MECHANICAL ENGINEERING FROM AN ACADEMIC PERSPECTIVE

Editör: Doç.Dr. Ahmet Beyzade DEMİRPOLAT

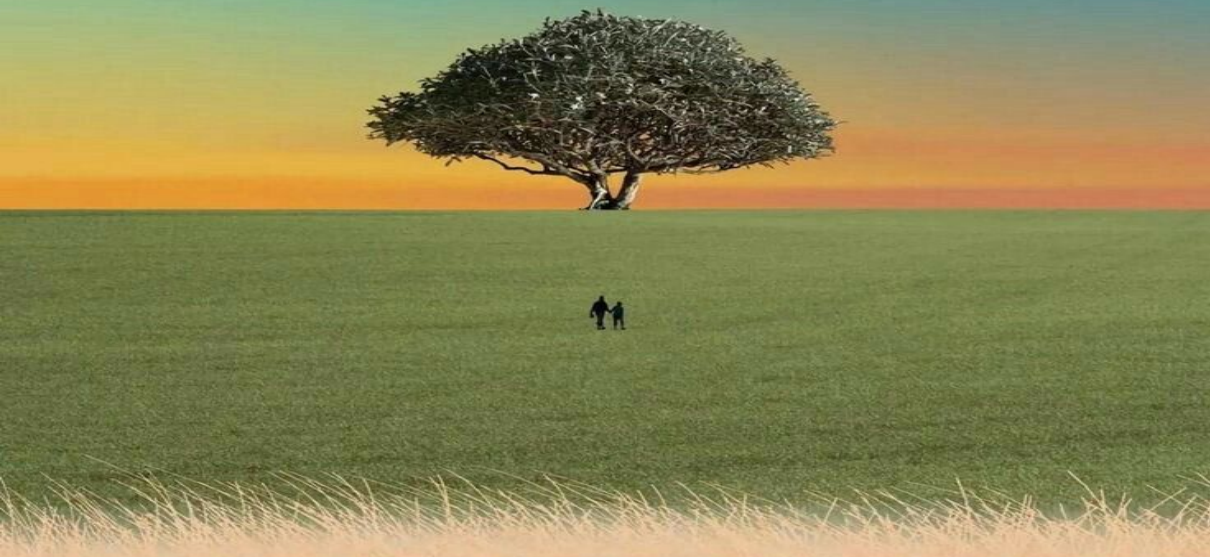

yaz
yayınları

Mechanical Engineering from an Academic Perspective

Editor

Doç.Dr. Ahmet Beyzade DEMİRPOLAT

yaz yayınları

2025

yaz
yayınları

Mechanical Engineering from an Academic Perspective

Editör: Doç.Dr. Ahmet Beyzade DEMİRPOLAT

E_ISBN 978-625-5596-71-0

Haziran 2025 – Afyonkarahisar

Dizgi/Mizanpaj: YAZ Yayınları

Kapak Tasarım: YAZ Yayınları

YAZ Yayınları. Yayıncı Sertifika No: 73086

M.İhtisas OSB Mah. 4A Cad. No:3/3
İscehisar/AFYONKARAHİSAR

www.yazyayinlari.com

yazyayinlari@gmail.com

info@yazyayinlari.com

CONTENTS

LPG CYLINDER DESIGN AND MANUFACTURING STAGES[1]

Hatice VAROL ÖZKAVAK[2]

Engin ALPER[3]

1. INTRODUCTION

Liquefied petroleum gas, known as LPG (Liquid Petroleum Gas), consists of a mixture of butane and propane gases. LPG is a colorless, odorless gas and is highly flammable. The properties of LPG gas are given in Table 1.

Table 1. Properties of LPG (Şaşmaz ve Altıntaş, 2021)

Properties of Liquefied Petroleum Gases (LPG)				
General Features	Unit	Commercial Propane	Commercial Butane	Milks LPG
Compound		C_3H_8	C_4H_{10}	%30 C_3H_8 + %70 C_4H_{10}
		The original is odorless, scented with ethyl mercaptan (C_2H_5SH)	The original is odorless, scented with ethyl mercaptan (C_2H_5SH)	The original is odorless, scented with ethyl mercaptan (C_2H_5SH)
Vapor pressures				
20°C	bar	9.2	1	3.5
40°C	bar	15.3	2.8	6.6

[1] This study is derived from the Master's Thesis Dissertion named "Desıgn Of Shrınk-Fıt Mold For Portable Steel Tube Manufacturıng And Determınatıon Of Suıtable Cord Blade Angle" in the department of Advanced Technologies (Interdisciplinary), Instıtute of Graduate Eduvation, Isparta University of Applied Sciences.

[2] Assoc. Prof., Isparta University of Applied Sciences, Technical Sciences Vocational School, Department of Mechanical and Metal Technology, Isparta, 32260, Turkey, haticevarol@isparta.edu.tr Orcid Id: 0000-0002-0314-0119

[3] Isparta University of Applied Sciences, Isparta University of Applied Sciences,The Institute of Graduate Education, engin.alper321@gmail.com Orcid Id: 0000-0002-2616-4228.

Boiling temperature	°C	-42	-9	-18
$1m^3$	kg	509	582	561
Relative Density (relative to Water)		0.509	0.532	0.561
Molecular Weight	g/gmol	44.1	58.1	53.5
Gas Volume / Liquid Volume		272	238	248
Lower Calorific Value	kCal/kg	11100	10900	10960
Ignition Temperature (in Air)	°C	493-549	482-538	482-549
After Evaporation				
Total Heating Value	kCal/kg	11950	11740	11800
Maximum Flame Temperature	°C	1980	2008	2000
95% Evaporation Temperature	°C	-38.3	2.2	2.2
Combustion Products				
CO_2	%	11.6	12	11.9
N_2	%	72.9	73.1	73
H_2O	%	15.5	15	15.1
Maximum Sulfur Content	Mg/kg	185	140	140
Explosive Limits in Air-Gas Mixture				
Lower	%	2,15		
Upper	%	9,6		

LPG is used in homes, hotels, hospitals or small commercial establishments in industry (Arayıcı, 2003; Anonim, 2003). Since it is used in many different areas, 3% of the world's energy needs are met by LPG (Öztop and Güven, 2000). This situation makes the storage of LPG gas important. Cylindrical pressure containers are used to store LPG gas. In the pressure container used for storing LPG, the LPG in liquid form turns into liquid gas due to the decrease in pressure when the valve on the

cylinder is opened. The LPG cylindrical containers manufactured for storing LPG in liquid form must be resistant to the internal pressure caused by the liquid. For this reason, LPG cylinder manufacturing is an important parameter and each country has determined its own standards.

2. LPG CYLINDER MANUFACTURING

2.1. LPG Cylinder Shapes and Materials

An LPG cylinder consists of a cylindrical body, lower dome, foot (base ring), cylinder valve, valve protection ring and cylinder plug components and are given in Figure 1 (Kiren and Sruthi, 2018). LPG cylinders are manufactured in 2-piece or 3-piece form. In 2-piece LPG cylinders, two domed ends are directly welded to each other. In 3-piece cylinders, two domed ends are joined to the cylindrical body. Domed ends used for LPG cylinders are classified as tori, spherical, hemispherical, and semi-ellipsoidal and are given in Figure 1 (Tom et al., 2014).

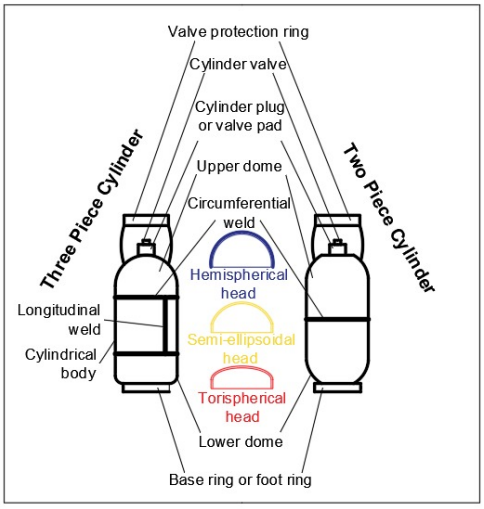

Figure 1. Components of LPG cylinders and the domed ends used for LPG cylinders (Tom et al., 2014; Kiran ve Sruthi, 2018)

In Turkey, TS EN 1442 standard is used for LPG cylinder manufacturing. This standard used is a European standard and includes the design, manufacturing and post-manufacturing tests required for circular section cylinders made of steel material that can be refilled and transported starting from 0.5 liters and up to 150 (inclusive). In addition, this standard is supported by TS EN 14140 standard. TS EN 14140 standard includes alternative design and manufacturing methods in addition to TS EN 1442 standard. Technical drawing details of LPG Cylinder according to TS EN 14140 standard are given in Figure 2.

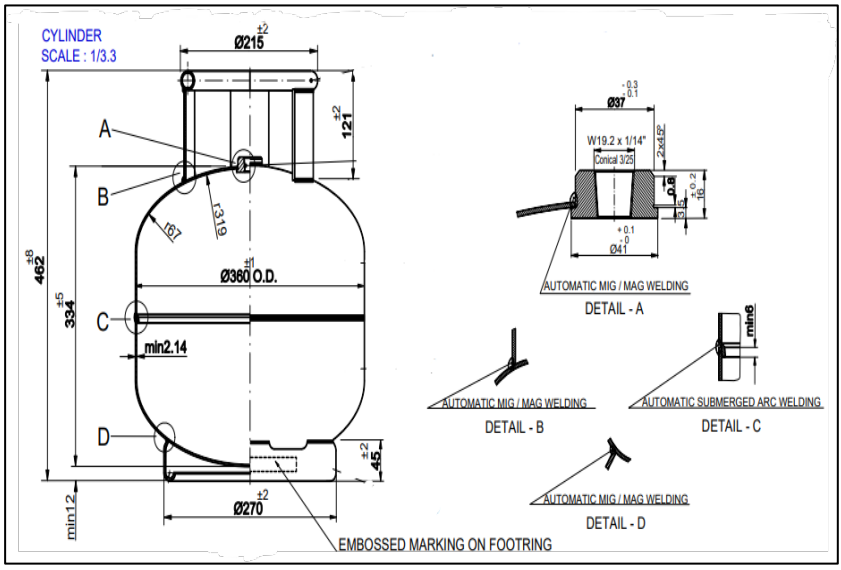

Figure 2. Technical drawing details of LPG Cylinder according to TS EN 14140 standard (TS EN 14140)

One of the important issues in LPG cylinder manufacturing is the selection of the material for cylinder manufacturing. LPG cylinders operate under high pressure. This requires the selected material to be resistant to pressure, lightweight, long-lasting, have safe operating properties, corrosion resistance and easy weldability. Considering these conditions, the most commonly used LPG cylinder material is

low carbon steel. As an alternative to this material, sheets manufactured using stainless steel, composite, and aluminum materials in accordance with the EN 10028-7 standard are also used in LPG manufacturing. The mechanical and chemical properties of the materials used in LPG cylinder manufacturing must be in accordance with the EN 10204:2004 standard. In addition, the materials and components used for LPG cylinder manufacturing must comply with the environmental policy of that country and EN 150 14021, EN 150 14024, EN 150 14025 standards.

2.2. Calculations Required for LPG Cylinder Manufacturing

Since LPG cylinders are cylinders operating under pressure, it is important to determine the cylinder wall thickness. The wall thickness depends on factors such as the yield strength of the material used, the welding joint factor, the cylinder test pressure, the cylinder dome shape, the outer diameter, the bowl radius, the joint radius, and the flat flange length (Sidduqui et al., 2013). Accordingly, the wall thickness is calculated as given in Equation 1.1.

$$a = \frac{P_c x D}{\frac{20 x R_O x J}{4/3} + P_c} \tag{2.1}$$

Here, the J value should be taken as J=0.9 for longitudinally welded tubes, while it should be taken as J=1 for tubes that are not longitudinally welded. Ro is the yield strength of the material, P_c is the test pressure and this value is taken as 15 bar for (UN1011, UK 1961 A, A01, A02, A0 mixtures and UN 1969) while it is taken as 30 bar for all other LPG cylinders. For longitudinally welded tubes: J = 0.9 For tubes that are not longitudinally welded: J = 1.0 Design of torispherical and semi-ellipsoidal concave dome heads subjected to pressure The shape

of the dome heads should be such that the following conditions are met:

• In torispheric dome heads; R < D; r 0.1 D; h 4b (Fig. 3),

• In semi-ellipsoidal dome heads; H 0.192 D; h 4b (Fig. 3)

Wall thickness (b) should not be less than the value calculated with the following equation:

$$b = \frac{P_c x D x C}{(15 x R_0) + P_c} \qquad (2.2)$$

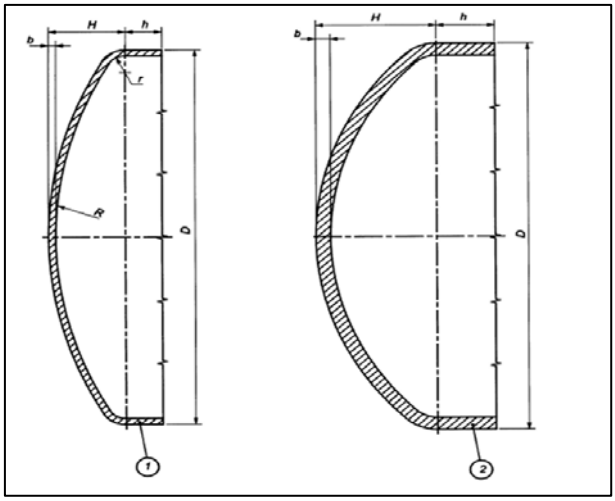

Figure 3. Examples of concave tube periods exposed to shelter (TS EN 1442-2017)

In Equation (2.2), "C" is the form factor value depending on the H/D ratio. When the H/D ratio is between 0.2 and 0.25, the "C" value is obtained from Figure 4a; when the H/D ratio is between 0.25 and 0.5, the "C" value is obtained from Figure 4b.

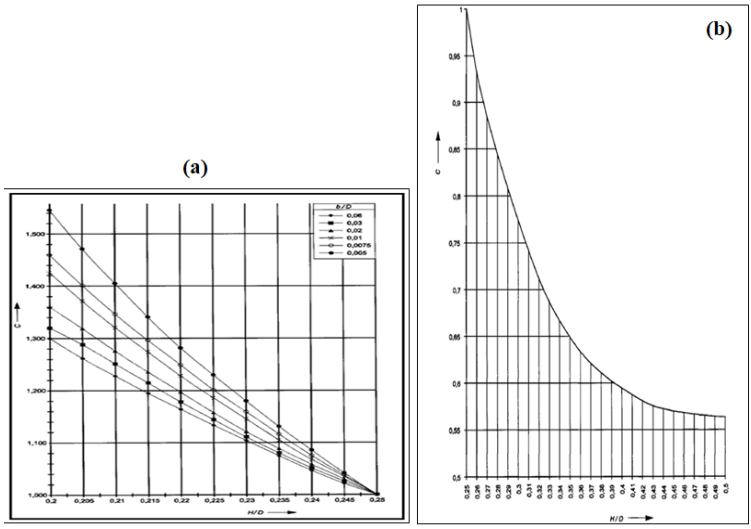

Figure 4. Finding the form factor (C) when the H/D ratio is between (a) 0.2-0.25 (b) 0.25-0.5 (TS EN 1442-2017)

2.3. LPG Cylinder Manufacturing Stages

The basic stages of LPG cylinder manufacturing from raw material to 2 or 3-piece LPG cylinder tube are given in Figure 5.

LPG cylinder manufacturing starts with cutting the raw material in the form of a sheet for the formation of the lower and upper domes. This process is called flake cutting. Then, a hole drilling process is applied so that the plug can be placed on the upper dome. The valve protection ring is manufactured by applying the processes of emptying, rolling and assembling to the raw material in order.

After the manufacturing of the parts, they need to be cleaned of defects such as oil and dirt before the welding process so that the welding procedure is not adversely affected. The cleaning process is followed by the welding process. Another important stage of LPG cylinder manufacturing is the welding and joining process. This stage must again be carried out in accordance with the standards. While the EN-130 15609-1

standard is used in the welding procedure applied in LPG cylinder manufacturing, scaling must be made in accordance with EN 15164-1 or EN 130 15613 for the welding process. There must be no errors such as porosity, incomplete joining, cracks in the welds made in LPG cylinder manufacturing. For this, it is applied on fully mechanical or automatic machines to eliminate operator errors. If welding personnel are used, it is required that this personnel meet the EN 130 4732 standard and the weld they make is behind the EN 1309606-1 standard. The welding surface must be smooth and 25% of the welding width is the allowed rates for overflows occurring after welding. Figure 6 shows the welding seam shape and dimensions specified in the TS EN 1442:2017 standard.

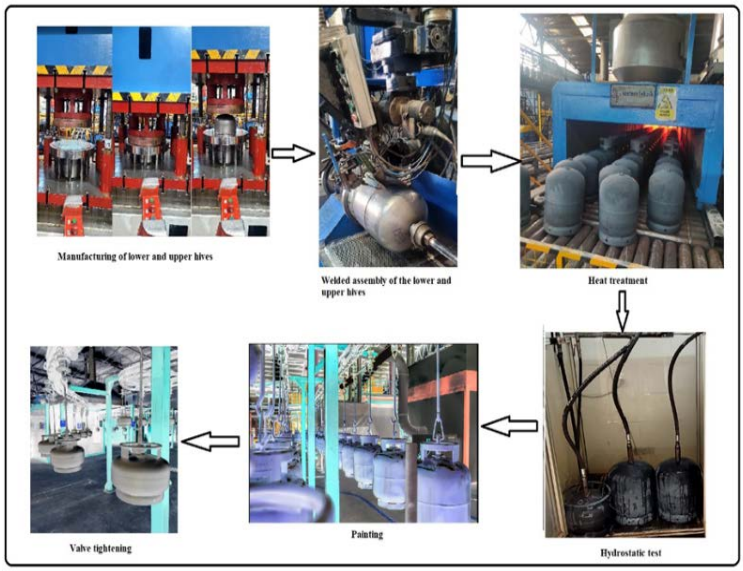

Figure 5. LPG Cylinder manufacturing stages (Alper,2025)

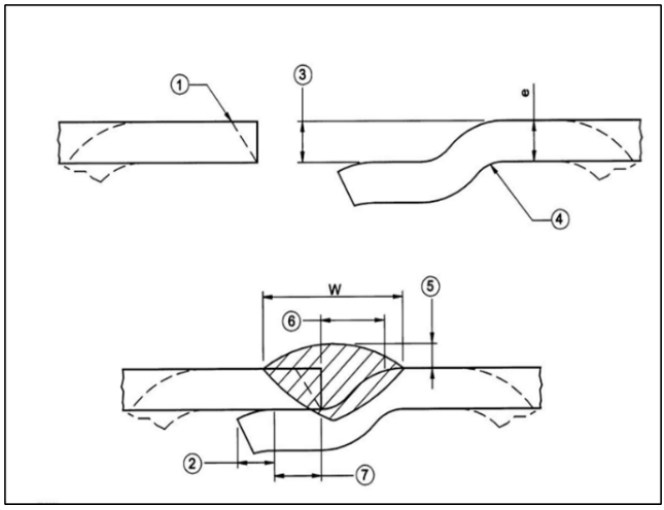

Figure 6. Illustration of a typical circumferential lap butt weld joint (TS EN 1442-2017)

Where 1 Optional beveling; 2 As desired; 3 Depth of misalignment for tight fit in insert; 4 Inside the tube – (sharp corners are avoided); 5 Weld height (excluding inner weld coating area) ≤ W/4 ; 6 Bevel width: 2.5e ≥ bevel width ≥ e; 7 Minimum contact length: 1.5e (e is the thickness of the misaligned metal and W is the weld width, and should be calculated so that 8e ≥ W ≥ 3e.

The submerged arc welding method is used as a welding method in LPG cylinder manufacturing. The submerged arc sliding method is a joining method that does not create smoke or radiation, has deep penetration and is very good in terms of reliability. The important parameters for this method are current, voltage and movement speed, and the adjustment of these parameters ensures successful welding.

After the welding process, heat treatment is applied to the tubes in order to eliminate the tensions caused by the welding. After the heat treatment, the tubes are subjected to hydrostatic

testing and then the valve tightening process is applied after the painting process and the manufacturing is completed.

2.4. Destructive and Non-Destructive Tests Applied to Cylinders in LPG Cylinder Manufacturing

During LPG cylinder manufacturing, destructive and non-destructive examinations are carried out under the conditions specified in the standards. Macro, micro and X-ray examinations are carried out on the tubes as non-destructive tests. Macro examinations applied to the tubes are carried out according to the TS EN ISO 17639 standard (Figure 7). Micro examinations are carried out on the samples prepared from LPG cylinders by grinding and etching.

Figure 7. Preliminary preparation stages for macro review (Alper,2025)

The manufactured LPG cylinder is subjected to X-Ray inspection before being subjected to heat treatment. X-Ray inspection is performed by certified personnel. X-Ray inspection determines whether there are any errors such as missing joints or gaps in the weld area. The X-Ray inspection setup used for LPG cylinders is given in Figure 8.

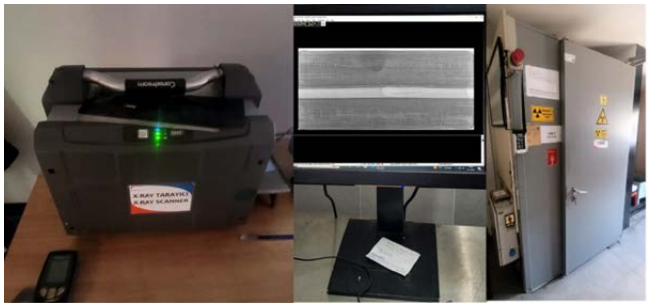

Figure 8. X-Ray inspection device used for LPG cylinders (Alper,2025)

In addition to non-destructive tests, destructive tests are also applied to LPG cylinders. Tensile, bending, pressure fatigue, burst-pressure and corrosion tests must be applied to manufactured LPG cylinders. These tests are applied to control the welding areas of the main metal used in tube manufacturing and the parts exposed to the pressure formed in the manufactured tube. The application number of the 2-piece prepared test samples is given in Table 2. In addition, the areas where samples should be taken are specified in the standard and are given in Figure 9.

Table 2. Tests to be applied to two-piece LPG cylinders and test descriptions

The experiment to be applied	The standard to which the experiment is based	The explanation of the experiment
Tensile test (1 time)	EN ISO 6892-1	In the longitudinal geometric direction of the tube or, when this is not possible, in the circumferential direction or from the centre of a domed head to the base metal
Tensile test (1 time)	EN ISO 4136	Perpendicular to the environmental source
Bending test (1 time)	EN ISO 5173	On the upper side of the environmental source
Tensile test (1 time)	EN ISO 5173	At the bottom of the environmental source
Macroscopic examination (1 time)	EN ISO 17639	At a randomly selected location in the environmental source

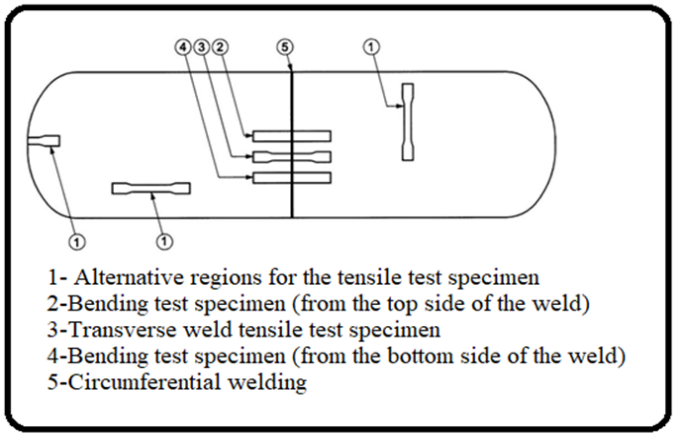

Figure 9. Areas where bending and tensile samples are taken in two-piece LPG cylinder manufacturing (TS EN 1442-2017)

EN ISO 6892-1 is the standard that includes sample preparation and application of the test for tensile tests on manufactured tubes. In addition, EN ISO 4136 standard gives the tensile sample properties made perpendicular to the source and the sample that complies with the standard is given in Figure 10.

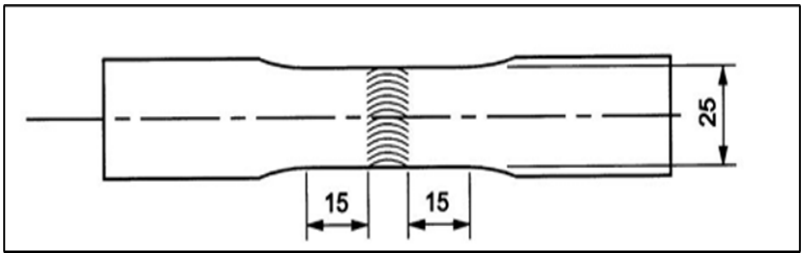

Figure 10. Test sample shape and dimensions for tensile test conducted perpendicular to the weld (TS EN 1442-2017)

The necessary procedures and sample shape and dimensions for bending test are given for tubes manufactured in EN ISO 5137 standard. Bending test sample dimensions and shapes are given in Figure 11. The bending sample is performed by bending 180° around the mandrel placed in the center of the

weld. In the bending test, the ratio of the mandrel diameter (Dp) / sample thickness (e) expressed as n is important and the tensile strength values according to this are given in Table 3. The absence of crack formation in the sample after the bending test is stated as a condition of success in the standard.

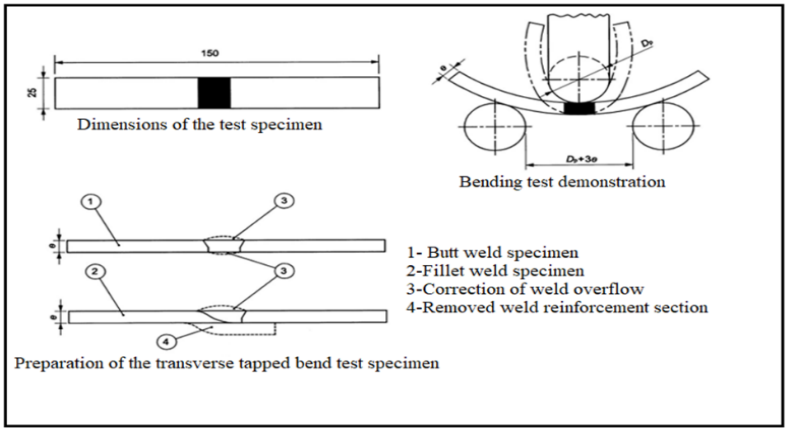

Figure 11. Bending test specimen shapes and dimensions (TS EN 1442-2017)

Table 3. Ratios of mandrel diameter and test piece thickness

Measured actual tensile strength (R_m) N/mm^2	n value
Up to and including 440	2
From 440 to 520 (inclusive)	3
From 520 to 600 (inclusive))	4
From 600 to 700 (inclusive)	5
From 700 to 800 (inclusive)	6
From 800 to 900 (inclusive)	7
Above 900	8

Bursting-pressure test must be applied to the manufactured tubes. This test is carried out in accordance with the TS EN 14140 standard. After the test, bursting curves of the tubes are drawn. The point to be noted here is given in the EN 12442 standard, and the bursting pressure must be 67.5 bar and the expansion in the tube must be at least 20%. In addition, the

bursting must occur perpendicular to the source area. The bursting pressure test system is given in Figure 12.

Figure 12. Bursting pressure test setup(Alper,2025)

One of the tests that must be applied in tube manufacturing is the pressure fatigue test. After this test, it is determined in which area the damage occurred in the tubes and whether it complies with the standards. In the pressure fatigue test, the tubes were subjected to a filling and emptying process at 35 bar pressure and 12100 cycles. The fact that no damage occurred after this test is an indication that the tubes comply with the standards. The pressure fatigue test setup is given in Figure 13.

The adhesion test, which is one of the external corrosion tests, is carried out according to the ENISO 2409:2013 standard. The EN ISO 11997-2 standard covers the climatic test conditions. In addition to this standard, the EN ISO 3231;1997 Article 9.3(b) standard also covers the climatic test conditions. The salt spray test, which is applied by spraying salt on the tube surfaces after they are scratched and exposing them to this for 720h, is carried out according to the EN ISO 9227 standard. The EN ISO 2812-2 standard covers the water resistance corrosion test, where the manufactured LPG cylinders are exposed to water for 400h. After the tests, the tensile test is also applied to the plates on which the

corrosion tests are applied, and the conditions are given in EN ISO 4624.

Figure 13. Compressive fatigue test setup (Alper,2025)

Corrosion is one of the damage mechanisms that LPG cylinders are exposed to. For this reason, corrosion tests are applied to manufactured LPG cylinders. External corrosion tests applied to coated cylinders are classified as adhesion climatic test, salt spray and water resistance. The salt spray test setup is given in Figure 14.

Figure 14. Salt Spray test setup (Alper,20005)

Impact test is applied to LPG cylinders in order to determine the ability of the cylinder design (thickness, material and mechanical properties) to withstand loads other than internal pressure. While applying these tests, there should be no internal

pressure in the cylinders and no covered casing on the cylinder. In the impact test, the impact speed and impact energy are obtained either by dropping the cylinder from a certain height or by hitting the cylinder with a mobile impact apparatus. In impact tests, the impact direction should intersect with the cylinder axis and the impact location should be selected in accordance with the test conditions. In addition, the hardness value of the impact apparatus used in the test should be greater than the hardness of the cylinder material and the absorption of the impact energy should be prevented. In addition, the surface used in the impact test should be flat; the impacting part length should be equal to the collection tube length and its width should be equal to the tube diameter. The impact energy in the impact test is given in Equation 2.3.

$$F = 30.M \tag{2.3}$$

In Equation 2.3, F: Energy (Joule) and M: Maximum operating mass of the tube (kg). The impact speed should be between 7 m/s and 8 m/s.

In the impact test, each tube should be impacted against a surface parallel to the tube. Following this, the tubes should then be impacted against a surface at 45º to the tube axis, on the convexity of the dome head (Figure 15). After both impacts, the tubes should be visually inspected for signs of damage and evaluated according to the rejection criteria determined in accordance with EN 1439. If both tubes are damaged equal to or worse than these rejection criteria, both tubes should be subjected to a burst test in accordance with the standard after two impacts. If the tubes withstand impacts with visible damage below the rejection criteria in EN 1439, after two impacts, one tube should be subjected to a burst test and the other to a fatigue test as appropriate. After the impacts, the pressurized tubes should not leak.

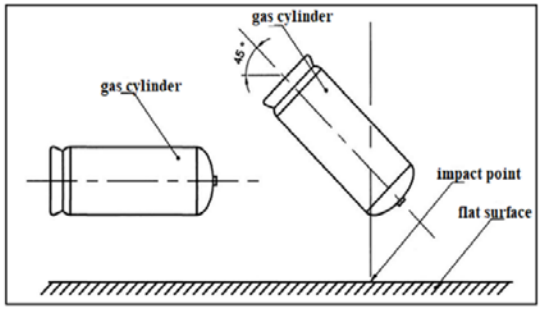

Figure 15. Schematic representation of impact test on flat surface (TS EN 1442-2017, Alper,2024)

The shape and dimensions of the apparatus used in the experiments using the impact apparatus are given in Figure 16. In case of using the impact apparatus, the impact energy is calculated as in Equation 2.4.

$$F=12.M \tag{2.4}$$

In Equation 2.4, F: Energy (Joule) and M: Maximum operating mass of the tube (kg). The impact speed should be between 4 m/s and 5 m/s. Each of the two tubes should be impacted from an edge parallel to the tube axis. The tubes should then be impacted with the edge perpendicular to the tube axis. The location of the two impacts should be separated by at least 45º around the tube circumference. Post-test checks are carried out in the same manner as in the flat surface impact test.

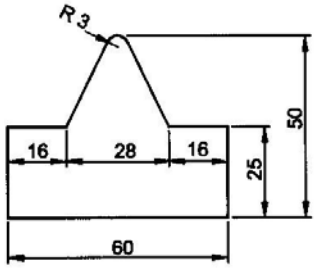

Figure 16. Impact apparatus shape and dimensions (TS EN 1442-2017, Alper,2024)

REFERENCES

Alper, E. (2025). Taşınabilir çelik tüp imalatı için sıkı geçme kalıp tasarımının yapılması ve uygun kordon bıçak açısının belirlenmesi. (Yüksek Lisans Tezi, Isparta Uygulamalı Bilimler Üniversitesi Lisansüstü Eğitim Enstitüsü).

Alper, E. (2024). Taşınabilir çelik tüp imalatı ve stndartları. (Yüksek Lisans Semineri, Isparta Uygulamalı Bilimler Üniversitesi Lisansüstü Eğitim Enstitüsü).

Arayıcı, S., Terzioğlu, G., Babaoğlu, M., Şafak, 5 , Yertutan, C., & Bener, O. (2003). Ev Yaşamında Güvenlik, Ekonomiklik, Pratiklik, TC. MEB. Çıraklık ve Yaygın Eğitim Genel Müdürlüğü ve İpragaz A.Ş. İşbirliği ile Hazırlanmış Bilgilendirme Semineri.

Anonim (2003). LPG'nin Doğru Kullanımı. http://www.ntvmsnbc.com/nevi's/190774.asp?cpl=l (Son erişim tarihi: 01 Kasım 2024)

Kiran, C. S., & Sruthi, J. (2018). Design and finite element analysis of domestic LPG cylinder using ANSYS Workbench. CVR Journal of Science and Technology, 14, 97-101. https://doi.org/10.32377/cvrjst1419

Öztop, H., & Güven, S. (2004). Kadınların tüp gaz kullanımına ilişkin bilgileri. Kadın/Woman 2000, 5(1-2), 117-130.

Siddiqui, N., Ramakrishna, A., & Lal, P.S. (2006). Review on liquefied petroleum gas cylinder design and manufacturing process as per Indian Standart, IS 3196. International Journal of Advanced Engineering Technology, 4(2), 1-4.

Şaşmaz, E., ve Altıntaş, A. (2021). Gaz Ve Tüp Valflerinin Tanıtımı Ve Çalışma Sistemi.Mühendis ve Makine,58.

Tom, A., Pius, G. M., Joseph, G., Jose, J., & Joseph, M. J. (2014). Design and analysis of lpg cylinder. International Journal of Engineering and Applied Sciences, 6(2), 17-31. https://doi.org/10.24107/ijeas.251225

TS EN 1442 (2017). LPG Donanım ve Aksesuarları- Taşınabilir, Yeniden Doldurulabilir. Kaynaklı Çelik LPG Tüpleri-Tasarım ve Yapım. Ankara.

TS EN 14140 (2015). LPG Donanım ve Aksesuarları- Taşınabilir, Yeniden Doldurulabilir. Kaynaklı Çelik LPG Tüpleri-Tasarım ve Yapım. Ankara.

TS EN ISO 17635 (2010). Kaynakların Tahribatsız Muayenesi Metalik Malzemeler İçin Kurallar. Ankara.

TS EN ISO 10028-7 (2016). Çelik yassı mamuller-Basınç amaçlı-Bölüm 7: Paslanmaz çelikler. Türk Standartları Enstitüsü, Ankara.

TS EN ISO 10204 (2007). Metalik mamuller- Muayene tipleri. tipleri. Türk Standartları Enstitüsü, Ankara.

TS EN ISO 17636-1 (2022). Kaynak Dikişlerinin Tahribatsız Muayenesi- Radyografik Muayene- Bölüm 1: Filmli X ve Gama Işını Teknikleri. Türk Standartları Enstitüsü, Ankara.

TS EN ISO 17637 (2017). Ergitme kaynaklarının Tahribatsız Muayenesi-Ergitme Kaynaklı Birleştirmeleri Gözle Muayene. Türk Standartları Enstitüsü, Ankara.

TS EN ISO 17637 (2022). Metalik Malzemelerdeki Kaynaklarda Tahribatlı Muayene- Kaynakların Makroskopik ve Mikroskopik Muayenesi. Türk Standartları Enstitüsü, Ankara.

TS EN ISO 19232-1 (2013). Tahribatsız Muayene-Radyografların Görüntü Kalitesi Kısım 1: Görüntü Kalite

Göstergeleri (Tel Tipi) – Görüntü Kalite Değerinin Tespiti. Türk Standartları Enstitüsü, Ankara.

TS EN ISO 19232-3 (2013). Tahribatsız Muayene – Radyografların Görüntü Kalitesi – Bölüm 3: Görüntü Kalite Sınıfları. Türk Standartları Enstitüsü, Ankara.

TS EN ISO 3834 (2007). Metalik Malzemelerin Ergitme Kaynağı İçin Kalite Şartları. Ankara.

TS EN ISO 6520-1 (2011). Kaynak ve İlgili İşlemler – Metalik Malzemelerde Geometrik Kusurların Sınıflandırılması – Bölüm 1: Ergitme Kaynağı. Türk Standartları Enstitüsü, Ankara.

TSE EN ISO/TR 16060 (2014). Metalik Malzemelerde Kaynaklar Üzerinde Tahribatlı Muayene- Makroskopik ve Mikroskopik İnceleme İçin Dağlayıcılar. Türk Standartları Enstitüsü, Ankara.

TS EN ISO 15609-1 (2019). Metalik malzemeler için kaynak prosedürlerinin şartnamesi ve vasıflandırılması- Kaynak prosedürü şartnamesi- Bölüm 1: Ark kaynağı. Türk Standartları Enstitüsü, Ankara.

TS EN 15613 (2005). Metalik malzemeler için kaynak prosedürlerinin şartnamesi ve vasıflandırılması- İmalât öncesi kaynak deneyini esas alan vasıflandırma. Türk Standartları Enstitüsü, Ankara.

TS EN ISO 9606-1 (2017). Kaynakçıların yeterlilik sınavı - Ergitme kaynağı- Bölüm 1: Çelikler. Türk Standartları Enstitüsü, Ankara.

AN OVERVIEW OF THE BORIDING PROCESS APPLIED TO IRON-BASED MATERIALS

Mehmet ÖZER[1]

Fatih BALIKOĞLU[2]

1. INTRODUCTION

Increasing the service life of materials used in the machinery industry, which are reduced because of tribological effects such as abrasion, corrosion and friction, can only be possible by improving the working surface areas. Because of abrasion and corrosion, there is a significant amount of material loss worldwide every year. It is known that the losses of countries due to corrosion vary between 3.5% and 5% of their gross national product. The loss in Turkey alone in 1991 is estimated to be 4.5 billion dollars (Özer, 2011).

One of the heat treatment methods that increases the strength value of machine parts is the "Boronizing" process. This process, first performed by Moissan in 1895, has a long history. Studies on the surface hardening of steels by boron diffusion have accelerated since the 1970s. Today, boronizing continues to be used in the industry, especially as an alternative surface hardening method, with further technological development (Özsoy, 1991).

When iron-based materials are boronized at 850 - 1150 ºC for 2 - 8 hours, a diffusion layer consisting of iron-boride (Fe_2B, FeB) phase is formed on the surface of the material, which can

[1] Öğr. Gör. Dr., Balıkesir Üniversitesi, Balıkesir MYO, İklimlendirme ve Soğutma Teknolojileri Programı, ozer@balikesir.edu.tr, ORCID: 0000-0002-6212-1217.

[2] Doç. Dr. Balıkesir Üniversitesi, Mühendislik Fak., Makine Mühendisliği Bölümü, fatih.balikoglu@balikesir.edu.tr, ORCID: 0000-0003-3836-5569.

reach a layer depth of ≈ 250μm and a layer hardness of ≈ 2500 HV0.06. This layer has a sawtooth-like form. In addition, the adhesion strength to the base material is very good, and it is known that the layer properties change depending on the process parameters (Çelikyürek, 2004; Karaman, 2003).

In terms of carbon content, iron containing less than 2% carbon is called steel, and more than 2% is called cast iron. In practice, carbon does not exceed 1.2% in steels other than plain carbon tool steels. In addition to iron and carbon, steels contain manganese, silicon and small amounts of phosphorus and sulphur from production. Especially in carbon steel and alloy steels, phosphorus and sulphur are tried to be kept at the lowest levels (Varol R., 2000).

2. BORON ELEMENT

It is an element with the atomic number 5, located at the top of Group 3A in the periodic table, and is represented by the symbol 'B' for boron. Pure boron was first obtained in 1808 by French chemists J.L. Gay-Lussac and Baron L. J. Thenard and English chemist H. Davy. It consists of isotopes 8, 10, 11, 12 and 13B. The most stable isotopes are 10 and 11B. Therefore, the 10B isotope is used in nuclear power plants and nuclear materials because it has a high thermal neutron capture property (Güner, 2023). The ratio of 10B isotopes in boron-extracted ores in our country is quite high. The boron element is widely found, especially in rocks, water and soil. It is found on average in soil at 10-20 ppm, in the sea at 0.5-9.6 ppm and in fresh water at 0.01-1.5 ppm. Due to its chemical affinity, it is found in nature as compounds. The physical and chemical properties of the boron element, which is heat resistant and almost as hard as diamond, are given in Table 1 and Table 2, respectively (Boren, 2025).

Table 1. Some physical properties of boron element (Boren, 2025).

Atomic weight	10,811u
Melting point	2300°C- 2573°K- 4172°F
Boiling point	4002°C- 4275°K- 7236°F
Density	2,34gr/cm^3
Hardness	Mohs: 9,3
Elastic modulus	Bulk: 320GPa
Heat of vaporization	489,7kJ/mol
Molar volume	4,68 cm^3/mol
Appearance	yellow- brown

Table 2. Some chemical properties of boron element (Boren, 2025).

Electronegativity	2,04
Electrochemical equivalent	0,1344g/amp-hr
Valence electron potential (-eV)	190
Ionization potential	First: 8.298, Second: 25.15, Third: 37.93
Fusion heat	50,2 kj/mol

The boron element has the opportunity to be used in a wide variety of areas in the industry, thanks to the different properties exhibited by the compounds it forms with some metals and nonmetals. It is known that there are approximately 230 types of boron minerals in nature. In addition, the boron element is also found in the form of salt in combination with other elements. Borax, colemanite, ulexite and kernite are some of the most common boron compounds used in industry (Güner, 2023). Boron mines generally gain value with the amount of B_2O_3 (boron oxide) they contain. Those with a high B_2O_3 content are considered valuable (BOREN, 2025). Boron ore is generally mined in the regions south of Uludağ in Turkey. It is intensively mined in Kırka in Eskişehir, Emet in Kütahya and Hisarcık, Bigadiç, Susurluk, Kestelek and Sultangazi in Balıkesir. 70% of the world's boron ore is produced in these regions. The quality of boron mined in our country is better than in other regions (Güner, 2023).

Boron products are used in the industry; glass; electronics and computers; energy; pharmaceuticals; paper; chemicals; machinery; nuclear; metallurgy; automobiles; agriculture; sports equipment; textiles; ceramics; medicine; and aviation sectors (Özer, 2011).

3. BORONIZING PROCESSES

3.1. Boronizing and Structure of Boride Layer

Boronizing is a method triggered by a diffusion mechanism and carried out by thermal activation. Therefore, it is among the thermochemical surface treatments that include nitriding and carburizing processes. In general, surface treatments are classified into four different methods (thermal-based, gas-phase, thermochemical-based, and galvanic-based) in practical applications. The place of boronizing among surface treatments is given in Figure 2 (Bolat, 2016).

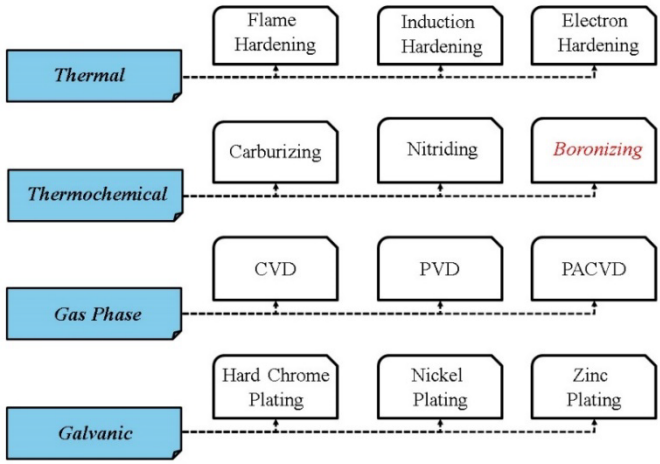

Figure 2. The Place of Boronizing Process Among Surface Treatments (Bolat, 2016).

In boronizing, since it is based on the diffusion mechanism, it is necessary to reach high temperature values and to perform thermal activation. Therefore, the realization of this mechanism is a basic requirement for all boronizing processes. The place of boronizing among all heat treatment processes is given in Figure 3 (Güner, 2023).

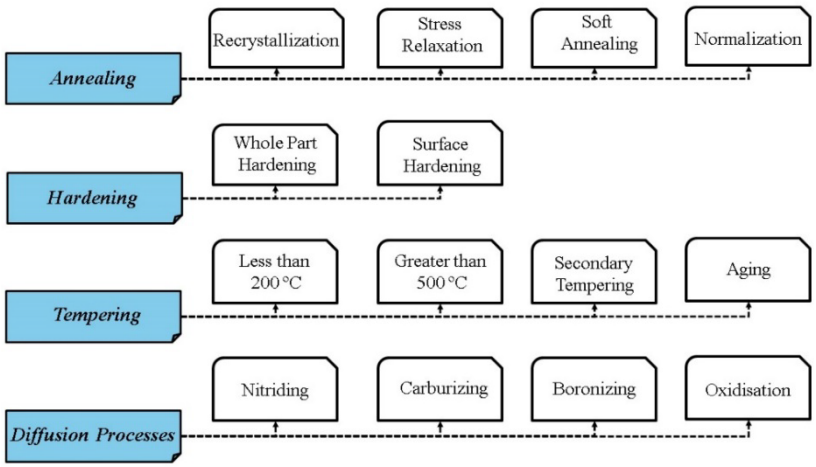

Figure 3. The Place of Boriding Process Among Heat Treatment Techniques (Bolat, 2016).

Since the boronizing process is carried out by diffusion, the driving force of temperature plays an important role. The boronizing process is carried out with the parameters of high temperatures and long processing times. Generally, when looking at boron-providing environments, there are applications such as solid, liquid and gas. In addition to these, the boronizing process is also applied with methods such as plasma, ion implantation, physical and chemical vapor deposition and electrochemical (Albayrak, 2021). The phase structure of the boride layer formed on the surface of the material after the diffusion process is determined by the boron potential of the boronizing environment, the chemical content of the material to be boronized, the process temperature and the process time (Cimenoğlu, 2014). In addition

to the boron source used during the boronizing process, activators, fillers and deoxidants are other elements that contribute to the process. The activator material allows the barite layer to grow regularly. In addition, fillers and deoxidants create a reducing environment by retaining oxygen, thus preparing the ground for a healthy boronizing process (Kondul, 2020).

The boronizing process has a two-stage process. First, the interaction between the surface to be coated and the boron-bearing medium occurs, and nucleation occurs. Then, with the second stage, diffusion begins to occur according to temperature and time. At the end of this successive process, the boride layers reach a certain thickness. The formation mechanism of the boride layer in all boronizing methods has been shown in many studies to exhibit similar behaviour. The formation mechanism of the boride layer is presented sequentially in Figure 4 (Ertürk, 2018).

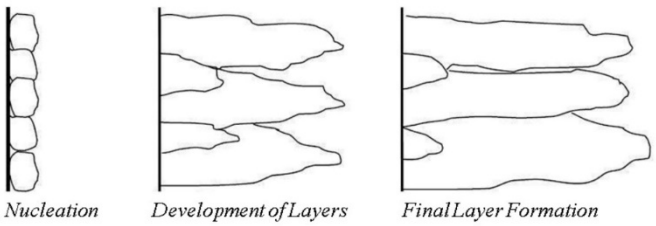

Figure 4. Boride Layer Formation Stage (Ertürk, 2018).

It is possible to create boride layers with various compositions depending on the type of substrate material. During boriding, boron atoms diffuse into the surface of the material, and the thickness of the new layer formed by the atoms of the substrate material depends on temperature and time, as in other diffusion-based surface treatments (Kartal, 2011).

The growth kinetics of boride layers is expressed in Equation 3.1 with the parabolic rate law.

$$d^2 = Kt \tag{3.1}$$

In this equation, ‘K’ indicates the layer formation rate constant, ‘d’ indicates the boride layer thickness and ‘t’ indicates the boronizing process time. Known as the Arrhenius relation and expressed as the formation rate constant in equation 3.2, ‘K’ depends on the degree of process temperature and the diffusion level of boron atoms.

$$K = K_0 exp(-Q/RT) \quad (3.2)$$

In the equation, K_0’ is the exponential factor, Q’ is the activation energy, T’ is the temperature and ‘R’ is the gas constant. Using these two equations, the thickness of the boride layer formed on the surface of the material at a certain time and temperature can be calculated (Sista, 2011).

The characteristics of the boride layer formed after the boronizing process are also affected by the number of alloying elements in the boronized material. As the content of alloying elements increases, the thickness of the obtained boride layer decreases and the diffusion between the boride layer and the surface of the material flattens. This is because the alloying elements act as barriers and allow limited diffusion (A Ertürk, 2018: 15). Some properties of different boride layers formed depending on the type of material are given in Table 3 (Kondul, 2020).

Table 3. Different Borides and Some of Their Properties (Kondul, 2020).

Boride	Crystal Structure	Density (gr/cm^3)	Melting Temperature (ºC)	Thermal Expansion (10^{-6}/K)	Thermal Conductivity (W/mK)	Hardness (GPa)	Electrical Resistance (10^6Ωcm)
CrB	Tetra.	6,14	--	12,3 (27-1027 ºC)	20,1 (20ºC)	11,8	46
Cr_2B	Ortog.	6,58	1870	14,2 (27-1027 ºC)	10,9 (20ºC)	13,2	107
FeB	Ortog.	6,73	1650	12 (400-1000 ºC)	12 (20ºC)	16,2-18,6	80
Fe_2B	Tetra.	7,34	1410	---	17,4	13,1-17,7	38
NiB	Ortog.	7,17	1590	---	21,9	15,2	50
Ni_2B	Tetra.	8,05	1225	---	58,4	14	14
TiB	Ortog.	4,56	2190	---	---	22,7	40
Ti_2B	Hegz.	4,52	3225	---	64,4 (27ºC)	33-25,5	9

3.2. Boronizing of Iron Based Materials

The purpose of imparting surface hardness to iron-based materials by boronizing is to obtain high wear resistance, a very hard surface, and to extend the service life in oxidizing and corrosive atmospheres (Allaoui, 2006).

Depending on the chemical content of the material used in the boronizing process, the boronizing time, temperature and the boron potential in the boronizing environment, a two-layer (FeB/Fe_2B) or single-layer (Fe_2B) boride layer is formed on the surface of the iron-based material (Türkmen, 2018). These iron borides provide both the properties of ceramics, such as high hardness, and the high electrical conductivity expected from metals (Toktaş, 2017).The outermost of the two layers formed on the surface of the material is called the FeB phase, which is denser in terms of boron, and the one below it is called the Fe_2B phase. These two layers are formed in different shapes depending on the number of alloying elements in the material. While it is formed in the form of a sawtooth in most steel materials, it is observed as a flatter structure in stainless steels and steels with high chromium content (Topuz, 2020).The image of the iron borides formed at the end of the boronizing process is shown in Figure 5 (Özer, 2011).

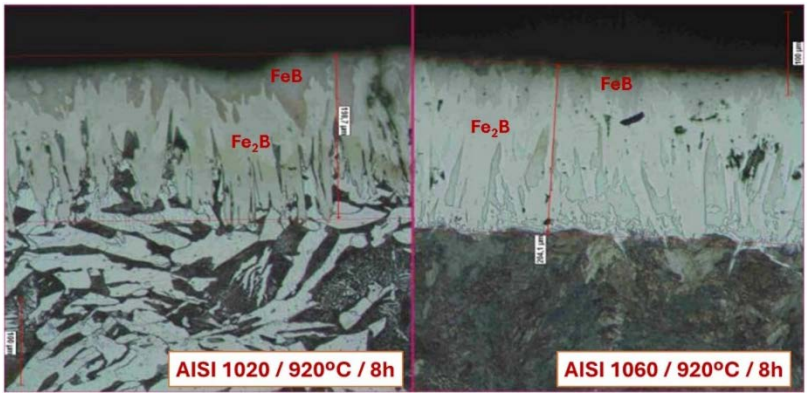

Figure 5. Appearance of Iron Boride Phases Formed as a Result of Boriding Process (Özer, 2011).

In industrial applications, monolayer (Fe_2B) formation is preferred over bilayer (FeB, Fe_2B) formation. This is because the boron-rich FeB phase is hard but more brittle than the Fe_2B phase (Mu, 2013). Another reason for preference is that compressive and tensile stresses occur between the Fe_2B and FeB phases during phase formation. It has been stated that cracks mostly occur between the two phases because of these stresses. While FeB creates tensile stress, Fe_2B creates compressive stress. As a result of this situation, the structures belonging to these phases separate from each other over time under the influence of mechanical stresses and cause damage by breaking off pieces in the form of layers (Özer, 2011; Yu, 2005). In addition, the large difference in thermal expansion coefficient between the two layers also causes crack formation between the phases. The thermal expansion coefficient for FeB is 23x10-6/°C, while it is 7.85x10-6/°C for Fe2B (Ozdemir, 2006). In two layered structures with a sawtooth structure, cracks may start due to the notching effect of the saw teeth. Figure 6 shows the crack between the two layers.

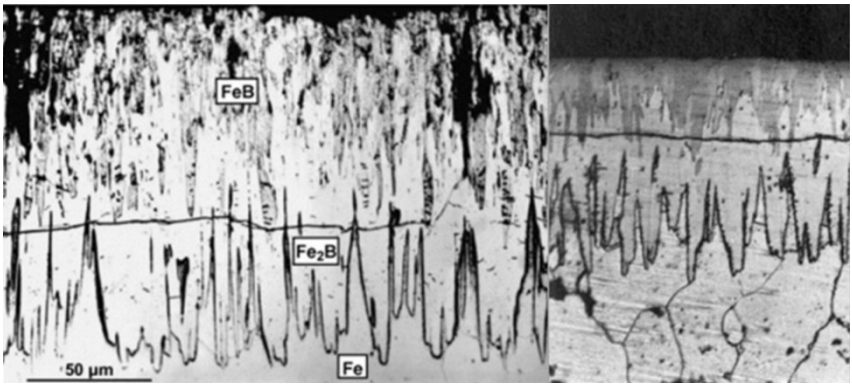

Figure 6. Crack Occurring Between Fe2B and FeB(Martini, 2004; Spence, 2005).

Fourteen different boride layers can be obtained by various boriding techniques. The systematic classification developed by Schaaber and Kunst is presented in Figure 7.

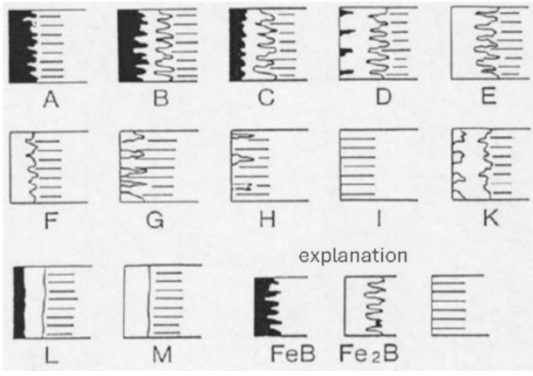

A: Dense FeB monolayer structure,
B: FeB and Fe2B bilayer structure,
C: Bilayer structure with thinner FeB layer,
D: Bilayer structure (isolated FeB teeth),
E: Fe2B monolayer structure,
F: Fe2B layer with fewer teeth,
G: Special layer (Fe2B teeth),
H: Isolated Fe2B teeth,
I: Transition region,
K: Distorted layer,
L: Flat biphasic layer,
M: Single phase layer.

Figure 7. Types of Boride Layers (Matuschka, 1980).

Typical properties of FeB and Fe_2B layers formed on the surface of iron-based materials are given in Table 4. It has been emphasized that the boronizing process increases the fatigue strength of iron-based materials by 25%, yield and rupture strengths by 10-20% and fatigue life by 200%, while it has been reported that it also reduces the deformation ability (Saygın, 2006).

Table 4. Some Properties of FeB and Fe2B Layers (Saygın, 2006).

Property	FeB	Fe_2B
Microhardness (GPa)	19-21	18-20
Boron Content (% by weight)	16,23	8,83
Density (gr/cm^3)	6,75	7,43
Melting Temperature (°C)	1540-1657	1389-1410
Electrical Resistivity (10^{-6}cm)	80	38
Crystal Structure	H. Centered Tetragonal	Orthorhombic
Module of Elasticity (GPa)	590	280-295

Since the boron atomic diameter is 25% smaller than the iron atomic diameter, these two elements form a solid solution. In the iron-boron equilibrium system, FeB compounds are formed at 16.23% boron by weight, and Fe_2B compounds are formed at 8.83% by weight. In the iron-boron equilibrium diagram in Figure 3.7, the eutectic phase is formed at 3.8% boron by weight and at a melting temperature of 1149 °C. For this reason, the boronized surface is not affected by heat up to this temperature.

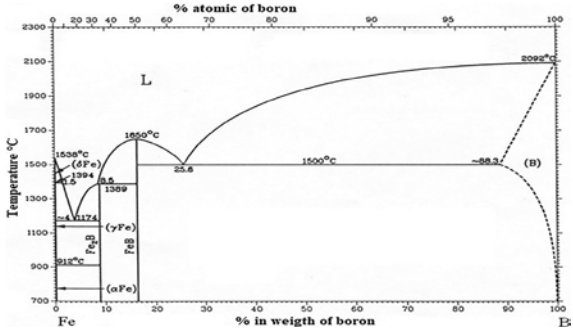

Figure 8. Iron-Boron Equilibrium Diagram (Hernández-Sánchez, 2018)

4. ADVANTAGES AND DISADVANTAGES OF THE BORONTING PROCESS

4.1. Advantages of the Boronizing Process

Some advantages of the boriding process, which is a thermochemical surface hardening process, can be listed as follows.

- Extremely high hardness values (between 1450 and 5000 HV) can be achieved after the boriding process. The hardness values of boronized steels according to hard materials and different processes are shown in Table 5. According to this table, it is seen that the hardness of the boride layer formed on the steel is much higher than the hardness values obtained with any traditional surface hardening methods. This hardness value obtained makes a significant contribution to the fight against main wear mechanisms such as abrasion, tribo-oxidation, adhesion, and surface fatigue (Sinha, 1991).

Table 5. Comparison of Hardness of Some Boronized Steels (Sinha, 1991).

Material	Microhardness (HV)
Diamond	>10000
AISI A2 Steel (Bored)	1900
AISI H13 Tool Steel (Bored)	1800
Mild Steel (Bored)	1600
Chrome Plating (Hard)	1000-1200
Quenched Steel	900
BM42 (High Speed Steel)	900-910
H13 Die Steel (Hardened & Tempered)	540-600
A2 Die Steel (Hardened & Tempered)	630-700
Steel (Nitrided)	650-1700
Low Alloy Steel (Carburized)	650-950

- The hardness of the boride layer formed by boronizing does not change under high temperatures.
- Boronizing can be applied to many different steels.

- Borided surfaces are resistant to oxidation up to 850 °C.
- Boronized materials have high fatigue life and service performance in corrosive and oxidizing environments (Sinha, 1991).
- After boronizing, corrosion-erosion resistance of ferrous materials in non-oxidizing dilute acids and alkaline environments increases (Oliveira, 2010).
- Boriding process, which is carried out for wide tribological applications where friction and wear are the priority, can be applied to a wide range of steel alloys, including low-carbon steel, low-alloy-steel, tool steel, and stainless steel. In addition, materials such as cobalt- and nickel-based alloys, molybdenum, and titanium can be boronized to obtain very high hardness and wear resistance on their surfaces. It can increase the resistance of low alloy steel to acids such as phosphoric, hydrochloric, and sulfuric acids. Austenitic stainless steel has excellent resistance to hydrochloric acid after boronizing. Boriding can be applied to materials with different geometries (Ozbek, 2004).

4.2. Disadvantages of Boronizing Process

The boriding process has advantages as well as undesirable disadvantages. These limitations can be listed as follows.

- It is not a flexible method; it is more costly than other thermochemical surface treatments (plasma nitriding and cementation in a gas environment). It is a labor-intensive process with special equipment. It is preferred in cases where high hardness, high corrosion, and wear resistance are desired.
- In works with sensitive tolerances, processing of the coating is possible with diamond tools. In case of

processing with traditional techniques, cracks occur in the coating layer.

- The rolling contact fatigue properties of boronized steel are fragile compared to nitrided and cemented steels. Therefore, boronizing has limited use in gear production (Sinha, 1991).
- Although boronized materials have good corrosion resistance against non-oxidizing acids such as H_2SO_4, they are weak against oxidizing acids such as HNO_3.
- In steels that will be subjected to heat treatment after boronizing, a vacuum or inert atmosphere is needed to maintain the properties of the coating layer (Kutucu, 2013).
- As the temperature of the boriding process increases, the resulting layer thickness also increases. The increase in this layer thickness increases the formation of porosity on the surface. The increased amount of porosity causes the boride layer to become brittle.
- Waste products formed after box boriding are harmful to nature (Öztürk, 2021).
- The deformation ability of materials that have undergone the boriding process, such as bending, is restricted, and surface roughness also increases (Kondul, 2020).

5. BORONIZING METHODS

In addition to traditional thermochemical boronizing methods (box, paste, liquid, and gas boronizing), techniques such as fluidized bed boronizing and plasma boronizing are also used depending on technological developments. Boriding is also performed by non-thermochemical ion deposition, plasma spray, chemical vapor deposition, and physical vapor deposition methods (Bora, 2017). The electrochemical boronizing phase

homogenization (PHEB) method, which allows thick and homogeneous boride layers to be formed easily and in a short time in terms of low cost, environmental sensitivity, and applicability, has been developed as an alternative to classical methods (Kartal, 2011; Mindivan, 2023).

5.1. Solid Media Boronizing

5.1.1. Box Boronizing

It is the most widely used boronizing technique due to its advantages of being safe, requiring simple equipment, and being able to be adjusted by changing the powder mixture ratio used in the process. It consists of boxing, heating, cooling, and cleaning stages. In the box boronizing process, the samples to be boronized are buried in the powdered traditional boronizing mixture or in the commercial mixture known as Ekabor powder, with a distance of at least 20 mm between the samples. The powder mixture in the box should surround the samples to be boronized with a thickness of 10-20 mm. Silica sand (SiO_2), Alüminyum oxide (Al_2O_3) or Ekrit (trade name) powder is filled on the boronizing powder as filler materials. The mouth of the crucible is closed with a lid to prevent air from entering the system (Aydoğmuş, 2019). Solid boron source, activators, and fluids are the components that make up the powder mixture. Amorphous boron, boron carbide (B_4C), and ferro boron are commonly used boron sources. Since amorphous boron is expensive and ferro boron cannot be produced in sufficient purity, boron carbide is used more in industrial applications. Some properties of solid boron sources are given in Table 6 (Bora, 2017).

Table 6. Some Properties of Solid Boron Sources (Bora, 2017).

Boron Source	Formula	Molecular Weight	Boron Ratio (%)	Melting Temperature (℃)
Amorphous Boron	(B)	10,82	95- 97	2050 ℃
Boron Carbide	(B_4C)	55,29	77,28	2450 ℃
Ferroboron	-	-	17- 19	-

The box boronizing process is carried out in a pre-prepared, atmosphere-controlled heat treatment furnace. The important parameters for the box boronizing process are temperature and time. This time and temperature vary depending on the type of material being boronized. The boronizing process is usually carried out in the temperature range of 800 to 1000 ℃ for 1-10 hours. The samples heated to the specified temperature are kept in the furnace for the desired time. The box left in the furnace is cooled until it reaches ambient temperature and then removed from the furnace. The schematic representation of the box boronizing system is shown in Figure 9a, and the schematic representation of the time- and temperature-dependent process is shown in Figure 9b (Öztürk, 2021). The most obvious disadvantage of the system is the need for high processing temperature (850-1050 ℃) and long processing time (3-16 h) to achieve an effective boronizing thickness (Xie et al., 2012: 2839).

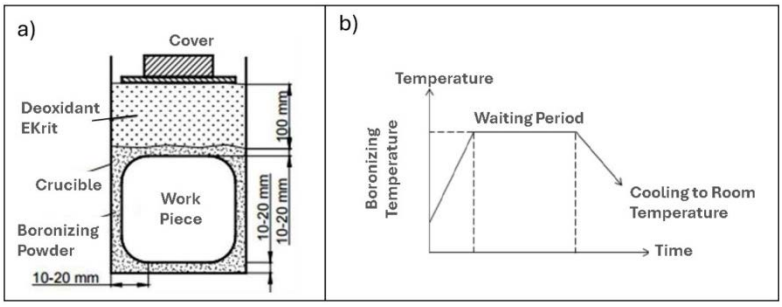

Figure 9. Box Boronizing System a) Schematic picture, b) Relationship between time and temperature (Öztürk, 2021).

5.1.2. Paste Boronizing

Paste boronizing process is preferred in cases where the box boronizing process is time-consuming, expensive, and difficult. In this process, boron carbide (45% B_4C), cryolite (55% Na_3AIF_6) or a traditional powder mixture (B_4C, SiC, KBF_4) and binding agents (ethyl silicate (hydrolysed), an aqueous solution of methyl cellulose, or nitrocellulose dissolved in butyl acetate) are used (G. Kartal, 2004). The mixture that turned into paste is sprayed or brushed onto the surface of the sample to be boronized at a depth of 1-2 mm. The paste-coated sample should be dried at a maximum temperature of 150 °C in a drying oven, preheating room, or hot air flow. Then, the paste-coated and dried samples are heated in a preheated oven to the boronizing temperature. After the boronized samples are removed from the oven, they are cooled, and the wastes adhering to the surface is cleaned. Obtaining a quality boride layer is possible by carrying out the boronizing process in a protective atmosphere (Ünal, 2013).

5.1.3. Fluidized Bed Boronizing

In fluidized bed boronizing, which is a type of solid medium boronizing method, a special boronizing powder (large-grained silicon carbide particles, EKabor) is used as a fluid medium. This powder is made fluid with an oxygen-free gas (N_2-H_2). The boronizing process is carried out in a fluidized bed containing the base material of the boronizing powder and oxygen-free gas. Electricity is used as a heat source to create a faster heat transfer medium in the base (P. Topuz, 2009). Some advantages of this process can be listed as follows.

- It is a low-cost method,
- The process is carried out in a short time with high speed in flow and heating,
- It can be used in continuous production, close tolerance and smooth surface,

- The bed is leak-proof due to the upward gas flow,
- Quenching can be done as a continuation of the process after the boronizing process,
- Heat distribution is homogeneous.

The disadvantage of fluidized bed boronizing is that the boron agents are continuously washed out with water along with the inert gas in the retorts. The waste gas contains fluoride and must be cleaned thoroughly (Sinha, 1991).

5.2. Liquid Medium Boronizing

The boriding process is carried out in a liquid environment at temperatures between 800 and 1000 °C by waiting for 2-6 hours. This process is the method of immersing the sample to be borided in a molten salt solution consisting of activator substance, boron compounds, and reducing substances. The duration of the boriding process is the immersion period. B_4C and SiC powders are generally used as reducing substances in the bath content, and borax is used as the boron source. If electric current is applied during the boriding process, it is called electrolytic boriding; if electric current is not applied, it is called normal liquid environment boriding (Alparslan, 2011).

Liquid environment boriding process is carried out in a normal atmosphere environment. Chemical reaction occurs quickly due to the liquid environment, so it is often preferred. The materials used are simple (Yamanel, 2018). If the boriding bath temperature drops below 850 °C, it will not be possible for the boriding process to take place since the bath fluidity will decrease. Therefore, temperature is a disadvantage of this method. For the boronizing process to be completed successfully, the viscosity of the boronizing medium should not increase. For this reason, salt (boron donor mixture) should not be added to the bath. After boronizing, salt deposits form on the surface of the sample and cleaning them is a disadvantage in terms of time and

cost. (Matuschka, 1980). The boronizing process carried out in a liquid medium is carried out in two groups; electroless boronizing in a salt bath and boronizing by the molten salt electrolysis method (G. Kartal, 2004). The main boron compounds and their properties used in these liquid medium boronizing techniques are given in Table 7.

Table 7. Basic Boron Sources and Properties Used in Liquid Media Boriding Process (Matuschka, 1980).

Material	Formula	Molecular weight (%)	Theoretical boron amount (%)	Melting temperature (°C)
Borax	($Na_2B_4O_7$-$10H_2O$)	381,42	11,35	-
Anhydrous Borax	($Na_2B_4O_7$)	201,26	21,50	741°C
Metaboric Acid	(HBO_2)	43,83	24,69	-
Sodium Boro fluoride	($NaBF_4$)	109,81	9,85	-
Boric Acid	(B_2O_3)	69,64	31,07	450°C
Boron Carbide	(B_4C)	55,29	7,28	2450°C

5.2.1. Electroless Boriding in Salt Bath

Borax is the main component in the environment, and chemicals such as B_4C, SiC, Zr, amorphous B, etc., are used as activators. This boriding process is carried out in borax, boric acid, sodium sulphate and ferrosilicon-based salt baths. It is a low-cost system that does not require much experience. The disadvantages of the method are that it cannot be applied to very large and complex parts, thermal shock, and the difficulty of cleaning the part after boriding. Boriding is generally carried out in the temperature range of 800-1000°C and in waiting times of 2-6 hours (G. Kartal, 2004).

5.2.2. Boriding with Molten Salt Electrolysis

The molten salt electrolysis boronizing method, which has survived to the present day and is still used, was first described by Origin and Schaaber. In the process, a graphite rod was used as the anode in molten borax, and the material to be boron was used as the cathode. Electrochemical boronizing is a method of electrolytically depositing boron atoms from a solution containing boron and activators (Na_2O, ZrO_2, NaCl, SiC, Potassium, Lithium, etc.) such as boric acid or borax, onto the material that serves as the cathode (Alparslan, 2011).

The boronizing process performed with this technique can be performed in 0.5-6 hours at a temperature range of 600-1000 °C and at a current density of 0.15-0.7 A/cm^2. While very thin coatings can be obtained in low-alloy steels with high current in a short time, high-alloy steels require low current density and long-term boronizing process to obtain a thick coating layer. The main electrolyte components used during the process are borax and boric acid, and because of the research, B_2O_3+MOH, B_2O_3+MF, B_2O_3+M_2CO_3 (M=Li, Na, K) compositions have also been developed to reduce the corrosive feature (G. Kartal, 2004).

5.3. Gas Environment Boriding

In this technique, where organic boron compounds, diborane, and boron halides are used, the diffusion of boron to the surface of the material is done by gas circulation. Its most important advantage is that uniform boron distribution can be achieved because of circulation. Another advantage of this boronizing technique is that a single-phase boride layer is obtained due to the control of boron potential. The pressure of the gas, the flow rate, and the composition of the gas environment are the most important parameters of the gas environment boronizing process.

If we look at the disadvantages of the technique, special devices are required to work with boronizing compounds in this method. Diborane, although it is the basic compound, is poisonous and very expensive, even compared to hydrogen. Boron halides can cause corrosion. Carburization is the case in boronizing made with triethylboron and trimethylboron due to their high carbon content (Gülsün, 2016).

5.4. Plasma Boriding

For many years, studies have been carried out to reduce the temperature and duration of the boriding process. According to the studies, it has been shown that these parameters can be reduced by ion implantation boriding, and plasma boriding processes. The plasma boriding process has superior advantages over traditional boriding processes. In this method, thanks to the use of less energy, the boriding process can be carried out at low temperatures, and shape distortions are minimized. The plasma boriding process can use Ar, H_2 gases and boron compounds such as BCl3, B_2H_6 at low temperatures such as 600 ℃, which is not possible with other boriding methods (Sinha, 1991). In addition, since the gas mixture ratios can be controlled, the amount of FeB can be reduced, and the formation of a single-layer Fe_2B layer can be made possible. The disadvantage of the plasma boriding technique can be shown as the gases (BCl_3, B_2H_6) used in boriding being toxic, explosive, and expensive. Another disadvantage is that the boride layer is porous in the boronizing process carried out in a BCl_3 environment (I., U. S., & T. S. Guneş, 2011). The disadvantages in plasma and gas boronizing processes can be eliminated with the plasma paste boronizing method. The paste used in this process consists of boron minerals that are harmless to the environment, and the gases generally have inert properties such as hydrogen, argon, and nitrogen (I. Guneş, 2013).

REFERENCES

Albayrak, M. G. (2021). *Düşük karbonlu Yüksek Mukavemetli Çeliklerde Borlama.* Elazığ: Doktora Tezi, Fırat Üniversitesi, Fen Bilimleri Enstitüsü,.

Allaoui, O. , B. N. , & S. G. (2006). Characterization of Borinezed Layers on a XC38 Steel. *Surface and Coatings Technology, , 201(6),* 3475–3482.

Alparslan, E. (2011). *Tekstil Endüstrisinde Borlama Uygulamaları.* Isparta: Süleyman Demirel Üniversitesi, Fen Bilimleri Enstitüsü, .

Aydoğmuş, T. (2019). *Tungsten Karbür Kesici Takımların Borlanması ve Karakterizasyonu.* Eskişehir: Doktora Tezi, Eskişehir Osmangazi Üniversitesi, Fen Bilimleri Enstitüsü, .

Bolat, Ç. (2016). *Orta Karbonlu DIN CK45 Çeliğinin Elektrokimyasal Yöntemle Borlanması*. İstanbul: Yüksek Lisans Tezi, İstanbul Teknik Üniversitesi, Fen Bilimleri Enstitüsü,.

Bora, A. B. (2017). *laşımsız Düşük Karbonlu Yassı Mamullerin Elektrokimyasal Olarak Borlanması ve Borlama İşleminin Mekanik Özelliklere Etkisi.* . İstanbul: Yüksek Lisans Tezi, İstanbul Teknik Üniversitesi, Fen Bilimleri Enstitüsü, .

BOREN. (2025). *Bor Araştırma Enstitüsü*.

Çelikyürek, Ġ. , B. B. , G. R. ,. (2004). Küresel Grafitli Dökme Demirlerin Borlanması. Eskişehir.: II. Uluslararası Bor Sempozyumu.

Cimenoğlu, H. , A. E. , & M. A. (2014). High Temparature Tribological Behaviour of Borided Surfaces Based on the

Phase Structure of the Boride Layer. In *Wear* (Vol. 309(1–2), pp. 152–158).

Ertürk, L. (2018). *Titanyum Alaşımlarının Borlama Yöntemi ile Yüzey Kalitesinin İyileştirilmesi.* . Sivas: Yüksek Lisans Tezi, Cumhuriyet Üniversitesi, Fen Bilimleri Enstitüsü, .

Gülsün, K. (2016). *Yüzey Borlanmış ve Farklı Matriks Yapılı Küresel Grafitli Dökme Demirin Aşınma Özelliklerinin İncelenmesi.* . Balıkesir: Yüksek Lisans Tezi, Balıkesir Üniversitesi, Fen Bilimleri Enstitüsü,.

Güner, R. (2023). *AISI 1020 çeliğinin elektrokimyasal olarak borlanması ve borlama işleminin darbeli kayma aşınma davranışına etkisi* . Bilecik: Bilecik Şeyh Edebali Üniversitesi, Lisansüstü Eğitim Enstitüsü.

Guneş, I. (2013). Wear Behaviour of Plasma Paste Boronized of AISI 8620 Steel with Borax and B2O3 Paste Mixtures. . *J. Mater. Sci. Technol., 29(7),* 662–668.

Guneş, I. , U. S. , & T. S. (2011). Plasma Paste Boronizing of AISI 8620, 52100 and 440C Steels. . *Meterials and Design, 32,* 2380–2386.

Hernández-Sánchez, E. , & V. J. C. (2018). Kinetics of growth of iron boride layers on a low-carbon steel surface. *In Laboratory Unit Operations and Experimental Methods in Chemical Engineering.* .

Karaman, Y. ,. (2003). *Endüstriyel Borlama ve Tekstil Endüstrisinde Bir Uygulama*. Isparta: Y.Lisans Tezi, Süleyman Demirel Ü. Fen Bil. Ens.,.

Kartal, G. (2004). *Ergimiş Tuz Elektroliz Yöntemiyle Çeliklerin Borlanması Proses Parametrelerinin Optimizasyonu.* . İstanbul: Yüksek Lisans Tezi, İstanbul Teknik Üniversitesi, Fen Bilimleri Enstitüsü,.

Kartal, G. , T. S. , S. V. , E. O. L. , & E. A. (2011). The Growth of Single Fe2B Phase on Low Carbon Steel Via Phase Homogenization in Electrochemical Boriding (PHEB). *Surface and Coatings Technology*, *206(7)*, 2005–2011.

Kondul, B. (2020). *Borlama İle Yüzeyi Sertleştirilmiş Ray Çeliğinin Aşınma davranışının İncelenmesi.* . Karabük: Yüksek Lisans Tezi, Karabük Üniversitesi, Lisansüstü Eğitim Enstitüsü,.

Kutucu, Y. K. (2013). *Yüksek Alaşımlı Çeliklerin Borlanması Sonucunda Oluşan Isıl Artık Gerilmelerin İncelenmesi.* Sakarya: Yüksek Lisans Tezi, Sakarya Üniversitesi, Fen Bilimleri Enstitüsü,.

Martini, C. , P. G. , P. G. , & P. D. (2004). Slinding and Abrasive Wear Behaviour of Boride Coatings. *Wear*, *256(6)*, 608–613.

Matuschka, A. G. (1980). Boronizing. *Heyden*, 11–45.

Mindivan, H. (2023). High-Temparature Wear and Oxidation Behaviour of Electrochemically Borided Low Carbon Steel. *Journal of the Faculty of Engineering and Architecture of Gazi University*, *38(2)*, 937–945.

Mu, D. , & S. B. (2013). The Kinetics and Dry-Sliding Wear Properties of Boronized Gray Cast Iron. *Hindawi Publishing Corparation Advances in Materials Science and Engineering*,.

Oliveira, C. K. N. , C. L. C. , N. A. L. , T. G. E. , & H. S. C. (2010). Production and Characterization of Boride Layers on AISI D2 Tool Steel. *Vacuum*, *84/6)*, 792–796.

Ozbek, I. , S. S. , I. M. , B. C. , Z. S. , & U. A. H. (2004). A Mechanical Aspect of Borides Formed on the AISI 440C Stainless-Steel. . *Vacumm*, *73*, 643–648.

Ozdemir, O. , U. M. , B. C. , & U. A. H. (2006). Hard Iron Boride (Fe2B) on 99.97 wt% Pure Iron. *Vacuum*, *80*, 1391–1395.

Özer, M. (2011). *Üç farklı çeliğe katı borlama işlemi yapılmasının içyapı ve sertlik üzerine etkisinin incelenmesi*.

Özsoy, A. ,. (1991). *Çeliğin Borlanmasında Borür Tabakası, Geçiş Zonu ve Ana Matriksin Özelliklerinin iyileştirilmesi*. Eskişehir: Doktora Tezi, Anadolu Ü. Fen Bil. Ens.,.

Öztürk, K. (2021). *Plastik Kalıp Çeliklerinin Korozyona Karşı Korunmasında Kutu Borlama İşleminin Etkileri.* . İzmir: Yüksek Lisans Tezi, Dokuz Eylül Üniversitesi, Fen Bilimleri Enstitüsü,.

Saygın, M. (2006). *AISI 1020 Çeliklerinde Borlamanın Yorulma Dayanımına Etkisi.* . Eskişehir: Yüksek Lisans Tezi, Osmangazi Üniversitesi, Fen Bilimleri Enstitüsü, .

Sinha, A. K. (1991). Boriding (Boronizing) of Steel. In *ASM Handbook* (Vol. 4, pp. 978–1000).

Sista, V. , K. O. , E. O. L. , E. A. , & T. B. (2011). Electrochemical Boriding and Characterization of AISI D2 Tool Steel. . *Thin Solid Films*, *520(5)*, 1582–1588.

Spence, T. W. , & M. M. M. (2005). Characterization of the Operative Mechanism in Potassium Fluoborate Activated Pack Boriding of Steels. . *Journal of Materials Processing Technology, , 168(1)*, 127–136.

Toktaş, G. , T. A. , & G. K. (2017). Effect of Matrix Structure and Boriding Time on the Wear Behaviour of Cu-Ni-Mo Alloyed Ductile Iron. *Journal of the Faculty of Engineering and Architecture of Gazi University*, *32(2)*, 449–457.

Topuz, P. (2009). *Akışkan Yataklı Fırında Farklı Çeliklerin Borlanması ve Borlama Parametrelerinin Geliştirilmesi.* İstanbul: Doktora Tezi, Marmara Üniversitesi, Fen Bilimleri Enstitüsü,.

Topuz, P. , A. Ö. , A. T. , & Ç. B. (2020). Borlanmış AISI 316 Üzerinde Oluşmuş FexB Tabakalarının Kırılma Tokluklarının İncelenmesi. . *Journal of Steel Research and Development,* 12–16.

Türkmen, İ. , & Y. E. (2018). Growth of the Fe2B Layer on SAE 1020 Steel Employed a Boron Source of H3BO3 During the Powder-Pack Boriding Method. *Journal of Alloys and Compounds , 744,* 658–666.

Ünal, F. (2013). *Cam Kalıplarında Kullanılan Küresel Grafitli Dökme Demirlerin (KGDD) Borlanması.* . İstanbul: Yüksek Lisans Tezi, Yıldız Teknik Üniversitesi, Fen Bilimleri Enstitüsü,.

Varol R. (2000). *Malzeme Bilgisi ve Muayenesi*. Isparta.

Yamanel, B. (2018). *Farklı Sıcaklıklarda Menevişlenmiş ve Borlama İşlemine Tabi Tutulmuş SAE 5140 Çeliğinin Mekanik ve Tribolojik Özelliklerinin İncelenmesi.* Kırıkkale: Yüksek Lisans Tezi, Kırıkkale Üniversitesi, Fen Bilimleri Enstitüsü,.

Yu, L. G. , C. X. J. , K. K. A. , & S. G. (2005). FeB/Fe2B Phase Transformation During SPS Pack Boriding: Boride Layer Growth Kinetics. *Acta Materialia, 53(8),* 2361–2368.

ADDITIVE MANUFACTURING OF TUNGSTEN CARBIDE CUTTING TOOLS: THEORETICAL FUNDAMENTALS AND TECHNOLOGICAL APPROACHES[1]

Tevfik Oğuzhan ERGÜDER[2]

1. INTRODUCTION

Today, the acceleration of technological advances and the increase in global population have significantly increased the demand for industrial products. In parallel, the increase in raw material, energy and labor costs directly affects the total costs of production systems and machines. As a result, users now expect longer service life and higher performance from high-cost products (Kalpakjian & Schmid, 2006; Šubić et al., 2022).

Advancements in engineering and manufacturing technologies have transformed production processes and driven demand for materials with high mechanical strength and wear resistance. Accordingly, tribological properties that ensure long service life and sufficient mechanical strength—particularly in cutting tool materials—have gained increasing importance (Trent & Wright, 2000).

---

[1] This study is derived from the master's thesis. Ergüder, Tevfik Oğuzhan. "Investigation of Structural, Tribological And Machining Performances of Tungsten Carbide Cutting Tools with Nickel Binder Produced by Selective Laser Melting Method". Erzurum Technical University, Graduate School of Natural and Applied Sciences, Department of Mechanical Engineering, Erzurum.

[2] Assistant Professor, Kafkas University, Faculty of Engineering and Architecture, Department of Mechanical Engineering, oguzhan.erguder@kafkas.edu.tr, ORCID: 0000-0002-8876-6152.

Cutting tools are divided into various classes according to their chemical composition, microstructure, manufacturing technique and mechanical-physical properties. Cutting tool materials commonly used in the machining industry include high speed steels (HSS), sintered carbides, cermets, diamond and cubic boron nitride (CBN) (Groover, 2010).

Cemented carbides are generally based on tungsten carbide (WC). WC-based cutting tools are widely preferred due to their superior performance in machining applications. The exceptional properties of WC—such as high hardness, wear resistance, and thermal stability—make it indispensable in both conventional and modern manufacturing processes (Dandekar & Shin, 2012). In order to increase the toughness of these structures, certain amounts of binder metals (Co, Ni, Cu, etc.) are added. The WC offers a hardness value of approximately 22 GPa and can maintain this property up to a temperature of 800 °C (Upadhyaya, 1998). For this reason, sintered carbides have a wide range of uses, especially in cutting tool and mold manufacturing. They can also preferred in other engineering applications that require high wear resistance.

2. PRODUCTION OF TRADITIONAL CARBIDE TOOLS AND THE NEED FOR TRANSITION TO ADDITIVE MANUFACTURING

The production of cemented carbide tools is a multi-stage process based on powder metallurgy and involving many processing steps (Figure 1) (Chen et al., 2019; Ku et al., 2019; K. Liu & Li, 2001; Upadhyaya, 1998). In the first stage of the production process, pure metal powders are obtained by reducing W, Ti and Ta oxides. These powders are converted into carbide form by reacting with carbon. Then, the carbide powders are mixed with binder metals such as Co or Ni and turned into

homogeneous granules by grinding. Then, the obtained granules are pressed under high pressure and shaped and structural stability is provided by pre-sintering. Pressed parts are subjected to a sintering process at a temperature range of 1400-1600 °C in order to gain their final mechanical properties. In the last stage, the products are brought to the desired geometric tolerances by precision grinding and ceramic coatings are applied by PVD or CVD methods to increase wear resistance. As a result of all these processes, the products are ready for use.

Figure 1. Traditional manufacturing of cemented carbide tools

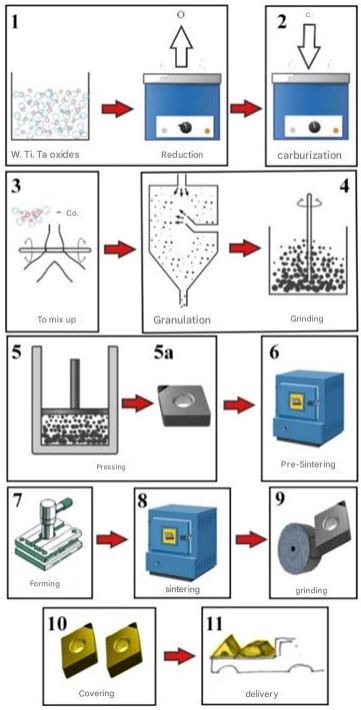

Reference: (Šubić et al., 2022)

Today, the production of cemented carbide cutting tools is largely carried out by traditional manufacturing methods. These methods are effective for manufacturing parts with high mechanical strength. However, these methods offer limited geometric flexibility and involve multi-stage, time-consuming

and costly processes. In particular, special cutting tool designs with internal contours, free-form cutting inserts and customized tool geometries are quite difficult to produce with these methods and require high costs (Groover, 2010; Herzog et al., 2016). Preforming of carbide materials is generally carried out by pressing in the form of a disk, and advanced cutting and processing techniques are required to obtain the target geometry. Integrating cooling channels into tools with traditional manufacturing methods presents significant limitations due to high initial costs and limited design flexibility. As a result, manufacturers are shifting toward more flexible and customizable production technologies. Additive manufacturing offers a direct way to transform digital tool designs into physical products, addressing the limitations of conventional methods. Specifically, for WC-based tools, this technology offers significant potential, especially in terms of low-volume, customized production and the production of complex geometries. In addition, thanks to near-net-shape production, material waste is reduced and production efficiency is increased (Uhlmann et al., 2015).

Literature studies show that powder bed based additive manufacturing systems, especially Selective Laser Melting (SLM), are increasingly being investigated for WC matrix composites. Optimization of laser parameters, improvement of binder distribution and prevention of crack formation are among the current research areas.

3. ADDITIVE MANUFACTURING TECHNOLOGIES AND SELECTIVE LASER MELTING METHOD

Additive manufacturing is a flexible technology that produces parts by depositing material layer by layer based on computer-aided design (Bourell & Wohlers, 2020). This method,

which allows the production of complex geometries with high precision without requiring molds or special tools (Huang et al., 2015), can be applied to many material classes, especially metals, ceramics and polymers. This technology, which was first used in the production of polymer-based objects in the 1980s, is now widely preferred for the manufacture of lightweight and unique parts in fields such as aviation and automotive (Lim et al., 2016). Although there are some limitations such as product quality, production speed and part size, it is aimed to overcome these difficulties thanks to the developing software and hardware infrastructures (Mhetre et al., 2022). The production process begins with the conversion of the model created with 3D CAD software to STL format and then separation into layers using 'slicer' software; the final form is created by adding each layer on top of each other at a certain thickness. The ability to produce complex geometries in a single step without the need for additional processing makes the process both time efficient and reduces production costs (Peleg, 2020).

The SLM method, which is among the additive manufacturing methods and allows the production of metallic materials with high precision, is based on the principle of laser melting of metal powders and thus enables the production of complex, high-performance parts. This method, the schematic representation of which is presented in Figure 2, is based on the layer-by-layer melting of metal or ceramic powders using a high-power laser. The production of ceramic materials such as WC is quite challenging due to their high melting temperatures and brittle structure. For this reason, WC powders are usually combined with binder metals and included in the production process. Powders between 30 and 200 μm are generally used and the powder is completely melted and rapidly solidified with the energy provided by the laser (Gu et al., 2012). However, this rapid thermal cycle can cause residual stresses in the part during

production. These problems can be reduced by keeping the temperature of the production platform high and by applying heat and surface treatments after production (Mercelis & Kruth, 2006; Mezzetta, 2017).

Figure 2. Schematic representation of the SLM method

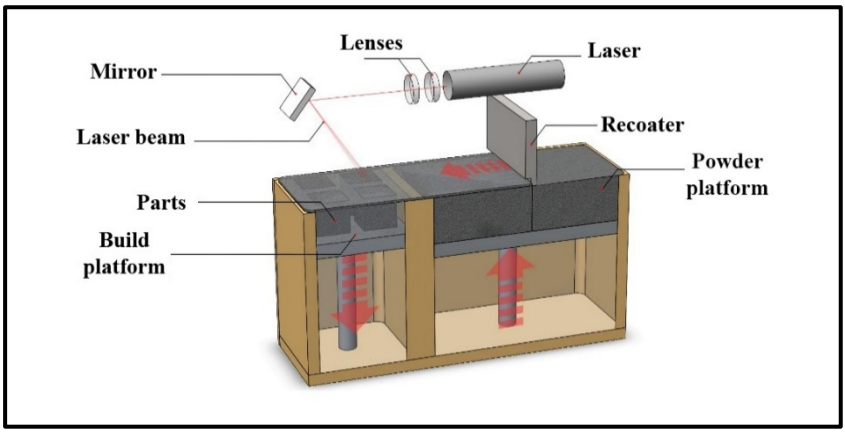

SLM is especially preferred for the production of complex geometries without molds and with minimum material loss. The production process proceeds with a cycle of layered powder laying, laser melting and powder laying again. Production is carried out in an inert gas environment to prevent oxidation. Parameters such as laser power, scanning speed, layer thickness and side slip distance have a direct effect on the microstructure and mechanical properties of the part. Therefore, determining the optimum production conditions is of critical importance (Bulut et al., 2024; Thijs et al., 2010).

4. PRODUCTION OF TUNGSTEN CARBIDE BASED CUTTING TOOLS BY ADDITIVE MANUFACTURING

Studies on laser additive manufacturing of WC-based materials are relatively scarce in the literature, with existing

research primarily focusing on WC-Co compositions using varying ratios of Co as a binder. The prevailing approach in these studies involves mixing WC powder with Co. Research by Kumar (2009), Uhlmann et al. (2015), (Enneti et al., 2018), Ku et al. (2019), Chen et al. (2019), Liu et al. (2020) and Liu et al. (2021) has examined factors such as microstructure, density, hardness, and grain growth. The results obtained in these studies have shown that the production parameters, especially laser power, scanning speed and strategy, play a critical role on the microstructure and mechanical properties. However, in these approaches, mixture of WC powder with the binder has some limitations in terms of homogeneous powder distribution and fluidity. Therefore, the use of WC powder by pre-coating it with metallic binders (Co, Ni, stainless steel, etc.) both improves the rheological behavior of the powder and ensures homogeneous distribution of the binder. Although this method is common in traditional powder metallurgy applications, studies on its integrated use with SLM are limited. Studies by Gu & Meiners, (2010), Davydova et al. (2016), Domashenkov et al. (2017), (Khmyrov et al. (2017), Cavaleiro et al. (2018), Grigoriev et al. (2019), Campanelli et al. (2019) and Ergüder et al. (2024) have provided detailed analyses of microstructure evolution, new phase formation, and hardness effects when using coated WC powders in additive manufacturing.

As a result, although studies on the production of WC-based hard materials by laser additive manufacturing are increasing, the literature on the use of binder-coated powders in this process is still open to development. This method offers significant potential for future studies in terms of microstructure control and production efficiency. At this point, studies carried out especially for the purpose of cutting tool production have a special importance. In the study conducted by Fortunato et al. (2019), the SLM method was used for the production of gear

cutting tools from WC-Co powders and then it was aimed to increase the density and toughness of the parts by applying HIP. In the study, the effects of powder size and chemical composition on the production process were evaluated for both the main structure and the support structures. In addition, cylindrical samples were produced using different laser parameters and scanning paths and their performances were tested. Especially thanks to the application of multiple scanning strategies, crack formation was reduced and parts with high density were obtained. Similarly, in the study conducted by Ergüder et al. (2025), turning inserts were produced by the SLM method using nickel-coated WC powders by electroless coating method. By applying surface grinding and TiN coating after production, the performance of the tips was improved and the tips obtained showed similar wear resistance compared to the products produced by the traditional method.

5. CONCLUSION AND FUTURE PERSPECTIVES

The applicability of additive manufacturing technologies to WC-based cutting tools has a strong potential both theoretically and practically. The literature evaluated in this study shows that additive manufacturing processes can be a serious alternative to traditional production methods if they are managed correctly and powder preparation is well optimized.

Successful examples have been presented in terms of performance criteria such as high hardness, low wear rate, homogeneous microstructure and surface integrity. However, there are still some problems to be solved:

- In-process monitoring systems to prevent crack formation,

- Specially developed forms of WC powders for additive manufacturing,
- Investigation of multiple combinations of binder systems,
- Integration of post-production heat treatment and coating methods.

In future studies, the integration of advanced technologies such as functional gradient structures (FGM), nano-reinforced WC systems, artificial intelligence-supported process optimization and real-time production control will increase the efficiency in this area. At the same time, the use of energy-efficient laser systems and recyclable powders is also gaining importance in terms of environmental sustainability.

As a result, the production of WC-based cutting tools through additive manufacturing stands out as an innovative and strategic production alternative that can find a response not only for research laboratories but also in industrial applications.

REFERENCES

Bourell, D., & Wohlers, T. (2020). Introduction to additive manufacturing. In *Additive Manufacturing Processes* (Vol. 24). ASM International.

Bulut, C., Yıldız, F., Varol, T., Kaya, G., & Ergüder, T. O. (2024). Effects of selective laser melting process parameters on structural, mechanical, tribological and corrosion properties of CoCrFeMnNi high entropy alloy. *Metals and Materials International*, *0123456789*. https://doi.org/10.1007/s12540-024-01694-w

Campanelli, S. L., Contuzzi, N., Posa, P., & Angelastro, A. (2019). Printability and Microstructure of Selective Laser Melting of WC/Co/Cr Powder. In *Materials* (Vol. 12, Issue 15). https://doi.org/10.3390/ma12152397

Cavaleiro, A. J., Fernandes, C. M., Farinha, A. R., Gestel, C. V., Jhabvala, J., Boillat, E., Senos, A. M. R., & Vieira, M. T. (2018). The role of nanocrystalline binder metallic coating into WC after additive manufacturing. *Applied Surface Science*, *427*, 131–138. https://doi.org/10.1016/j.apsusc.2017.08.039

Chen, Huang, M., Fang, Z. Z., Koopman, M., Liu, W., Deng, X., Zhao, Z., Chen, S., Wu, S., Liu, J., Qi, W., & Wang, Z. (2019). Microstructure analysis of high density WC-Co composite prepared by one step selective laser melting. *International Journal of Refractory Metals and Hard Materials*, *84*(June), 104980. https://doi.org/10.1016/j.ijrmhm.2019.104980

Dandekar, C. R., & Shin, Y. C. (2012). Modeling of machining of composite materials: A review. *International Journal of Machine Tools and Manufacture*, *57*, 102–121.

Davydova, A., Domashenkov, A., Sova, A., Movtchan, I.,

Bertrand, P., Desplanques, B., Peillon, N., Saunier, S., Desrayaud, C., Bucher, S., & Iacob, C. (2016). Selective laser melting of boron carbide particles coated by a cobalt-based metal layer. *Journal of Materials Processing Technology*, *229*, 361–366. https://doi.org/https://doi.org/10.1016/j.jmatprotec.2015.09.033

Domashenkov, A., Borbély, A., & Smurov, I. (2017). Structural modifications of WC/Co nanophased and conventional powders processed by selective laser melting. *Materials and Manufacturing Processes*, *32*(1), 93–100. https://doi.org/10.1080/10426914.2016.1176195

Enneti, R. K., Prough, K. C., Wolfe, T. A., Klein, A., Studley, N., & Trasorras, J. L. (2018). Sintering of WC-12%Co processed by binder jet 3D printing (BJ3DP) technology. *International Journal of Refractory Metals and Hard Materials*, *71*(October 2017), 28–35. https://doi.org/10.1016/j.ijrmhm.2017.10.023

Ergüder, T. O., Güler, O., & Yıldız, F. (2024). Determination of selective laser melting process parameters of tungsten carbide powders coated with nickel via electroless plating for improved interface properties. *International Journal of Refractory Metals and Hard Materials*, *122*, 106735. https://doi.org/https://doi.org/10.1016/j.ijrmhm.2024.106735

Ergüder, T. O., Yıldız, F., Güler, O., Sevim, M. İ., & Varol, T. (2025). Development of cutting tools with selective laser melting from electroless nickel-coated tungsten carbide powder material. *International Journal of Refractory Metals and Hard Materials*, *130*, 107169.

Fortunato, A., Valli, G., Liverani, E., & Ascari, A. (2019). Additive manufacturing of WC-Co cutting tools for gear

production. *Lasers in Manufacturing and Materials Processing*, *6*(3), 247–262. https://doi.org/10.1007/s40516-019-00092-0

Grigoriev, S., Tarasova, T., Gusarov, A., Khmyrov, R., & Egorov, S. (2019). Possibilities of manufacturing products from cermet compositions using nanoscale powders by additive manufacturing methods. In *Materials* (Vol. 12, Issue 20). https://doi.org/10.3390/ma12203425

Groover, M. P. (2010). *Fundamentals of modern manufacturing: materials, processes, and systems*. John Wiley & Sons.

Gu, D. D., Meiners, W., Wissenbach, K., & Poprawe, R. (2012). Laser additive manufacturing of metallic components: materials, processes and mechanisms. *International Materials Reviews*, *57*(3), 133–164.

Gu, D., & Meiners, W. (2010). Microstructure characteristics and formation mechanisms of in situ WC cemented carbide based hardmetals prepared by Selective Laser Melting. *Materials Science and Engineering A*, *527*(29–30), 7585–7592. https://doi.org/10.1016/j.msea.2010.08.075

Herzog, D., Seyda, V., Wycisk, E., & Emmelmann, C. (2016). Additive manufacturing of metals. *Acta Materialia*, *117*, 371–392.

Huang, Q., Liu, X., Yang, X., Zhang, R., Shen, Z., & Feng, Q. (2015). Specific heat treatment of selective laser melted Ti–6Al–4V for biomedical applications. *Frontiers of Materials Science*, *9*(4), 373–381. https://doi.org/10.1007/s11706-015-0315-7

Kalpakjian, S., & Schmid, S. (2006). *Manufacturing, engineering and technology SI 6th edition-serope kalpakjian and stephen schmid: manufacturing, engineering and technology*. Digital Designs.

Khmyrov, R. S., Safronov, V. A., & Gusarov, A. V. (2017). Synthesis of nanostructured WC-Co hardmetal by selective laser melting. *Procedia IUTAM*, *23*, 114–119. https://doi.org/https://doi.org/10.1016/j.piutam.2017.06.011

Ku, N., Pittari, J. J., Kilczewski, S., & Kudzal, A. (2019). Additive manufacturing of cemented Tungsten Carbide with a cobalt-free alloy binder by selective laser melting for high-hardness applications. *Jom*, *71*(4), 1535–1542. https://doi.org/10.1007/s11837-019-03366-2

Kumar, S. (2009). Manufacturing of WC-Co moulds using SLS machine. *Journal of Materials Processing Technology*, *209*(8), 3840–3848. https://doi.org/10.1016/j.jmatprotec.2008.08.037

Lim, C. W. J., Le, K. Q., Lu, Q., & Wong, C. H. (2016). An overview of 3-D printing in manufacturing, aerospace, and automotive industries. *IEEE Potentials*, *35*(4), 18–22.

Liu, J., Chen, J., Liu, B., Lu, Y., Wu, S., Deng, X., Lu, Z., Xie, Z., Liu, W., Liu, J., Wang, Z., & Qu, Z. (2020). Microstructure evolution of WC-20Co cemented carbide during direct selective laser melting. *Powder Metallurgy*, *63*(5), 359–366. https://doi.org/10.1080/00325899.2020.1815996

Liu, J., Chen, J., Zhou, L., Liu, B., Lu, Y., Wu, S. H., Deng, X., Lu, Z., Xie, Z., Liu, W., Liu, J., & Qu, Z. (2021). Role of Co content on densification and microstructure of WC–Co cemented carbides prepared by selective laser melting. *Acta Metallurgica Sinica (English Letters)*, *34*, 1245–1254.

Liu, K., & Li, X. P. (2001). Ductile cutting of tungsten carbide. *Journal of Materials Processing Technology*, *113*(1–3),

348–354. https://doi.org/10.1016/S0924-0136(01)00582-9

Mercelis, P., & Kruth, J. (2006). Residual stresses in selective laser sintering and selective laser melting. *Rapid Prototyping Journal*, *12*(5), 254–265.

Mezzetta, J. (2017). *Process-property relationships of Ti6Al4V fabricated through selective laser melting*. McGill University (Canada).

Mhetre, G. N., Jadhav, V. S., Deshmukh, S. P., & Thakar, C. M. (2022). A review on additive manufacturing technology. *ECS Transactions*, *107*(1), 15355.

Peleg, J. (2020). Additive and traditionally manufactured components a comparative analysis of mechanical properties. In *Additive and Traditionally Manufactured Components*. https://doi.org/10.1016/c2019-0-04180-5

Šubić, J., Slokar Benić, L., Selanec, M., & Erman, Ž. (2022). Effect of hard metal production on the environment. *Holistic Approach to Environment*, *12*(3), 102–109. https://doi.org/10.33765/thate.12.3.2

Thijs, L., Verhaeghe, F., Craeghs, T., Humbeeck, J. Van, & Kruth, J. P. (2010). A study of the microstructural evolution during selective laser melting of Ti-6Al-4V. *Acta Materialia*, *58*(9), 3303–3312. https://doi.org/10.1016/j.actamat.2010.02.004

Trent, E. M., & Wright, P. K. (2000). *Metal cutting*. Butterworth-Heinemann.

Uhlmann, E., Bergmann, A., & Gridin, W. (2015). Investigation on additive manufacturing of Tungsten Carbide-cobalt by selective laser melting. *Procedia CIRP*, *35*, 8–15. https://doi.org/10.1016/j.procir.2015.08.060

Upadhyaya, G. S. (1998). *Cemented tungsten carbides: production, properties and testing*. William Andrew.

EFFECT OF CARBON-BASED AND CERAMIC-BASED NANO-MATERIALS ON BALLISTIC BEHAVIOURS OF FIBER-REINFORCED POLYMER COMPOSITE ARMOURS

Ege Anıl DİLER[1]

Fatih BALIKOĞLU[2]

1. INTRODUCTION

The continuous effort to improve protection against kinetic threats has been a primary objectives in engineering. From the earliest forms of defensive gear, like rudimentary shields and woven chainmail, to the sophisticated multi-layered composite armours of today, the goal remains steadfast: to effectively dissipate, deflect, or absorb incident kinetic energy to minimize harm to personnel or critical assets. Conventional armour systems, while undoubtedly effective within their established design parameters, frequently encounter inherent compromises. These trade-offs are particularly evident in the delicate balance required between the levels of protection offered, the areal density of the material, its ergonomic flexibility, and overall manufacturing cost. For instance, achieving superior protective capabilities often necessitates increasing the thickness and density of the material. This leads to heavier, more cumbersome solutions that can significantly impede mobility, increase

[1] Assoc. Prof. Dr., Ege University, Faculty of Engineering, Department of Mechanical Engineering, ege.anil.diler@ege.edu.tr, ORCID: 0000-0002-1667-5737.

[2] Assoc. Prof. Dr., Balıkesir University, Faculty of Engineering, Department of Mechanical Engineering, fatih.balikoglu@balikesir.edu.tr, ORCID: 0000-0003-3836-5569.

logistical burdens, and reduce operational effectiveness across diverse applications, ranging from individual soldier protective equipment to advanced aerospace and vehicular platforms.

In recent decades, the burgeoning field of nanotechnology has emerged as a truly pioneering frontier in material design. It offers unprecedented opportunities to manipulate and engineer matter at its most fundamental level, the atomic and molecular scales. Nano-materials exhibit extraordinary physical, chemical, and mechanical properties that frequently deviate profoundly and advantageously from those observed in their bulk counterparts. These unique attributes are rooted in several key factors: their exceptionally high surface-area-to-volume ratio, the manifestation of quantum mechanical effects at these scales, and the potential for novel crystallographic or molecular architectures that are unattainable in larger forms. Consequently, the judicious and precise integration of these exquisite nanoscale building blocks into existing or entirely novel material systems presents a compelling and revolutionary pathway to overcome the intrinsic limitations of traditional engineering materials and push the boundaries of protective technology.

This chapter presents the profound impact of nano-materials on the ballistic performance of armours. The strategic incorporation of various nanostructures enhances critical material properties. These enhancements include, but are not limited to, significant improvements in tensile strength, fracture toughness, specific energy absorption capacity, and overall impact resistance. This study will directly link the intricate fundamental mechanisms driving these improvements with the specific nano-materials that enable them. This integration will cover everything from the complex processes of enhanced kinetic energy dissipation through tortuous crack pathways and localized shear banding, to the optimization of interfacial adhesion and highly efficient stress distribution at the nanoscale. Furthermore, this

chapter will present specific exemplars of nanomaterial applications across a spectrum of armour types, ranging from advanced lightweight flexible armours designed for personal protection. This will involve a critical examination of pivotal experimental findings and the sophisticated theoretical models that provide the intellectual framework for their enhanced performance. By scrutinizing the advancements in this profoundly interdisciplinary field, this chapter aims to furnish a comprehensive and authoritative overview of potential of nanotechnology to fundamentally revolutionize the future trajectory of protective materials. This will pave the way for the development of armours that are intrinsically lighter, demonstrably stronger, and remarkably more versatile in addressing the multifaceted and evolving ballistic threats of the contemporary operational environment.

2. NANO MATERIALS

The rapidly evolving landscape of nano-materials for armour applications is remarkably diverse, with each class offering unique advantages and tailored functionalities for ballistic protection. These materials augment or fundamentally change the response of conventional armour components by introducing novel energy dissipation and strengthening mechanisms at the nanoscale.

Among various advanced materials, carbon nanotubes (CNTs) and graphene have emerged as highly promising candidates for personal protection applications. Figure 1 illustrates the CNTs and graphene incorporated into armour for ballistic protection of individuals. Extensive research, both experimental and computational, consistently highlights their exceptional mechanical stability, impressive energy absorption capabilities, and remarkable multi-hit resistance under impact

conditions. These properties, combined with their inherent lightweight, resilience, and stiffness, position CNTs and graphene as strong alternatives to traditional materials like aramid and ultra-high molecular weight polyethylene (Sharma et al., 2023).

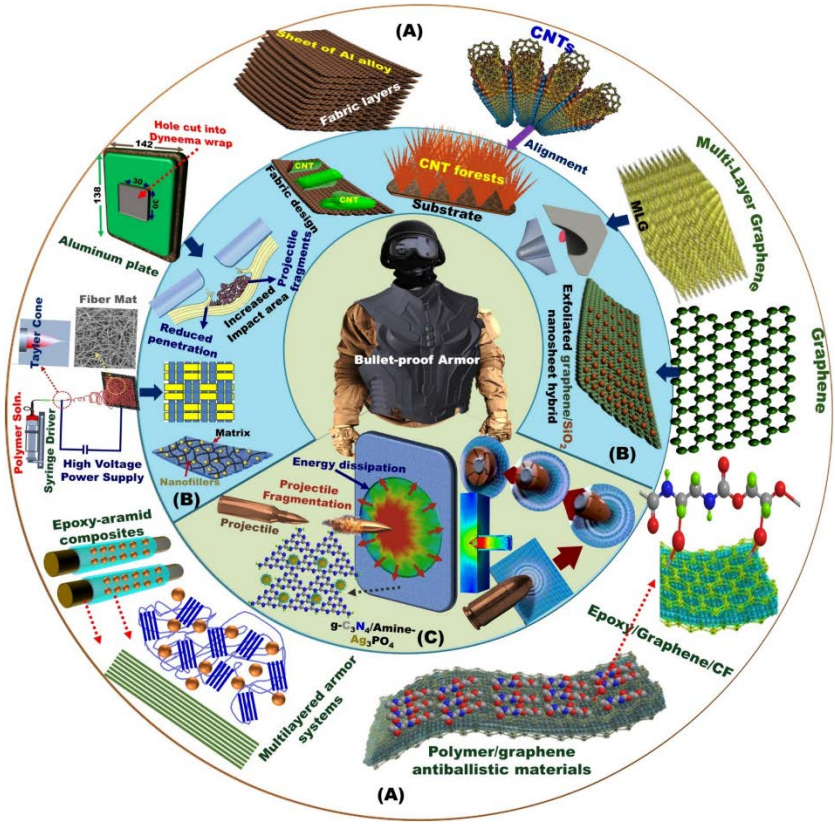

Figure 1. (a) and (b) Conceptual design and foundational elements of anisotropic nanocomposite materials for creating protective clothing, and (c) The energy absorption and dispersion process in anti-ballistic armors, leading to projectile mushrooming against high-velocity threats (Mohamed et al., 2024)

This section aims to elucidate the substantial potential of CNTs and graphene in improving the energy absorption, penetration resistance, and ballistic limits vital for personal armour. Furthermore, the contributions of nano-ceramic materials to advanced ballistic applications will be detailed.

2.1. Carbon-Based Nanomaterials

Carbon, in its various nanoscale allotropes, has catalyzed a revolution in materials science due to its extraordinary mechanical, thermal, and electrical properties, combined with its remarkably low density. These attributes make carbon nano-materials exceptionally attractive for advanced ballistic protection.

Within the realm of carbon-based nano-materials, particular attention has been drawn to two structures for their exceptional promise in enhancing protective materials. The discussion will first examine Carbon Nanotubes (CNTs), detailing their unique architecture and the translation of this into superior ballistic performance. Following this, the focus will turn to Graphene and Graphene Oxide, assessing their distinct properties and the groundbreaking ways they contribute to next-generation armour solutions.

2.1.1. Carbon Nanotubes (CNTs)

Carbon Nanotubes (CNTs), particularly multi-walled carbon nanotubes (MWCNTs) and single-walled carbon nanotubes (SWCNTs), stand out as among the most promising reinforcements or fillers for advanced armours (Srinivasan et al., 2021). With their impressive aspect ratios, remarkable tensile strength, extreme hardness, high stiffness, good ductility, and low density, CNTs hold considerable promise for ballistic applications and in high-strength, high energy-absorption materials (Mylvaganam & Zhang, 2006; Pandya & Naik, 2015). The unique tubular structure of CNTs provides exceptional axial strength and stiffness, while their nanoscale dimensions allow for their seamless integration into various matrices. CNTs are extensively utilized as primary reinforcements in polymer matrix composites (PMCs), forming the backbone of advanced soft and rigid body armours (Figure 2).

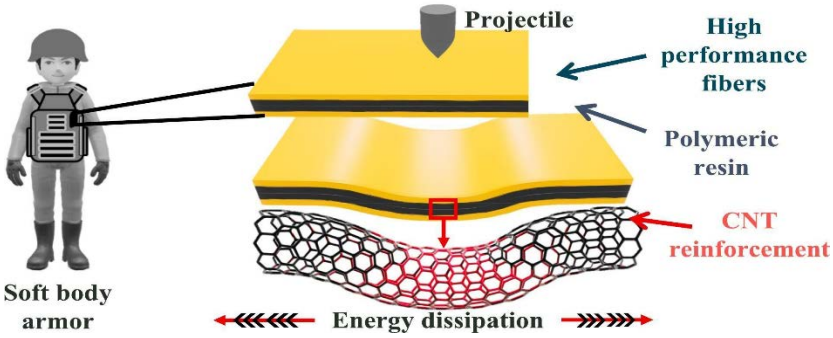

Figure 2. Schematic illustration of carbon nanotube-based soft body armour (Rani et al., 2024)

They have been demonstrably shown to significantly enhance the ballistic limit of high-performance fibre fabrics such as aramid (Kevlar) (Micheli et al., 2016; Nitin & Kumar, 2022) and ultra-high molecular weight polyethylene (UHMWPE) (Kukle et al., 2024).

The incorporation of carbon nanotubes (CNTs) into fibre-reinforced composite materials generally leads to a notable improvement in their ballistic performance, as seen in Figure 3. This enhancement is consistently observed across various impact scenarios and is fundamentally linked to the unique properties of CNTs and their interaction within the composite structure.

Composites containing CNTs exhibit a significantly increased capacity to absorb and dissipate impact energy. This is achieved by converting the kinetic energy of the projectile into various forms of internal energy, such as localized deformation and microstructural damage. This higher energy absorption is often reflected in reduced projectile residual velocities and greater energy absorption percentages compared to unreinforced counterparts.

A critical aspect of the effectiveness of CNT lies in their ability to reinforce the interfaces between the primary fibres and the polymer matrix. When CNTs are effectively dispersed and

chemically bonded, they create connections that enable more efficient transfer and distribution of stress throughout the composite. This means that during an impact, the load is shared across a larger volume of the material, preventing localized stress concentrations that can lead to premature failure.

CNTs contribute to the overall toughness of the composite by acting as a barrier to crack propagation. They can bridge incipient cracks or force them to deflect around the rigid nanotube structures, requiring significantly more energy for the crack to advance (Lubineau, et al., 2024). This toughening effect fundamentally can increase the ballistic performance of the material.

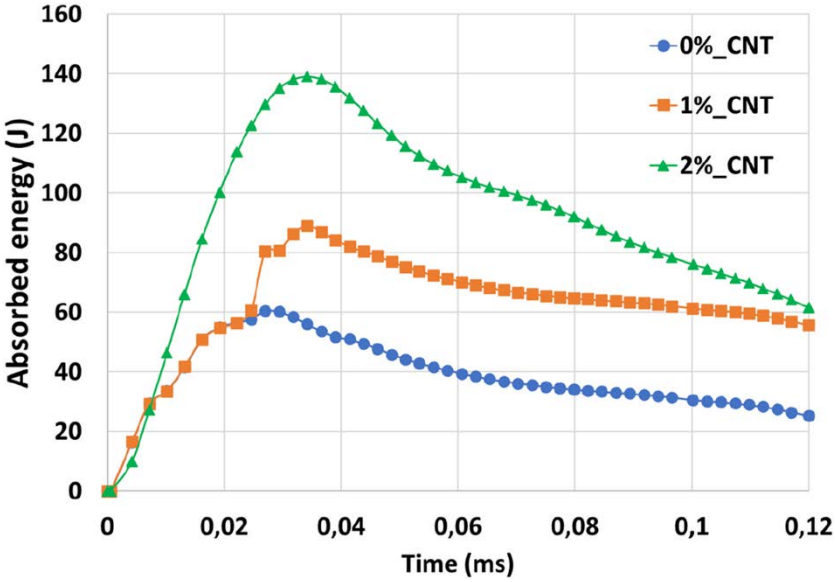

Figure 3. Absorbed energy of CNT-modified fibre-reinforced polymer composite (Namena et al., 2024)

While CNTs are often lauded for their potential to enhance material properties, their actual impact on composite ballistic performance is highly dependent on effective incorporation. Adding CNTs, particularly MWCNTs, does not guarantee improved ballistic performance; in fact, agglomeration of

MWCNTs can lead to a reduction in this property. Figure 4 illustrates the formation of MWCNT agglomerates within the material. These agglomerations, along with the resulting matrix voids, can lead to a reduction in the ballistic performance of the material. (Ravindran et al., 2023). Thus, the dispersion of CNTs within the polymer matrix is crucial. When CNTs, despite their strength, agglomerate, they can introduce significant porosity and act as stress concentration points within the composite. Instead of reinforcing the material, these agglomerates become weaknesses, compromising the ability of the composite to resist impact. This can manifest as decreased energy absorption, greater deformation, and an increased damaged area upon ballistic impact, effectively making the material less protective. Therefore, for CNTs to fulfill their promise in ballistic applications, overcoming the challenge of uniform dispersion and strong interfacial bonding remains a critical engineering imperative. Without it, the very properties that make CNTs attractive can inadvertently lead to performance degradation.

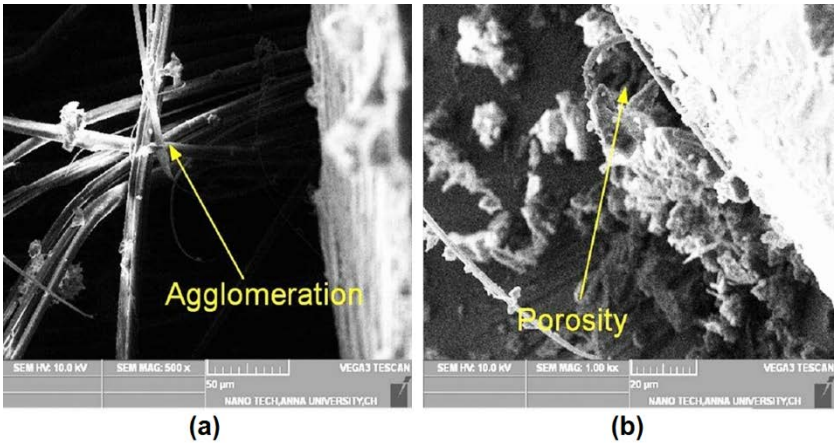

Figure 4. SEM analysis showing (a) CNT agglomerates (clusters) and (b) voids or pores in the matrix of Plain Kevlar and a CNT-reinforced Kevlar epoxy polymer composite (Ravindran et al., 2023)

Ultimately, while CNTs offer exceptional potential for enhancing ballistic performance through superior mechanical properties and improved energy dissipation mechanisms, their efficacy is critically contingent upon achieving uniform dispersion and robust interfacial bonding within the composite matrix, as agglomeration can paradoxically compromise the material's protective capabilities.

2.1.2. Graphene and Graphene-Oxide

Graphene-based materials are other nano-sized carbon-based materials used in ballistic applications (Worku & Ayele, 2023).

Graphene, a single atomic layer of carbon atoms arranged in a hexagonal lattice, is unequivocally the strongest material known to humanity while simultaneously exhibiting remarkable flexibility. Its two-dimensional nature allows for unique interactions. Graphene Oxide (GO), a chemically functionalized derivative of graphene, maintains many of the desirable properties of graphene but offers superior dispersibility and processability, particularly in aqueous solutions and various polymer matrices due to its oxygen-containing functional groups.

Graphene is intensely investigated for their transformative potential in lightweight composite armours (Naven et al., 2021). Due to their prodigious surface area, they further contribute to enhanced energy dissipation capabilities. Adding even small percentages of graphene to fibre-reinforced polymer matrix composites can significantly improve their ballistic limits. Figure 5 shows energy absorption, indicating ballistic performance, of aramid (Twaron) fabric modified with polyethylene (LDPE) and graphene. As seen in Figure 5, the energy absorption capability of aramid (Twaron) fabric-reinforced composite can be improved by modifiying graphene (GR) and LDPE. A critical explanation for the improved ballistic performance is the considerable

increase in inter-yarn friction within the modified fabrics (Cao et al., 2020). The GR/LDPE coatings adhere to the aramid yarns, resulting in more integrated connections between adjacent yarns. This heightened friction necessitates greater energy for a projectile to cause yarn separation or sliding, contributing significantly to the dissipation of the kinetic energy of the projectile. While an increase in friction is generally beneficial, excessive inter-yarn friction can have adverse effects. This explains why the GR/LDPE/aramid fabric, despite incorporating graphene, exhibited slightly weaker ballistic performance than the LDPE-only modified fabric. An overly high friction coefficient may lead to premature fabric failure, potentially by restricting necessary deformation or inducing localized stress concentrations. This implies an optimal range for inter-yarn friction to achieve maximum ballistic resistance (Wang et al. 2023).

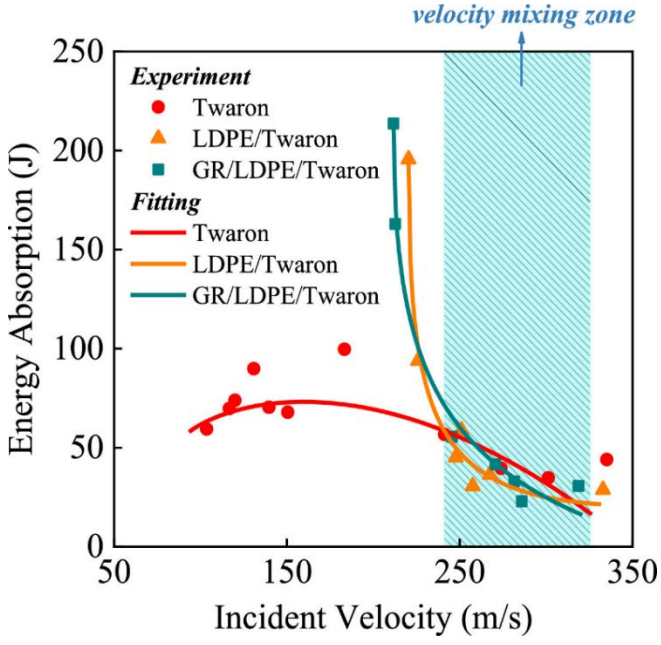

Figure 5. Energy absorption characteristics of graphene modified aramid (Twaron) fabrics (Wang et al. 2023)

While graphene itself is typically incorporated directly into the polymer matrix, graphene oxide (GO) is also applied as a coating to the fibres. Figure 6 shows the influence of GO on the ballistic absorbed energy of aramid fabric. The direct correlation between GO coating and enhanced ballistic performance indicates a promising pathway for developing more effective protective materials. The most prominent reason for the increased ballistic resistance is the higher friction between the fibres within the GO-coated fabric. The GO coating on the aramid fibres likely increases their surface roughness and introduces more contact points, leading to greater resistance when fibres slide against each other or when the projectile interacts with the fabric. This heightened friction translates directly into more efficient energy dissipation, as a greater amount of the energy of the projectile is converted into frictional work. Moreover, the heat treatment applied after GO deposition improves the adhesion of the GO sheets to the aramid fibres. This stronger interface contributes to the overall integrity of the material under impact. The GO-coated fabric exhibits a greater amount of microfibrillation in the fractured fibres. This indicates a more extensive energy absorption process, where the fibres undergo significant internal deformation and breaking into smaller fibrils, rather than simply shearing or displacing. This tensile rupture accompanied by microfibrillation significantly contributes to the increased energy absorption (Da Silva et al., 2020).

As a result, the integration of graphene and graphene oxide significantly enhances the ballistic performance of composite materials, primarily by optimizing inter-fibre/inter-yarn friction and promoting energy-dissipating microfibrillation, though achieving an optimal balance in these mechanisms is crucial to avoid detrimental effects.

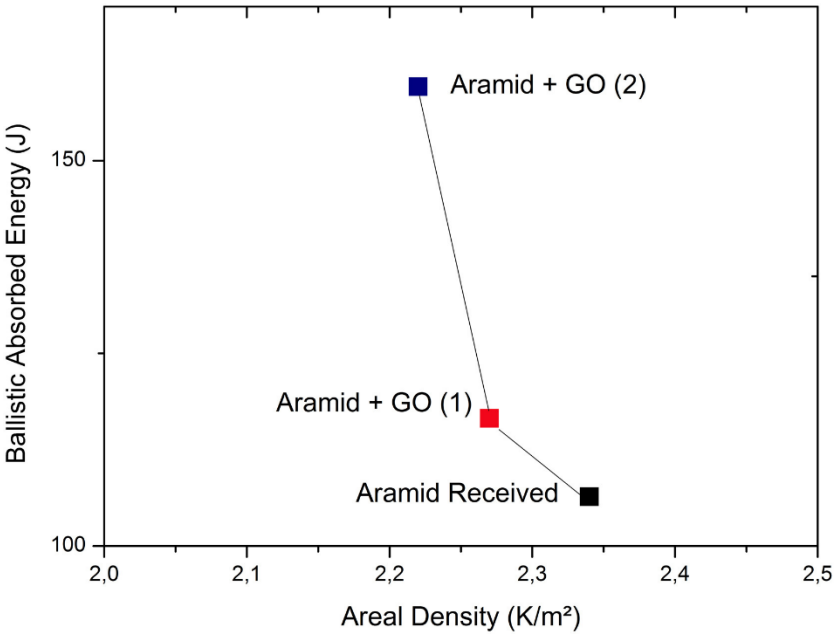

Figure 6. Ballistic absorbed energy of the received-aramid fabric and GO-modified aramid fabric a function of the fabric areal density (Da Silva et al., 2020)

Incorporating both CNTs and graphene is an effective way to improve the ballistic performance of fibre-reinforced polymer composites. This significantly enhances the ballistic performance of this type of composites. Hybrid configurations exhibits superior ballistic resistance, evidenced by reduced projectile exit velocities, and increased impact energy absorption, as seen in Figure 7. These improvements are attributed to the synergistic effects of enhanced matrix toughening, strengthened interfacial bonding between the fibres and nano-fillers, and the collective action of crack bridging of CNT with encapsulation behaviour of graphene. These mechanisms concurrently contribute to a more effective energy dissipation and load transfer within the composite, highlighting the potential of such hybrid nano-filler systems for advanced protective materials.

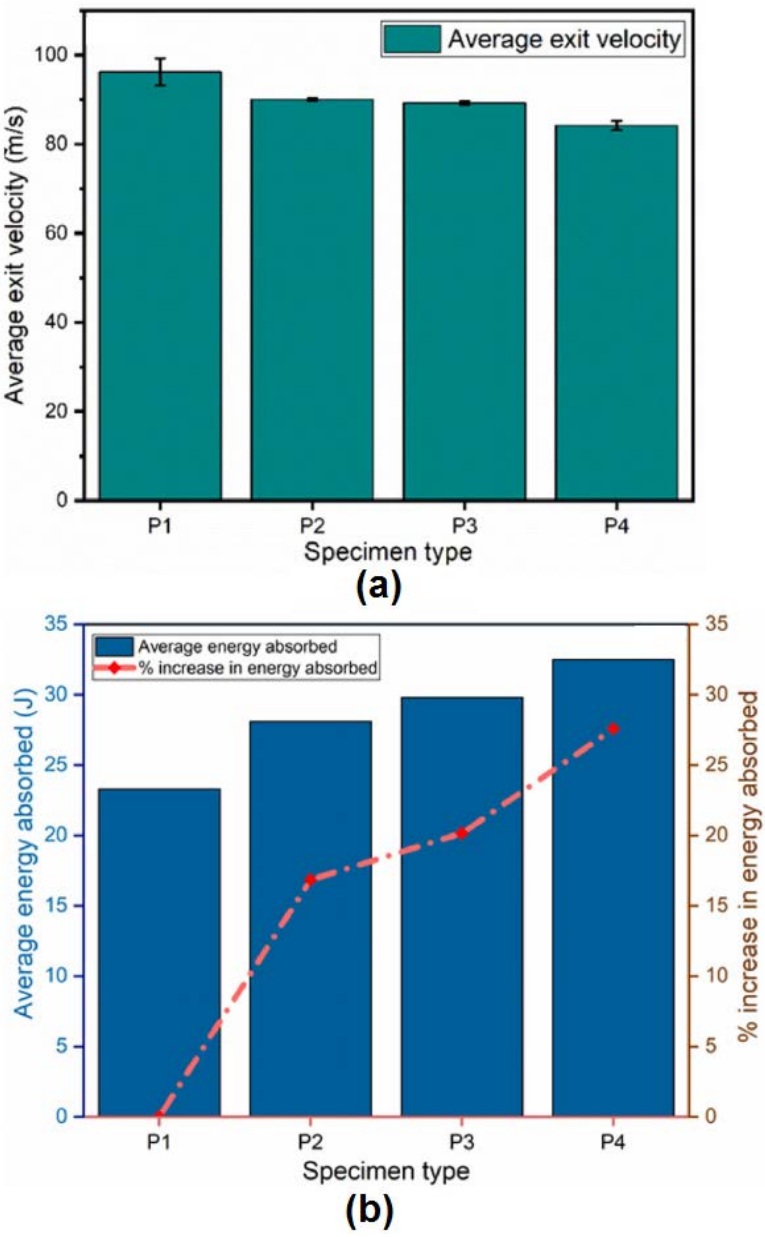

Figure. 7. (a) Average exit velocity and (b) energy absorbed for P1: Kevlar / Epoxy, P2: Kevlar + (0.5 wt.%)MWCNT / Epoxy, P3: Kevlar + (0.5 wt.%)GNP / Epoxy, and P4: Kevlar + (0.5 wt.%)MWCNT+ (0.5 wt.%) GNP / Epoxy composites (Nitin & Kumar, 2022)

2.2. Nano Ceramic-Based Reinforcements and Fillers

The addition of ceramic particles, ranging from nanoscale to microscale, into the fibre reinforced polymer matrix alters ballistic performance of the composite (Gaikwad et al., 2025). Unlike traditional macroscopic reinforcements, these ceramic reinforcements or fillers interact with the matrix and fibres at a much finer level, leading to a synergistic improvement in mechanical properties. Their unique stiffness, hardness, and fracture behaviour at various scales contribute significantly to enhanced ballistic resistance (Lach et al., 2015).

Among the nano-ceramic particles commonly utilized to elevate composite ballistic performance, Al_2O_3, SiO_2, and clay are certainly at the forefront.

The integration of Al_2O_3 particles within a Kevlar fibre/epoxy matrix demonstrate a positive and significant impact of Al_2O_3 on the ability of the composite to resist high-velocity impacts. The composite, when incorporating Al_2O_3, exhibits enhanced energy absorption capabilities. This improvement is attributed to the capacity of the material to effectively distribute and dissipate kinetic energy upon impact, primarily through mechanisms involving elastic work, and radial and tangential stretching. The presence of Al_2O_3 particles appears to augment these deformation mechanisms, contributing to a more robust energy absorption profile. Crucially, the ballistic limit velocity of the material is notably improved with the inclusion of Al_2O_3. This indicates a superior resistance to penetration at higher projectile velocities compared to other composite materials. This enhanced performance stems from the contribution of Al_2O_3 particles to the overall mechanical integrity of the composite, particularly in terms of stiffness and strength, which are vital for mitigating severe impact forces. Ultimately, the addition of Al_2O_3 particles in Kevlar/epoxy hybrid composites presents a promising avenue

for advancing target performance in bulletproof applications. The improved energy absorption and ballistic limit velocity of the material emphasize the practical benefits of this specific composite structure (Talib et al., 2012).

Regarding the influence of Al_2O_3 nanoparticles, these particles significantly impact the ballistic performance of fibre (Kevlar)-reinforced polymer composites (Haro et al., 2017). Al_2O_3 nanoparticles demonstrably improve the stiffness of the composite, contributing a notable increase. Also, they provide the high energy absorption capability to the composite. These performance gains are primarily attributed to the nanoscale size and the high inherent rigidity of the ceramic Al_2O_3 nanoparticles. This combination allows for superior interaction within the polymer matrix, facilitating more efficient load transfer and energy dissipation. The elevated flow stress observed further indicates an increased resistance to plastic deformation, enabling greater energy absorption before material failure.

SiO_2 nanoparticles significantly enhance the dynamic impact response and energy absorption capabilities of composite materials, particularly those reinforced with Kevlar in matrix, such as HDPE matrix (Haro et al., 2017). Their incorporation can lead to substantial improvements in stiffness. Dynamic impact resistance is also bolstered, as materials containing SiO_2 nanoparticles consistently exhibit higher maximum flow stress. Moreover, these composites show a reduced propensity for cracking under high-impact loads, thus maintaining their structural integrity more effectively. These performance benefits largely stem from the nanoscale dimensions and inherent rigidity of the ceramic SiO_2 filler. Such characteristics facilitate more effective force distribution and energy dissipation throughout the composite structure. The resulting increase in flow stress further suggests an enhanced capacity for plastic deformation and energy absorption prior to failure.

Figure 8 shows effectiveness of incorporating nano-sized silicon dioxide (SiO_2) particles into polyvinyl alcohol (PVA)/aramid fibre composite. As seen in Figure 8, the addition of nano-SiO_2 significantly enhances the ballistic resistance of these composites. Nano-SiO_2 enhances ballistic performance by reinforcing the properties of the matrix and improving the bonding of fibres within that matrix. This fortification at the nanoscale allows the composite system to more effectively withstand and dissipate the energy from ballistic impacts, validating its suitability for lightweight protective armour applications (Gencheva and Djerahov, 2018).

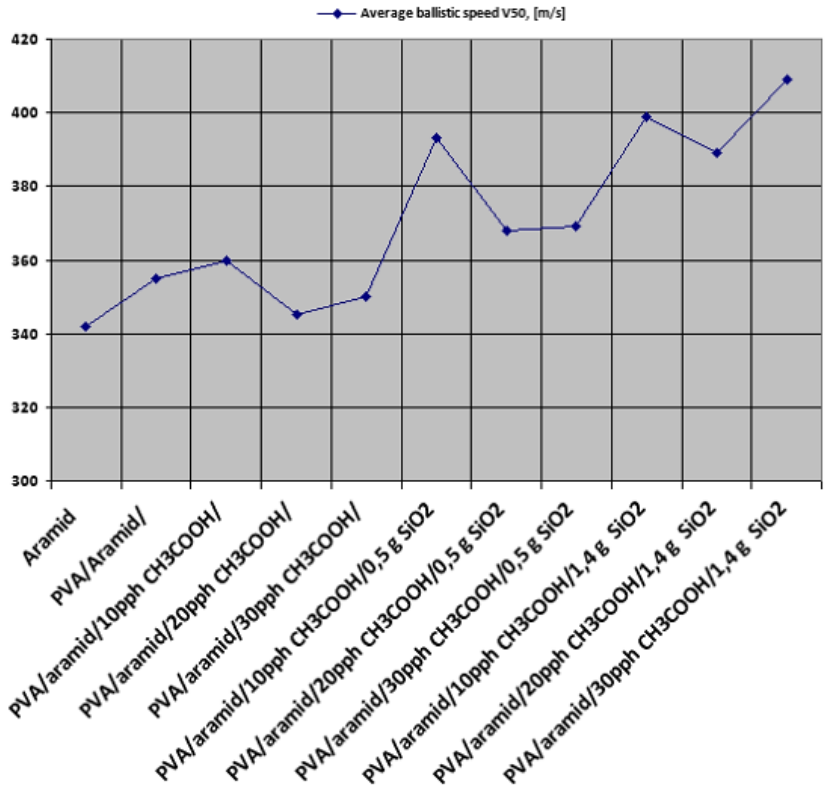

Figure 8. Ballistic test results of PVA/aramid fibre and nano-SiO_2 reinforced composites (Gencheva and Djerahov, 2018)

Figure 9 depicts that adding clay nanoparticles significantly improves the ballistic properties of fibre reinforced composite laminates. This enhancement stems from the increased ability of the material to absorb energy and its higher ballistic limit. This superior performance is primarily attributed to the influence of the nano clay particles on various failure mechanisms. While the deformation of fibres remains the primary energy absorber, clay nanoparticles particularly amplifies energy dissipation through delamination and matrix cracking. Also, the increased clay content leads to larger delamination areas, effectively creating more pathways for energy to be dissipated throughout the material.

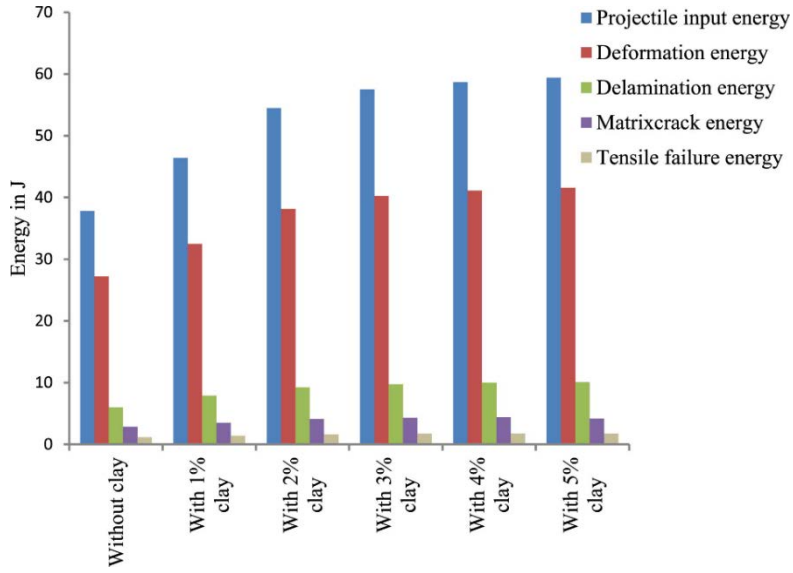

Figure 9. Ballistic limit energy absorption and failure modes of three-layer laminates with and without clay (Balaganesan et al., 2014)

As seen in the results above, while nano-ceramic particles can positively influence the ballistic properties of fibre-reinforced composites, they might not achieve the same level of effectiveness as reinforcements or fillers like carbon nanotubes (CNTs). Figure 10 presents the impact of SiO_2 nanoparticles and

COOH-MWCNTs on the percentage of energy absorption observed in the glass fibre reinforced epoxy matrix composite, in that order.

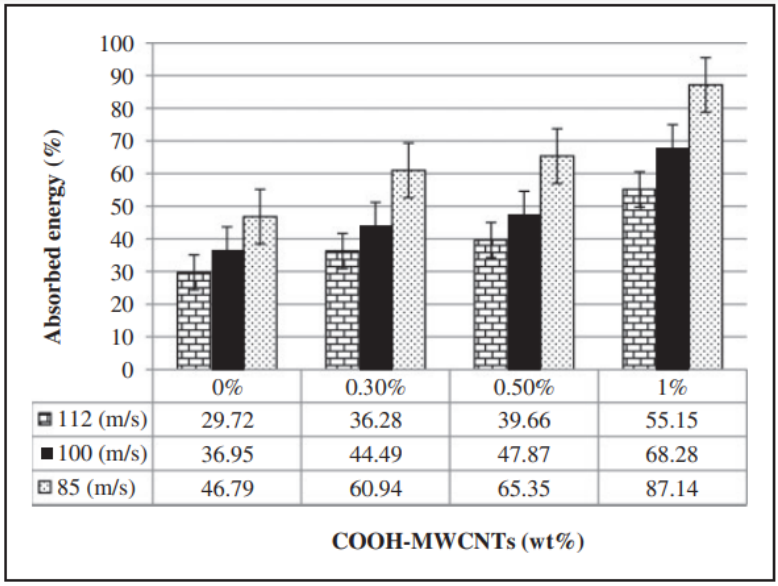

	0%	0.30%	0.50%	1%
112 (m/s)	29.72	36.28	39.66	55.15
100 (m/s)	36.95	44.49	47.87	68.28
85 (m/s)	46.79	60.94	65.35	87.14

(a)

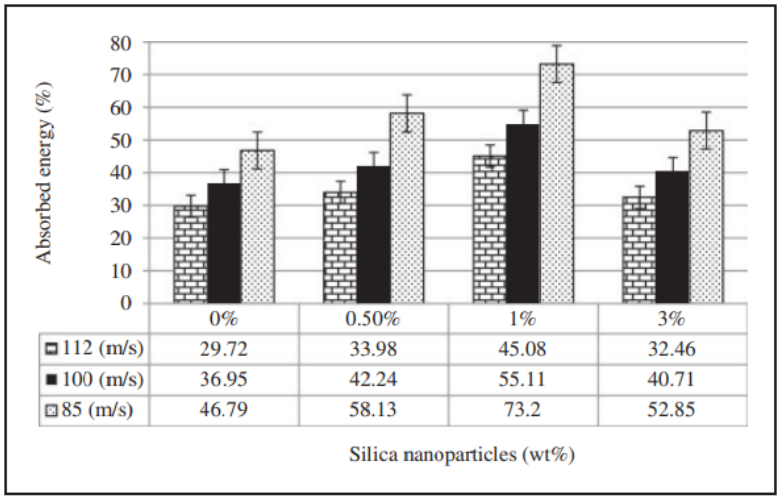

	0%	0.50%	1%	3%
112 (m/s)	29.72	33.98	45.08	32.46
100 (m/s)	36.95	42.24	55.11	40.71
85 (m/s)	46.79	58.13	73.2	52.85

(b)

Figure 10. The effect of (a) COOH-MWCNTs and (b) silica (SiO_2) nanoparticle on the absorbed energy of glass fibre reinforced epoxy matrix composite (Naghizadeh et al., 2016)

The impact resistance of fibre-reinforced polymer composites with nano-materials, MWCNTs tend to be more effective than silica (SiO_2) nanoparticles in improving ballistic performance (Figure 10). This difference is often attributed to several factors: MWCNTs possess exceptional strength, stiffness, and aspect ratio (length to diameter ratio). This allows them to effectively bear and distribute impact forces throughout the material, leading to better energy absorption. Silica nanoparticles, while improving properties, generally do not offer the same level of individual mechanical superiority. MWCNTs contribute to energy absorption through various mechanisms, such as pull-out, fracture, and large deformations, which dissipate more kinetic energy from the projectile. While silica nanoparticles can improve matrix toughness and distribute stress, their energy dissipation mechanisms might not be as extensive. This suggests that MWCNTs are more effective at containing the damage and preventing it from spreading, which is crucial for ballistic performance.

Fundamentally, the unique combination of high strength, high stiffness, and efficient energy dissipation mechanisms makes MWCNTs a more potent reinforcement for enhancing the ballistic resistance of fibre-reinforced polymer matrix composites.

3. CONCLUSION

This chapter comprehensively analysed the significant influence of nano-materials on the ballistic performance of fibre-reinforced polymer composite armours. The advent of nanotechnology, with its unprecedented ability to tailor materials at the atomic and molecular scales, emerged as a truly revolutionary pathway to circumvent these traditional limitations.

The strategic integration of various nano-materials fundamentally improves critical material properties. Notably, carbon-based nano-materials, such as carbon nanotubes (CNTs) and graphene, have shown exceptional promise. Their remarkable strength, stiffness, and aspect ratios allow for significant contributions to energy absorption and multi-hit resistance. CNTs, for instance, improve ballistic performance by promoting mechanisms like crack bridging and localized deformation, effectively dissipating more kinetic energy upon impact. Graphene, with its extraordinary strength and two-dimensional nature, enhances inter-yarn friction and promotes energy-dissipating microfibrillation, leading to increased ballistic limits. However, a crucial aspect surfaced: the efficacy of these materials is critically contingent upon uniform dispersion and robust interfacial bonding. Agglomeration, particularly with MWCNTs, can ironically undermine the very protective capabilities these nano-materials are meant to provide, transforming potential strengths into weaknesses.

In addition to carbon-based structures, the chapter also detailed the contributions of various nano-ceramic particles, including Al_2O_3 and SiO_2. These materials have demonstrated a positive influence on ballistic properties by enhancing stiffness, increasing energy absorption, and fostering larger delamination areas, which aid in energy dissipation. For example, Al_2O_3 nanoparticles improve composite stiffness and energy absorption through better load transfer, while SiO_2 nanoparticles bolster dynamic impact response and reduce cracking. Nevertheless, a comparative analysis revealed that while nano-ceramic particles offer valuable improvements, they may not achieve the same pinnacle of effectiveness as carbon nanotubes. This distinction largely stems from the distinct energy absorption mechanisms and the inherently superior individual mechanical properties inherent to CNTs.

The progression of nano-materials marks a defining frontier for next-generation protective technologies. By strategically leveraging the distinct properties of these nanoscale constituents, the development of armours that are not only lighter and stronger but also significantly more adaptable becomes feasible. This advancement is crucial for confronting the increasingly complex and dynamic kinetic threats prevalent in modern operational settings.

REFERENCES

Balaganesan, G., Velmurugan, R., Srinivasan, M., Gupta, N. K. & Kanny, K. (2014). Energy absorption and ballistic limit of nanocomposite laminates subjected to impact loading. *International Journal of Impact Engineering, 74*, 57-66. https://doi.org/10.1016/j.ijimpeng.2014.02.017.

Cao, S., Pang, H., Zhao, C., Xuan, S., & Gong, X. (2020). The CNT/PSt-EA/Kevlar composite with excellent ballistic performance. *Composites Part B: Engineering, 185*, 107793. https://doi.org/10.1016/j.compositesb.2020.107793.

Da Silva, A. O., Weber, R. P., Monteiro, S. N., Lima, A. M., Faria, G. A., Da Silva, W. O., Oliveira, S. D. S. A., Monsores, K. G. D. C., & Pinheiro, W. A. (2020). Effect of graphene oxide coating on the ballistic performance of aramid fabric. *Journal of Materials Research and Technology, 9*(2), 2267-2278. https://doi.org/10.1016/j.jmrt.2019.12.058.

Gaikwad, N. S. Deshmukh, D. D., & Kakade, S. P. (2025). Fiber-reinforced polymer matrix composites for improved defence armor - A comprehensive review. *Smart Materials in Manufacturing, 3*, 100084. https://doi.org/10.1016/j.smmf.2025.100084.

Gencheva, P. & Djerahov, L. (2018). High-strength synthetic fibers and nano-sized particles of SiO_2 combined into one composite system for ballistic protection. *Journal of Mining and Geological Sciences, 61*, 82-86.

Haro, E. E., Odeshi, A. G., & Szpunar, J. A. (2017). The effects of micro- and nano-fillers' additions on the dynamic impact response of hybrid composite armors made of HDPE reinforced with Kevlar short fibers. *Polymer-*

Plastics Technology and Engineering, 57(7), 609-624. https://doi.org/10.1080/03602559.2017.1332207

Kukle, S., Valisevskis, A., Briedis, U., Balgale, I., & Bake, I. (2024). Hybrid soft ballistic panel packages with integrated graphene-modified para-aramid fabric layers in combinations with the different ballistic Kevlar textiles. *Polymers, 16*, 2106. https://doi.org/10.3390/polym16152106.

Lach, E., Wolf, T., & Scharf, M. (2015). Submicro and nano ceramic as ballistic protective material. *Mechanik, 2*, 45-46. http://dx.doi.org/10.17814/mechanik.2015.2.76.

Lubineau, G., Alfano, M., Tao, R., Wagih, A., Yudhanto, A., Li, X., Almuhammadi, K., Hashem, M., Hu, P., Mahmoud, H. A., & Oz, F. (2024). Harnessing extrinsic dissipation to enhance the toughness of composites and composite joints: A state-of-the-art review of recent advances. *Advanced Materials, 36*(51), 2407132. https://doi.org/10.1002/adma.202407132.

Micheli, D., Vricella, A., Pastore, R., Delfini, A., Giusti, A., Albano, M., Marchetti, M., Moglie, F., & Primiani, V. M. (2016). Ballistic and electromagnetic shielding behaviour of multifunctional Kevlar fiber reinforced epoxy composites modified by carbon nanotubes. *Carbon, 104*, 141-156. https://doi.org/10.1016/j.carbon.2016.03.059.

Mohamed S. S., El-Safty, S. A., Shenashen, M. A., & Elmarakbi. A. (2024). Advances in polymer/inorganic nanocomposite fabrics for lightweight and high-strength armor and ballistic-proof materials. *Chemical Engineering Journal, 493*, 152422. https://doi.org/10.1016/j.cej.2024.152422.

Mylvaganam, K. & Zhang, L. C. (2006). Energy absorption capacity of carbon nanotubes under ballistic impact.

Applied Physics Letters, 89(12), 123127. https://doi.org/10.1063/1.2356325.

Naghizadeh, Z., Faezipour, M., Pol, M. H., Liaghat, G. H., & Abdolkhani A. (2016). Improvement in impact resistance performance of glass/epoxy composite through carbon nanotubes and silica nanoparticles. *Proceedings of the Institution of Mechanical Engineers, Part L: Journal of Materials: Design and Applications. 232*(9), 785-799. https://doi.org/10.1177/1464420716649403.

Nanema, B. L. T., Mejri, M., & Salah N. B. (2024). Numerical study of composite structures behavior under ballistic impacts. *International Journal of Protective Structures, 16*(1), 252-265. https://doi.org/10.1177/20414196241284417.

Naveen, J., Jawaid, M., Goh, K. L., Reddy, D. M., Muthukumar, C., Loganathan, T. M., & Reshwanth, K. N. G. L. (2021). Advancement in graphene-based materials and their nacre inspired composites for armour applications—A review. *Nanomaterials, 11*, 1239. https://doi.org/10.3390/nano11051239.

Nitin, M. S., & Kumar, S. S. (2022). Ballistic performance of synergistically toughened Kevlar/epoxy composite targets reinforced with multiwalled carbon nanotubes/graphene nanofillers. *Polymer Composites, 43*(2), 639-1214. https://doi.org/10.1002/pc.26409.

Pandya, K. S. & Naik, N. K. (2015). Analytical and experimental studies on ballistic impact behavior of carbon nanotube dispersed resin. *International Journal of Impact Engineering, 76*, 49-59. https://doi.org/10.1016/j.ijimpeng.2014.09.003.

Rani, M., Sehrawat, M., Sharma, S., Bharadwaj, S., Chauhan, G. S., Dhakate, S. R., & Singh, B. P. (2024). Carbon nanotube-based soft body armor: Advancements, integration strategies, and future prospects. *Diamond and Related Materials*, *148*, 111446. https://doi.org/10.1016/j.diamond.2024.111446.

Rashid, A. B., Haque, M., Islam, S. M. M., & Labib, K. M. R. U. (2024). Nanotechnology-enhanced fiber-reinforced polymer composites: Recent advancements on processing techniques and applications. *Heliyon*, *10*(2), e24692. https://doi.org/10.1016/j.heliyon.2024.e24692.

Ravindran, P., Kumar, K. M., Rangasamy, S., Rajammal, K., & Kumar, V. (2023). Plain Kevlar and a CNT-reinforced Kevlar epoxy polymer composite: Comparative study of its mechanical, low velocity and ballistic impact properties. *Iranian Polymer Journal*, *32*, 239-249. https://doi.org/10.1007/s13726-022-01122-z.

Sharma, S., Goyal, R., Rani, M., Dhakate, S., & Singh, B. P. (2023). Carbon Nanotubes and Graphene for Ballistic Protection. In *Advanced Carbon Materials for Defense Applications* (pp. 23-48). CRC Press.

Srinivasan, V., Kunjiappan, S., & Palanisamy, P. (2021). A brief review of carbon nanotube reinforced metal matrix composites for aerospace and defense applications. *International Nano Letters*, *11*, 321-345. https://doi.org/10.1007/s40089-021-00328-y.

Talib, A. R. A., Abbud, L. H., & Mustapha, A. A. F. (2012). Ballistic impact performance of Kevlar-29 and Al_2O_3 powder/epoxy targets under high velocity impact. *Materials & Design*, *35*, 12-19. https://doi.org/10.1016/j.matdes.2011.08.045.

Wang, Z., Zhang, H., Dong, Y., Zhou, H., & Huang, G. (2023). Ballistic performance and protection mechanism of aramid fabric modified with polyethylene and graphene, *International Journal of Mechanical Sciences, 237*, 107772. https://doi.org/10.1016/j.ijmecsci.2022.107772.

Worku, A. K. & Ayele, D. W. (2023). Recent advances of graphene-based materials for emerging technologies. *Results in Chemistry, 5*, 100971. https://doi.org/10.1016/j.rechem.2023.100971.

SURFACE PRETREATMENT METHODS FOR ENHANCING BONDING PERFORMANCE IN POLYMER MATRIX COMPOSITES: A COMPREHENSIVE INVESTIGATION INTO LASER ABLATION MECHANISMS

Elif BAŞER[1]

Ege Anıl DİLER[2]

1. INTRODUCTION

A worldwide need for enhanced structural performance, coupled with demands for lightweighting and sustainability, has firmly established polymer matrix composites (PMCs) as indispensable materials in a diverse array of advanced engineering applications. From the demanding confines of aerospace and defence to the high-volume production of automotive and marine components, PMCs offer a remarkable confluence of specific strength, stiffness, fatigue resistance, and corrosion immunity. However, the seamless integration of these high-performance materials into complex, multi-component assemblies necessitates reliable joining methodologies. While traditional mechanical fastening systems introduce stress concentrations, increase weight, and often complicate manufacturing, adhesive bonding stands as a superior alternative. This technique facilitates a more uniform stress distribution

[1] B. Eng., Ege University, Graduate School of Natural and Applied Sciences, Mechanical Engineering Program, baserelif4@gmail.com, ORCID: 0009-0002-7125-9901.

[2] Assoc. Prof. Dr., Ege University, Faculty of Engineering, Department of Mechanical Engineering, ege.anil.diler@ege.edu.tr, ORCID: 0000-0002-1667-5737.

across the joint, suppresses fatigue crack initiation, and simplifies structural geometries, ultimately leading to lighter and more efficient designs.

Despite these advantages, the achievement of durable and high-strength adhesive bonds in PMCs is profoundly challenged by the characteristics of their surfaces. Polymer matrices, by design, often possess low surface energy, are chemically inert, and frequently harbour process-induced contaminants such as mould release agents, unreacted oligomers, or weak boundary layers. These surface characteristics collectively impede effective wetting by adhesives and inhibit the formation of strong interfacial bonds, relegating the bond line to the weakest link in the entire structural system. Consequently, surface treatment methodologies are not merely beneficial enhancements but rather fundamental, non-negotiable prerequisites for maximizing the adhesive bond strength and ensuring the long-term reliability of PMC joints. These treatments are engineered to alter the typically passive composite surface into a highly active, wettable, and structurally receptive substrate, thereby maximizing the work of adhesion and promoting strong inter-molecular or inter-atomic interactions across the interface.

This treatise aims to provide an exhaustive scientific exposition on advanced surface treatment strategies for PMCs. This chapter will systematically dissect the underlying principles, mechanisms, and comparative efficacy of prominent surface pretreatment methods. A significant emphasis will be placed on an unrivaled deep dive into laser ablation, a cutting-edge, non-contact technology. This chapter will also detail the intricate physics of laser-material interaction within the multi-phase composite structure, elucidating the resultant hierarchical morphological, profound chemical, and energetic transformations, ultimately correlating these changes to the improvements in bonding performance of composite materials.

2. SURFACE PRETREATMENT METHODS for PMCs

Beyond the absolute prerequisite of rigorous cleaning, which removes contaminants, a suite of advanced surface modification techniques is employed to engineer the surface of PMC for enhanced adhesion. Each method operates via distinct mechanical, physical, and chemical mechanisms, offering unique advantages and posing specific limitations. Figure 1 depicts the surface treatment methods applied for the adhesive bonding of PMCs.

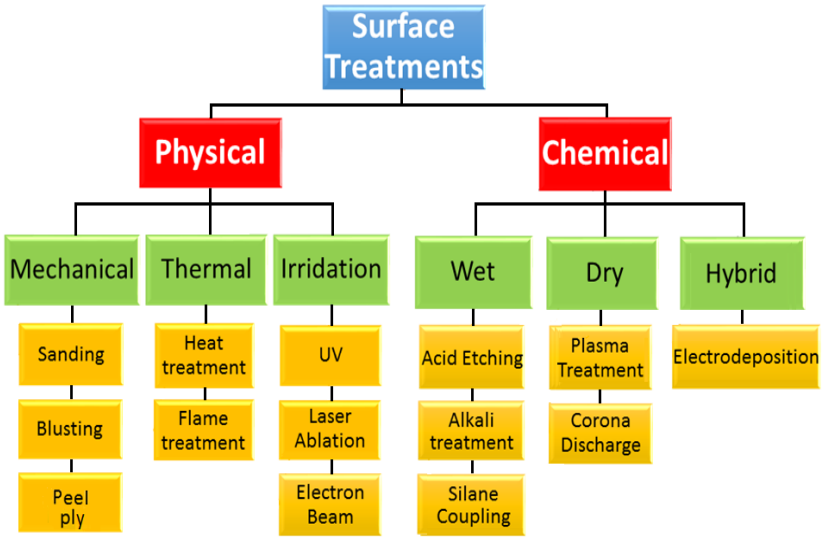

Figure 1. Surface pretreatment methods applied for adhesive bonding of PMCs

When considering adhesive bonding for composite materials, the efficacy of the surface treatment process is essential. Several key factors significantly influence its outcome, ultimately determining the strength and durability of the bond. These influencing factors include the type of composite material itself, particularly the specific resin matrix and fibre reinforcement used, as their chemical and physical properties

dictate the appropriate treatment. Furthermore, the chosen surface treatment method, whether it be mechanical abrasion, chemical etching, or plasma treatment, plays a critical role, as each technique modifies the surface in distinct ways. Process parameters such as treatment time, temperature, and power settings for physical methods are also crucial, requiring precise control to achieve optimal surface morphology and chemistry (Figure 2). Finally, environmental conditions during and after treatment, including humidity and cleanliness, can profoundly impact surface reactivity and the potential for contamination, which directly affects adhesive wettability and bond formation.

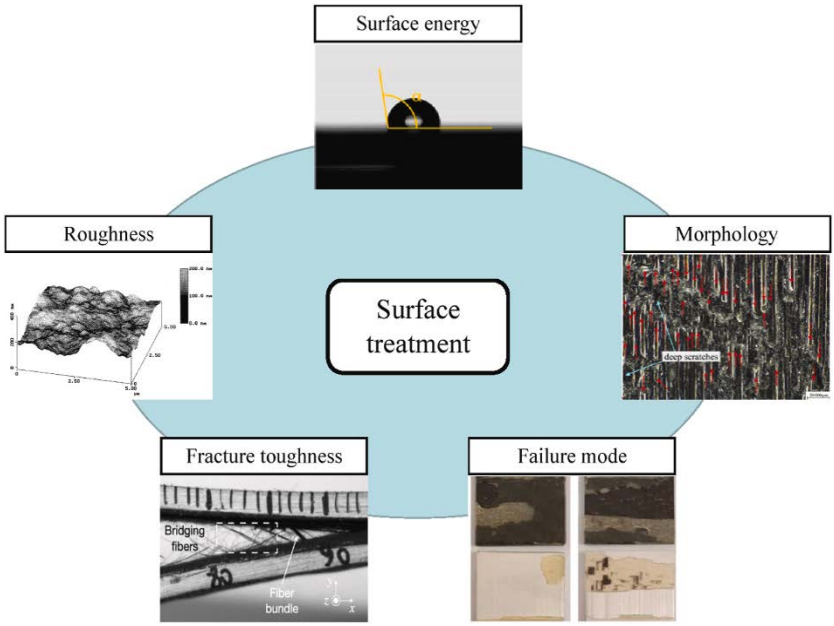

Figure 2. Factors of surface treatment process for the composite bondings (Liu et al., 2023)

2.1. Mechanical Surface Treatments

These methods primarily focus on modifying the surface topography to enhance mechanical interlocking via some methods including sanding, blasting, and peel ply.

2.1.1. Sanding

Sanding is a mechanical surface treatment method and offers a straightforward, affordable, and versatile way to roughen the surface of the materials, which in turn enhances their bonding strength with other components. However, this method comes with drawbacks; it is highly dependent on the operator, often leading to significant inconsistencies in surface profile and residual contamination. Additionally, there is a higher risk of fibre damage and abrasive particle embedment compared to more controlled blasting techniques.

This process creates surface roughness and removes outer layers. The severity of the treatment depends on grit size and applied pressure. The roughness of a surface plays a crucial role in the adhesive bonding, but it is a delicate balance. Generally, increasing surface roughness to an optimal level can significantly enhance bond strength (Figure 3). This occurs because a moderately roughened surface provides more area for the adhesive to grab onto, creating a stronger mechanical interlock and often improving the ability of the surface to be wetted by the adhesive. However, pushing that roughness too far can actually backfire. Excessive roughness can make it difficult for the adhesive to fully fill all the microscopic valleys and crevices (Nazari et al., 2024a), leaving voids that act as stress concentration points. In some cases, over-roughening leads to a weaker bond than if the surface had not been treated at all (Figure 3). This highlights the importance of finding that sweet spot for surface preparation.

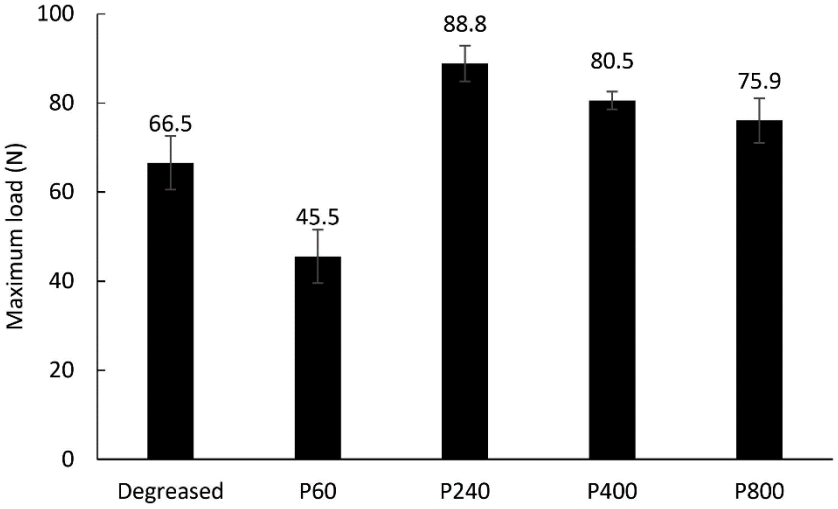

Figure 3. Effect of sanding process on the strength of adhesive bonding (lower value of sanding number of P denotes higher roughness) (Nazari et al., 2024b)

2.1.2. Blasting

Blasting is another mechanical surface treatment to improve the strength of adhesive-bonded polymer matrix composites. It is highly effective at creating significant surface roughness and dislodging stubborn contaminants (Marques et al., 2020).

While other mechanical methods like sanding are also scientifically recognized for surface preparation, blasting specifically excels at removing superficial resin layers, mould release agents, and inducing a desirable macro- and micro-roughened topography. This is achieved as the kinetic energy of the blasting particles transfers to the surface, leading to localized fracture and plastic deformation.

Blasting treatment is applicable across a wide array of composite types and geometries. However, blasting is not without its drawbacks. The uncontrolled nature of particle impingement can cause localized damage or even sever reinforcing fibres. This,

in turn, can create stress concentrators within the material and diminish the overall mechanical properties of the composite.

2.1.3. Peel Ply

Among mechanical surface treatments, peel ply offers a convenient and effective method for surface preparation. The peel ply acts as a sacrificial layer, effectively encapsulating the contaminants found on the surface of the composite. Upon removal, it carries these contaminants away, exposing a significantly cleaner, untainted surface that is inherently more receptive to adhesive wetting and chemical interaction.

The textured weave of the peel ply imparts a characteristic micro-roughness to the composite surface as it cures against it. This controlled surface topography is highly beneficial for adhesive bonding. The increased surface area and the creation of micro-indentations allow the liquid adhesive to penetrate more effectively. This mechanism, often referred to as mechanical keying, significantly enhances the strength of the bond by providing a physical anchor for the adhesive.

The primary advantage of the peel ply process lies in its ability to simultaneously achieve surface cleanliness and controlled roughening without introducing potential damage to the underlying fibres (Li et al., 2021).

Compared to the mechanical surface treatments, blasting, such as sandblasting, consistently yielded the highest bonding strength for fibre-reinforced composite bondings, while sanding resulted in the lowest, as seen in Figure 4.

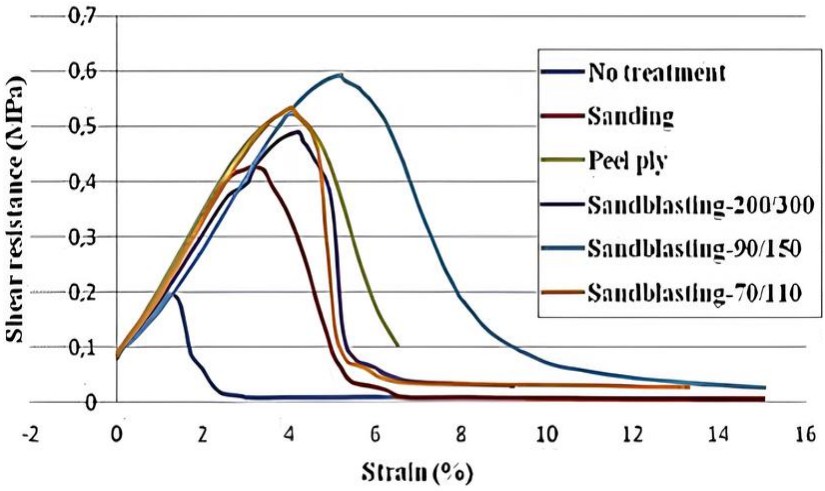

Figure 4. Influence of mechanical surface treatments on the shear strength of adhesive-bonded flax fiber/epoxy coomposites (Bechikh et al., 2022)

Sandblasting performance is directly linked to its capacity to create a highly non-homogeneous surface topography with the highest arithmetic mean height. This significant roughening provides superior mechanical interlocking with the adhesive, enhancing the physical bond.

Furthermore, sandblasted surfaces exhibited the highest surface free energy (SFE), particularly its dispersive component. A higher SFE promotes better wettability by the adhesive, allowing it to spread effectively and improve adhesion with the adherend (Aliheidari & Ameli, 2024). Critically, sandblasting treatment also led to fibre exposure at the surface of the composite. This exposure of the hydrophilic fibres likely facilitated a more favourable chemical compatibility with the adhesive, contributing significantly to the overall bond strength. The strong linear correlation observed between shear strength and the surface free energy dispersive component further reinforces these findings.

2.2. Chemical Surface Treatments

Chemical surface treatments employ chemical reactions to alter the surface chemistry and energy of the polymer matrix. These treatments often include methods like chemical etching and various plasma treatments, such as those performed under vacuum or in atmospheric conditions.

2.2.1. Chemical Etching

Chemical etching treatment has highly effective method in forming a rough surface (Olonisakin et al., 2021) and creating chemical bonding sites, leading to strong and durable adhesion. However, it involves the use of highly corrosive, toxic, and environmentally hazardous chemicals.

During chemical etching treatment, strong oxidizing acids or alkaline solutions chemically attack and remove the outermost layer of the polymer matrix through oxidative degradation and dissolution. This process not only removes weak boundary layers but also introduces a high density of polar, functional groups (hydroxyl, carboxyl, etc.) onto the surface. These functional groups significantly increase the surface energy and provide active sites for chemical bonding with the adhesive.

The optimal etchant and processing parameters are highly specific to the polymer matrix type. Aggressive etchants can severely degrade or weaken reinforcing fibres if not precisely controlled, compromising the structural integrity of the composite.

2.2.2. Plasma Surface Treatments

Plasma treatments utilize a partially ionized gas (plasma) containing highly reactive species to modify the outermost atomic layers of the composite surface. Vacuum plasma and atmospheric plasma are the most frequently employed methods.

2.2.2.1.Vacuum Plasma (Low-Pressure Plasma)

Vacuum plasma surface treatment provides a clean surface and allows for highly controlled introduction of specific chemical functionalities, tailoring the surface properties for optimal adhesion (Pitto et al., 2024). Also, it operates at low temperatures, preventing thermal degradation of the composite bulk material. Figure 5 illustrates a low-pressure plasma surface treatment applied to fibre-reinforced polymer matrix composites.

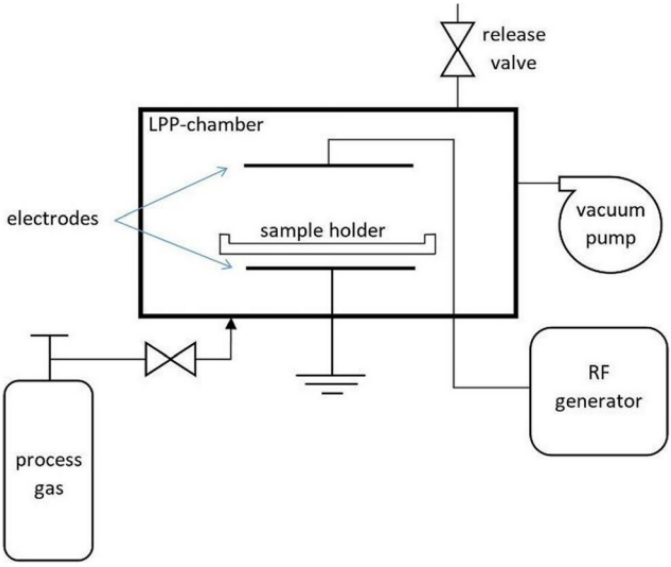

Figure 5. Schematic diagram of the low-pressure plasma (LPP) surface treatment (Pizzorni et al., 2019)

In this treatment, the composite is placed in a vacuum chamber, and a process gas (argon, oxygen, nitrogen, air, etc.) is introduced and ionized by an electromagnetic field. The plasma species (ions, electrons, radicals, photons) interact with the surface through several mechanisms. High-energy ions bombard the surface, physically removing atoms or molecules and creating nanoscale roughness. Reactive radicals from the plasma break chemical bonds on the polymer surface and incorporate new atoms, leading to the introduction of highly polar functional

groups. This treatment can induce cross-linking of surface polymer chains, increasing surface hardness and chemical resistance; moreover, it effectively removes ultra-thin organic contaminants at a molecular level without damaging the bulk material.

2.2.2.2.Atmospheric Plasma

The other plasma treatment method is the atmospheric plasma method. Similar to vacuum plasma, but the plasma is generated at atmospheric pressure by a high-voltage electrical discharge across a small gap. Reactive species are formed in the gas phase and interact with the composite surface. Figure 6 depicts the atmospheric plasma surface treatment employed on the carbon fibre-reinforced epoxy matrix composite to improve the bonding strength.

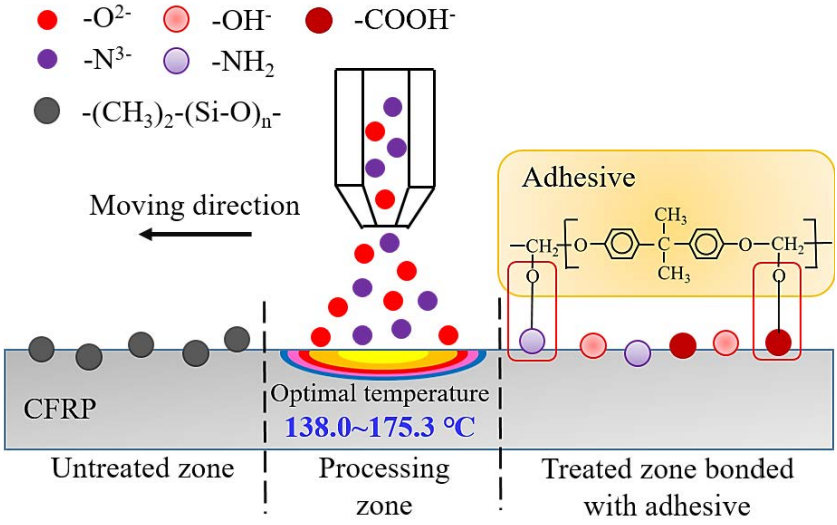

Figure 6. Schematic diagram of the atmospheric pressure plasma surface treatment employed on the carbon fibre-reinforced epoxy matrix composite (Sun et al., 2019)

Both plasma treatments work by cleaning the surface (removing contaminants and weak boundary layers) and activating it by introducing reactive functional groups and/or

increasing surface roughness. This leads to improved surface energy and wettability, allowing the adhesive to spread more effectively and form stronger chemical bonds (Guo et al., 2024).

The choice between vacuum and atmospheric plasma largely depends on the specific application requirements, including part geometry, production volume, desired level of precision, and cost considerations. Both are effective, modern approaches to enhance adhesive bonding in composite materials, offering significant improvements over traditional mechanical or chemical methods.

While plasma treatment effectively enhances the chemical reactivity and cleanliness of composite surfaces for adhesive bonding, it typically does not significantly increase surface roughness. This lack of surface modification means plasma alone cannot fully leverage the benefits of mechanical interlocking in adhesive joints. However, a synergistic approach, wherein pre-treatment with mechanical abrasion methods like sanding is employed to augment surface roughness, can be highly advantageous (Guo et al., 2024). This initial roughening, combined with the chemical activation and cleaning provided by subsequent plasma treatment, creates a multi-faceted surface ideal for strong adhesion. Such a combined strategy allows for the maximization of both mechanical interlocking and chemical bonding mechanisms, leading to a substantial enhancement in the overall strength and durability of the adhesive joint.

3. LASER ABLATION TREATMENT for PMCs

Laser ablation represents a non-contact, and highly controllable method for surface modification (Wang et al., 2021). It leverages the directed energy of a focused laser beam to precisely remove material from the substrate, inducing profound changes in surface morphology, chemistry, and energy. This

makes it an exceptionally powerful tool for preparing PMC surfaces for adhesive bonding, offering advantages over conventional techniques.

The interaction between a laser beam and a PMC is intrinsically complex due to the heterogeneous nature of the composite, comprising a polymer matrix and reinforcing fibres, each with distinct optical and thermophysical properties. The primary mechanisms of material removal (ablation) are fundamentally dependent on the laser pulse duration and the absorption characteristics of the material.

When using laser ablation, the type of laser significantly impacts the treatment mechanism. Ultraviolet (UV) lasers, with their high photon energy, primarily induce photochemical ablation. This means the high-energy photons directly break molecular bonds in the material (Manshina et al., 2024). In contrast, infrared (IR) lasers have lower photon energy. Their ablation mechanism is predominantly photothermal. Here, the material absorbs the laser energy, which then converts into heat, leading to rapid temperature increase and material removal.

3.1. Photothermal Ablation

Photothermal ablation is a process where the material absorbs laser energy, converting it into heat that rapidly removes the matrix, often by vaporizing or degrading it. When a laser pulse with a duration in the nanosecond to microsecond regime interacts with the composite, the absorbed photon energy is rapidly converted into vibrational (thermal) energy within the irradiated volume. If the laser fluency (energy per unit area) exceeds a specific material-dependent threshold, the temperature of the illuminated region, primarily the polymer matrix, escalates rapidly beyond its decomposition temperature.

In this surface treatment, the following mechanisms can occur: vaporization/sublimation, thermal degradation, melt ejection, and thermal diffusion (Gu et al., 2024).

The polymer converts from solid to gas, resulting in material expulsion. Chemical bonds within the polymer matrix break down due to extreme localized heating, resulting in the formation of volatile organic compounds and often a carbonaceous char layer. This char can be detrimental to adhesion and may require secondary removal. Rapid heating can lead to localized melting, followed by explosive expulsion of molten material due to the rapid pressure build-up from vaporization. This can result in resolidified droplets and debris on the surface. A critical challenge with longer pulse durations is that the laser pulse duration is comparable to or longer than the characteristic time for thermal diffusion within the material. This leads to significant heat conduction into the surrounding, un-irradiated material, creating a substantial Heat-Affected Zone (HAZ). Within the HAZ, the polymer matrix can undergo undesirable thermal degradation, micro-cracking, residual stress formation, and changes in its mechanical properties, potentially compromising the structural integrity of the material. This is a primary limitation for precise surface engineering. Figure 7 depicts the maximum measured heat-affected zone (HAZ) for laser ablation of carbon fibre-reinforced epoxy matrix composite. Notably, the infrared (IR) laser causes a larger HAZ compared to other wavelengths, a finding attributed to its more prominent photothermal effect.

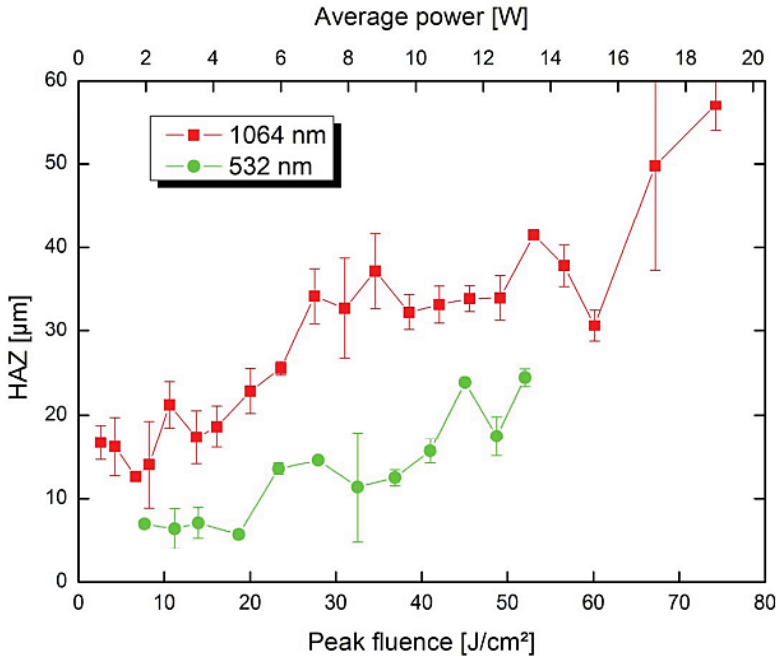

Figure 7. Highest measured heat affected zone in laser-ablated carbon fibre-reinforced composite (Wolynski et al., 2011)

For removing resin and contaminants, the thermal process driven by an infrared (IR) laser is generally less efficient compared to the direct photochemical ablation achieved with a UV laser (Ledesma et al., 2020). This difference arises because UV lasers directly break molecular bonds, while IR lasers rely on a heating process that can be less precise for material removal.

3.2. Photochemical Ablation

Photochemical ablation for polymer matrix composites is a technique where high-energy laser light directly severs molecular bonds within the material, allowing for highly precise removal with minimal thermal side effects.

For polymer matrix composites, nanosecond UV laser processing primarily removes material through two mechanisms: photochemical fracture and thermal evaporation. The intense

energy from the laser photons can actually break apart molecular bonds, leading to a chemical breakdown of the material. Figure 8 illustrates this well: when laser pulses hit the surface of the composite, the interplay of photochemical fracturing and thermal evaporation produces both fibre strands and a melted matrix.

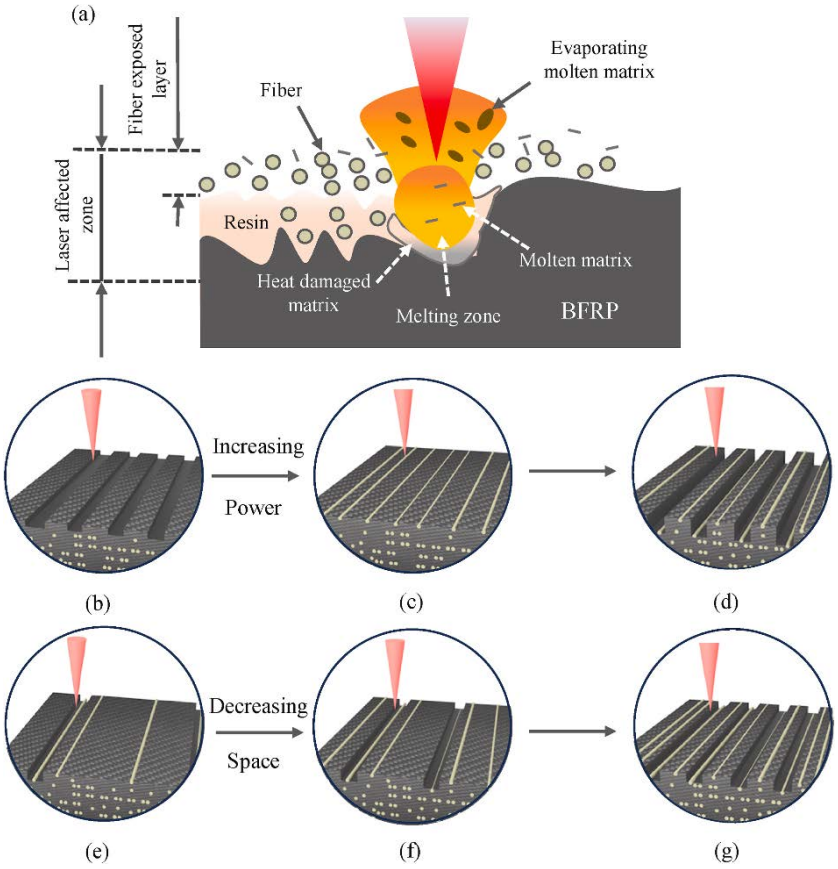

Figure 8. Schematic diagram of (a) Nanosecond Nd laser ablation of basalt fibre-reinforced polymer composite, and (b)-(g) Surface texture variations with laser line spacing and power (Zhang et al., 2024).

As the temperature rises and reaches the evaporation threshold of the materials, two distinct regions emerge: the laser-affected zone and the layer where the fibres are exposed. In the laser-affected zone, the material absorbs energy, which damages

the matrix and turns it into a molten state. Because fibres, such as basalt, vaporize at a significantly higher temperature than the matrix material, the matrix breaks down first, revealing the underlying fibres (Zhang et al., 2024).

If a series of ultra-short pulses hits the material too quickly, the heat builds up in the area absorbing the laser light. This causes the heat to spread, making the damaged zone larger. This issue becomes more noticeable with high repetition rates and is also affected by how easily heat moves through the material being processed. Multiple low-energy photons are simultaneously absorbed to collectively provide enough energy to excite electrons to higher energy levels or directly break chemical bonds (Bernabeu et al., 2024).

In very strong laser fields, electrons can tunnel out of atoms, leading to rapid ionization of the material and the formation of a highly localized, dense non-thermal plasma. The highly energetic, superheated plasma expands explosively, driving material removal. Crucially, because the energy delivery is orders of magnitude faster than the timescale for electron-phonon coupling and thermal diffusion, there is minimal energy transfer to the surrounding lattice. The hallmark of ultrashort pulse laser ablation is the extremely confined HAZ, often on the order of tens of nanometers or less. Material is removed with exceptional precision, leaving behind minimal thermal damage to the adjacent bulk material.

This cold ablation mechanism is vital for PMCs, as it allows for precise surface modification without compromising the integrity of the heat-sensitive polymer matrix or the reinforcing fibres. It avoids char formation and molten material deposition, leading to cleaner ablated surfaces.

3.3. Comparison of Photochemical and Photothermal Ablation

When considering laser-based processing of polymer composites, two primary mechanisms come into play: photochemical ablation, typically associated with UV lasers, and photothermal ablation, commonly seen with IR lasers. Understanding their fundamental differences is crucial for selecting the appropriate technique for specific applications.

Photochemical ablation relies on the high energy of UV photons to directly break molecular bonds within the polymer. This process, often termed cold ablation, minimizes heat transfer, leading to extremely precise material removal. It is ideal for applications demanding fine structuring or when preserving the integrity of heat-sensitive materials and fibres is essential, as it produces clean cuts with minimal, if any, thermal damage or residues.

Conversely, photothermal ablation operates by converting absorbed laser energy into heat. This heat causes the material to degrade or vaporize. In composites, the IR laser often heats the reinforcing fibres, which then indirectly affects the surrounding polymer matrix. While effective for selective matrix removal, particularly where the matrix strongly absorbs IR, this method can result in a more pronounced HAZ. This can lead to thermal degradation, charring, or delamination, and potentially leave behind residues. Careful control is vital to mitigate these thermal side effects.

Figure 9 shows the influence of short pulse (SP)-UV laser and ultra-short pulse (USP)-IR laser processes on the carbon fibre-reinforced epoxy matrix composites.

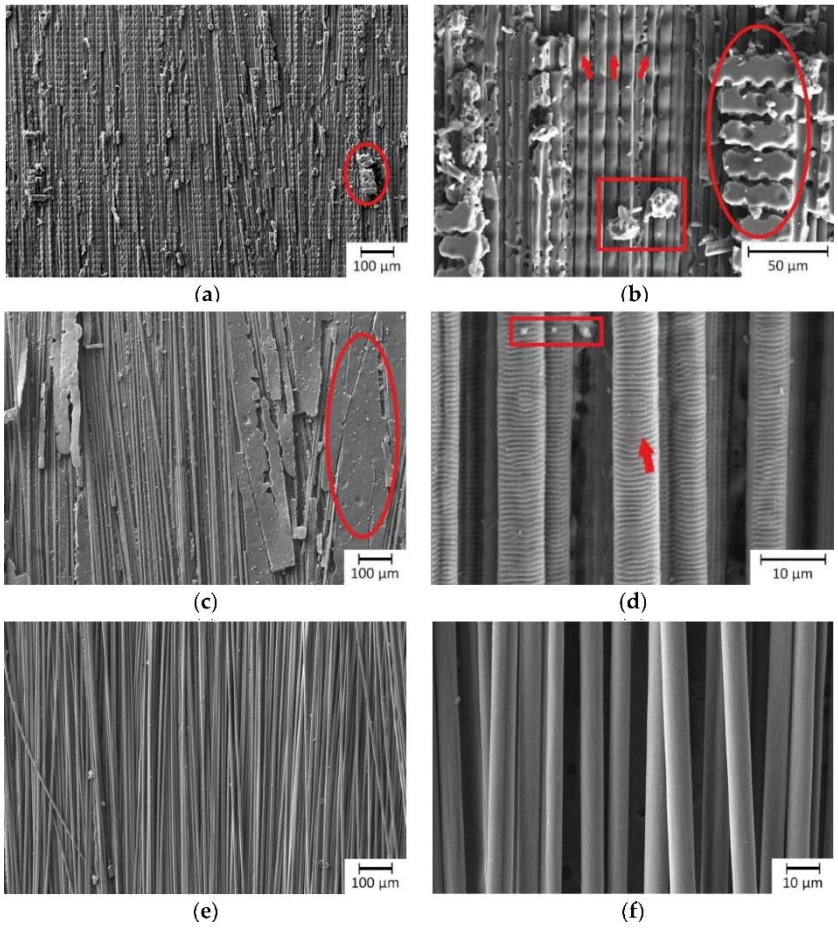

Figure 9. SEM analysis of fibre exposure following selective matrix removal. (a) and (b) SP-UV, (c) and (d) USP-IR-A, and (e) and (f) SP-IR-C lasers, residual epoxy (red circles), various residues (red rectangles), damaged carbon fibres (red arrows) (Gebauer et al., 2020)

As mentioned before, UV lasers use high-energy photons to break polymer bonds, leading to cold and precise material removal. This minimizes heat, ideal for exposing fibres cleanly with minimal damage, as seen in Figures 8(a) and (b). The laser primarily targets fibres, but some epoxy may remain due to differing absorption. Sharp epoxy edges suggest interfacial stresses contribute to material chipping. While photochemical effects dominate, some thermal fibre ablation is not excluded.

Residue-free matrix removal is often possible even without focused beams. IR lasers convert absorbed energy into heat, vaporizing material. In composites, fibres often heat up, affecting the surrounding epoxy. While effective for selective matrix removal, expect a heat-affected zone (HAZ). A post-ablation cleaning step may be necessary. Fibres can show a structure like in Figure 8(d), enhancing bonding without weakening the fibres. These patterns confirm the main interaction with the fibres of the laser, with interfacial stresses also aiding matrix detachment. Some epoxy residue is common after both UV and IR treatments. CO_2 lasers typically provide the most uniform selective matrix removal, completely ablating the matrix to expose fibres, as shown in Figure 8(e) and (f). This method usually leaves no structural fibre damage or residues (Gebauer et al., 2020).

4. CONCLUSION

The effective adoption of fibre-reinforced polymer matrix composites (PMCs) in challenging applications relies fundamentally on forming strong and long-lasting adhesive bondings. While various surface treatment strategies aim to address the inherent challenges posed by PMC surfaces, namely their low surface energy, chemical inertness, and susceptibility to contamination, this comprehensive investigation highlights the privilege of laser ablation as a premier surface modification technique.

Traditional methods, ranging from mechanical abrasion like sanding and blasting to chemical etching, each offer distinct advantages but also present notable limitations. Mechanical techniques, while straightforward, often risk fibre damage, inconsistent surface profiles, or abrasive particle embedment. Chemical etching, though effective in enhancing surface energy, introduces concerns about corrosive and hazardous substances.

Plasma treatments, whether vacuum or atmospheric, provide cleaner surfaces and controlled chemical functionalization but can be complex in application.

Amidst these approaches, laser ablation stands out as a highly controllable, non-contact method capable of inducing profound and precise changes in PMC surface morphology, chemistry, and energy. Its effectiveness arises from the collaboration of laser parameters and material properties, which produces different ways the material gets removed.

There is a crucial differentiation between photochemical ablation (UV lasers) and photothermal ablation (IR lasers). Photochemical ablation, driven by high-energy UV photons, directly breaks molecular bonds, leading to a cold ablation process. This mechanism is exceptionally precise, minimizing thermal damage and residue formation, which is vital for preserving the integrity of heat-sensitive polymer matrices and reinforcing fibres. It is particularly adept at creating intricate surface structures. Conversely, photothermal ablation, characteristic of IR lasers, relies on converting absorbed laser energy into heat, which then vaporizes or degrades the material. While effective for selective matrix removal, especially with CO_2 lasers that can achieve homogeneous fibre exposure, it often results in a more significant heat-affected zone (HAZ) and can leave behind residues. The insights gained from comparing these distinct laser-material interactions are invaluable for tailoring surface properties to specific bonding requirements.

Ultimately, the inherent heterogeneity of PMCs, comprising a polymer matrix and reinforcing fibres with disparate optical and thermophysical properties, demands a subtle approach to surface modification. Laser ablation is a versatile process. By choosing the right wavelength and pulse duration, it allows for precise control over ablation mechanisms, from photochemical to

photothermal, giving it a significant capability to precisely modify PMC surfaces. This leads to enhanced surface cleanliness, tailored topography for mechanical interlocking, and optimized surface chemistry for strong adhesive bonds. As the demand for lightweight, high-performance composites continues to grow across industries, advanced laser ablation techniques will play a vital role in effectively incorporating these materials into complex assemblies, thereby establishing their significance in engineering designs.

REFERENCES

Aliheidari, N. & Ameli, A. (2024). Retaining high fracture toughness in aged polymer composite/adhesive joints through optimization of plasma surface treatment. *Composites Part A: Applied Science and Manufacturing, 176*, 107835. https://doi.org/10.1016/j.compositesa.2023.107835.

Bechikh, A., Klinkova, O., Maalej, Y., Tawfiq, I., & Nasri, R. (2022). Effect of dry abrasion treatments on composite surface quality and bonded joints shear strength. *International Journal of Adhesion and Adhesives, 113*, 103058. https://doi.org/10.1016/j.ijadhadh.2021.103058.

Bernabeu, A. P., Puerto, D., Ramirez, M. G., Nájar, G., Francés, J., Gallego, S., Márquez, A., Pascual, I., & Beléndez, A. (2024). Controlled photothermal ablative processing of commercial polymers minimizing undesired thermal effects under high frequency femtosecond laser irradiation. *Optics & Laser Technology, 177*, 111069. https://doi.org/10.1016/j.optlastec.2024.111069.

Gebauer, J., Burkhardt, M., Franke, V., & Lasagni, A. F. (2020). On the ablation behavior of carbon fiber-reinforced plastics during laser surface treatment using pulsed lasers. *Materials, 13*(24), 5682. https://doi.org/10.3390/ma13245682.

Gu, J., Su, X., Jin, Y., Zhang, D., Li, W., Xu, J., & Guo, B. (2024). Research progress and prospects of laser cleaning for CFRP: A review. Composites Part A: Applied Science and *Manufacturing, 185*, 108349. https://doi.org/10.1016/j.compositesa.2024.108349.

Guo, W., Lim, Y. C., Ong, C. H., & Senthil K. A. (2024). Atmospheric pressure plasma application on the adhesive

bonding improvement of CFRP via surface configuration comparison. *Polymer Composites, 45*(2), 1461-1471. https://doi.org/10.1002/pc.27866.

Ledesma, R. I., Palmieri, F. L., Lin, Y., Belcher, M. A., Ferriell, D. R., Thomas, S. K., & Connell, J. W. (2020). Picosecond laser surface treatment and analysis of thermoplastic composites for structural adhesive bonding. *Composites Part B: Engineering, 191*, 107939. https://doi.org/10.1016/j.compositesb.2020.107939.

Li, H., Zhao, L., Qiao, Y., Bai, X., Wang, D., Qu, C., Liu, C., & Wang, Y. (2021). Surface treatment of composites with bismaleimide resin-based wet peel ply for enhanced adhesive bonding performance. *Polymers, 13*(20), 3488. https://doi.org/10.3390/polym13203488.

Liu, J., Xue, Y., Dong, X., Fan, Y., Hao, H., & Wang, X. (2023). Review of the surface treatment process for the adhesive matrix of composite materials. *International Journal of Adhesion and Adhesives, 126*, 103446. https://doi.org/10.1016/j.ijadhadh.2023.103446.

Manshina, A. A., Tumkin, I. I., Khairullina, E. M., Mizoshiri, M., Ostendorf, A., Kulinich, S. A., Makarov, S., Kuchmizhak, A. A., & Gurevich, E. L. (2024). The second laser revolution in chemistry: Emerging laser technologies for precise fabrication of multifunctional nanomaterials and nanostructures. *Advanved Functional Materials, 34*, 2405457. https://doi.org/10.1002/adfm.202405457.

Marques, A. C., Mocanu, A., Tomić, N. Z., Balos, S., Stammen, E., Lundevall, A., Abrahami, S. T., Günther, R., de Kok, J. M. M., & de Freitas, S. T. (2020). Review on adhesives and surface treatments for structural applications: Recent developments on sustainability and implementation for

metal and composite substrates. *Materials, 13*(24), 5590. https://doi.org/10.3390/ma13245590.

Nazari, R., Hakimi, R., Daneshfar, M., & Talebi, B. (2024a). Improving mode I fracture response of glass fiber-epoxy composite adhesive joints using sanding treatment and MWCNTs inclusion. *Discover Applied Sciences, 6*, 479. https://doi.org/10.1007/s42452-024-06186-5.

Nazari, R., Khoramishad, H., & Hakimi, R. (2024b). The effect of abrading treatment method on the bonding surface characteristics and fracture behavior of glass fiber-epoxy composite adhesive joints. *Journal of Adhesion Science and Technology, 38*(13), 2405-2424. https://doi.org/10.1080/01694243.2024.2302259.

Olonisakin, K., Fan, M., Xin-Xiang, Z., Ran, L., Lin, W., Zhang, W., & Wenbin, Y. (2021). Key improvements in interfacial adhesion and dispersion of fibers/fillers in polymer matrix composites; focus on PAL matrix composites. *Composite Interfaces, 29*(10), 1071–1120. https://doi.org/10.1080/09276440.2021.1878441.

Pitto, M., Fiedler, H., Kim, N. K., Verbeek, C. J. R., Allen, T. D., & Bickerton, S. (2024). Carbon fibre surface modification by plasma for enhanced polymeric composite performance: A review. *Composites Part A: Applied Science and Manufacturing, 180*, 108087. https://doi.org/10.1016/j.compositesa.2024.108087.

Pizzorni, M., Lertora, E., Gambaro, C., Mandolfino, C., Salerno M., & Prato, M. (2019). Low-pressure plasma treatment of CFRP substrates for epoxy-adhesive bonding: an investigation of the effect of various process gases. *The International Journal of Advanced Manufacturing Technology, 102*, 3021-3035. https://doi.org/10.1007/s00170-019-03350-9.

Sun, C., Min, J., Lin, J., & Wan, H. (2019). Effect of atmospheric pressure plasma treatment on adhesive bonding of carbon fiber reinforced polymer. *Polymers, 11*(1), 139. https://doi.org/10.3390/polym11010139.

Wang, H., Tong, X., Chen, Y., Hua, L., Wu, M., & Ji, W. (2021). Study on ultrasonic vibration-assisted adhesive bonding of CFRP laminates with laser ablation-treated surfaces. *Composite Structures, 268*, 113983. https://doi.org/10.1016/j.compstruct.2021.113983.

Wolynski A, Herrmann T, Mucha P, Haloui H, & L'huillier J. (2011). Laser ablation of CFRP using picosecond laser pulses at different wavelengths from UV to IR. *Physics Procedia, 12*, 292-301. https://doi.org/10.1016/j.phpro.2011.03.136.

Zhang, A., Jiang, H., Li, Y., Hu, R. Ren, Y., & Jiang, S. (2024). Effects of surface micro-texturing laser-etching on adhesive property and failure behaviors of basalt fiber composite single-lap-joint. *International Journal of Adhesion and Adhesives, 135*, 103831. https://doi.org/10.1016/j.ijadhadh

SEÇİCİ LAZER ERİTME (SLM) YÖNTEMİYLE EKLEMELİ İMALAT

Zehra SEVER[1]

1. GİRİŞ

Eklemeli imalat, aynı zamanda 3D baskı, hızlı prototipleme veya serbest formlu üretim olarak da adlandırılmaktadır. ASTM F2792-10 standardına göre, bu üretim yöntemi, geleneksel talaşlı imalat gibi malzeme çıkarma tekniklerinin aksine, nesnelerin üç boyutlu model verilerinden oluşturulması için malzemenin katmanlar halinde üst üste eklenmesi sürecine dayanır [1,4].

Havacılık, uzay, enerji, otomotiv, tıp, alet üretimi ve tüketici ürünleri gibi birçok sektörde eklemeli imalat, hem tasarım süreçlerinde hem de üretim tekniklerinde köklü değişiklikler yaratmaktadır [6].

Bu teknolojinin avantajları arasında geniş tasarım özgürlüğü, minimum malzeme israfı, düşük maliyetli prototipleme, kısa üretim süresi ve kişiselleştirilmiş üretim imkânı bulunmaktadır. Bununla birlikte, belirli malzemelerle sınırlı olması, üretim hızının görece düşük kalması, yüksek birim maliyetler, yüzey kalitesinin değişkenliği ve gelişmiş teknik bilgi ile özel makineler gerektirmesi gibi dezavantajları da mevcuttur.

[1] Ostim Teknik Üniversitesi, MYO, Makine ve Metal Teknolojileri, zehra.sever@ostimteknik.edu.tr, ORCID: 0000-0002-2928-1323.

2. EKLEMELİ İMALAT YÖNTEMLERİNİN SINIFLANDIRILMASI

Eklemeli imalat teknolojileri, kullanılan malzeme türü ve üretim sürecindeki farklı prensiplere göre çeşitli kategorilere ayrılmaktadır. Bu sınıflandırma, genellikle işlem mekanizmasına, malzemenin birleştirilme yöntemine ve uygulama alanlarına göre yapılmaktadır. ASTM 52900 standardına göre eklemeli imalat, yedi ana kategori altında sınıflandırılmaktadır Şekil1'de verilmektedir (ASTM, 2015).

Şekil1. Eklemeli İmalatın Sınıflandırılması

2.1. Vat Polimerizasyonu (Vat Photopolymerization)

Bu yöntemde sıvı fotopolimer reçine, belirli bir ışık kaynağı (genellikle lazer veya UV ışık) ile seçici olarak sertleştirilerek katmanlar oluşturulur. Stereolitografi (SLA) ve Dijital Işık İşleme (DLP**)** bu kategoriye giren başlıca yöntemlerdir. Yüksek hassasiyet ve pürüzsüz yüzey kalitesi sunmasıyla öne çıkar (Gibson, Rosen ve Stucker, 2015).

2.2. Malzeme Ekstrüzyonu (Material Extrusion)

Bu teknikte, termoplastik malzeme ısıtılarak eritilir ve katmanlar halinde biriktirilir. Eriyik Yığma Modelleme (FDM – Fused Deposition Modeling) bu sınıfta yer alır. Yaygın olarak kullanılan bir yöntem olup düşük maliyetli ve pratik olması avantajları arasındadır (Gupta, 2021).

2.3. Toz Yataklı Füzyon (Powder Bed Fusion - PBF)

Bu yöntemde, ince bir toz tabakası serilir ve belirli bölgeler yüksek enerjili bir ışın (lazer veya elektron ışını) kullanılarak eritilir veya sinterlenir. Bu gruptaki başlıca yöntemler şunlardır:

Seçici Lazer Sinterleme (SLS): Genellikle plastik ve kompozit malzemeler için kullanılır.

Seçici Lazer Eritme (SLM) ve Elektron Işınıyla Eritme (EBM): Metal tozlarının eritilerek güçlü ve dayanıklı parçalar oluşturulmasını sağlar (ASTM, 2015).

2.4. Doğrudan Enerji Depozisyonu (Directed Energy Deposition - DED)

Bu teknik, metal tozu veya telin, yüksek enerjili bir lazer ya da plazma arkı yardımıyla eritilerek yüzeye katman katman eklenmesine dayanır. Büyük ölçekli endüstriyel parçaların üretimi ve tamiratında yaygın olarak kullanılır (Gibson, Rosen ve Stucker, 2015).

2.5. Malzeme Jetleme (Material Jetting)

Mürekkep püskürtme yazıcılarına benzer şekilde çalışan bu yöntemde, fotopolimer damlacıkları katmanlar halinde biriktirilerek nesneler oluşturulur. Yüksek yüzey kalitesi ve çok renkli baskı imkanı sunar (Gupta, 2021).

2.6. Bağlayıcı Püskürtme (Binder Jetting)

İnce bir toz tabakası üzerine sıvı bağlayıcının püskürtülerek katmanların birleştirilmesi prensibine dayanır. Metal, seramik ve kum malzemelerle üretim yapılabilir (ASTM, 2015).

2.7. Sac Levha Laminasyonu (Sheet Lamination)

Bu yöntemde, ince levhalar üst üste yerleştirilerek birleştirilir. Yapıştırıcı veya ultrasonik kaynak ile birleştirme işlemi gerçekleştirilir. Genellikle düşük maliyetli ve hızlı prototipleme süreçlerinde kullanılır (Gibson, Rosen ve Stucker, 2015).

ASTM 52900 standardına göre eklemeli imalat teknolojileri farklı malzemeler ve üretim süreçlerine göre sınıflandırılmıştır. Her yöntem, belirli avantajlar ve dezavantajlar sunarak farklı endüstriyel ihtiyaçlara hizmet etmektedir. Gelişen teknolojiyle birlikte eklemeli imalat yöntemleri daha geniş bir kullanım alanına yayılmaktadır.

3. SEÇİCİ LAZER ERİTME (SLM) YÖNTEMİ

Metal eklemeli imalat teknolojilerinden biri olan Seçici Lazer Eritme (SLM – Selective Laser Melting)**,** toz yatağı esasına dayanan bir üretim yöntemidir. Bu yöntemde, metal tozları ince katmanlar halinde serilir ve yüksek enerjili bir lazer ile belirlenen bölgeler eritilir. Lazer, belirli bir enerji yoğunluğuyla metal tozlarını tamamen eriterek katı bir yapı oluşturur Şekil 2.

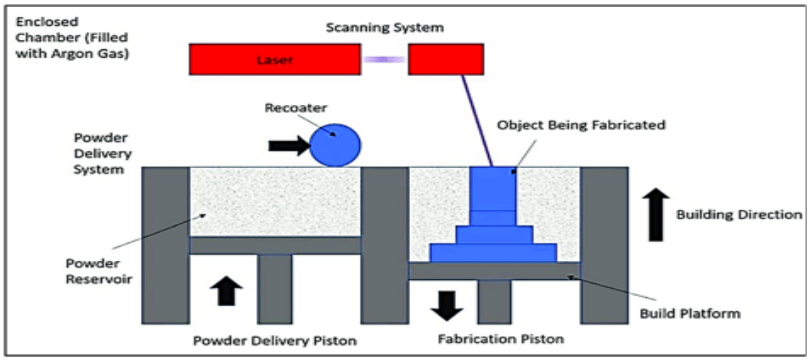

Şekil 2. SLM Yöntemi Şematik Gösterimi (Padmakumar M. (2020)).

Her katmanda, lazerle eritilen bölge katılaşarak parçanın belirli bir kısmını oluşturur. Katman tamamlandıktan sonra, sistem yeni bir toz tabakası yayar ve lazer bu tabakayı tekrar eriterek parçanın bir sonraki katmanını oluşturur. Bu işlem, nesne tamamen üretilene kadar devam eder (Gibson, Rosen ve Stucker, 2015; Kruth, Mercelis, Van Vaerenbergh, Froyen ve Rombouts, 2005).

SLM, yüksek yoğunluklu ve dayanıklı metal parçalar üretmeye olanak tanıdığı için havacılık, otomotiv ve tıp gibi sektörlerde yaygın olarak kullanılmaktadır.

4. SLM İLE ÜRETİMDE İŞLEM PARAMETRELERİ

Seçici Lazer Eritme **(**SLM – Selective Laser Melting**)** yöntemi, eklemeli imalat süreçlerinde yaygın olarak kullanılan bir toz yatağı füzyon tekniğidir. Bu yöntemde, üretim kalitesini doğrudan etkileyen çeşitli parametreler bulunmaktadır. Lazer gücü, tarama hızı, katman kalınlığı, tarama stratejisi ve toz özellikleri gibi faktörler, üretilen parçanın mekanik özellikleri, yoğunluğu ve yüzey kalitesi üzerinde belirleyici rol oynamaktadır (Kruth, Mercelis, Van Vaerenbergh, Froyen & Rombouts, 2005).

4.1. Lazer Gücü (Laser Power)

Lazer gücü, metal tozunun tam olarak eritilebilmesi için yeterli enerji sağlamada kritik bir parametredir. Yüksek lazer gücü, daha iyi bir birleşme sağlarken aşırı enerji, malzeme hatalarına yol açabilir (Padmakumar, 2020).

4.2. Tarama Hızı (Scanning Speed)

Lazerin toz yatağı üzerinde hareket hızı, enerji yoğunluğu ile doğrudan ilişkilidir. Daha düşük tarama hızları, daha fazla enerji girişi sağlayarak yoğunluk artışına neden olabilir, ancak

aşırı düşük hızlar malzeme deformasyonuna sebep olabilir (Gibson, Rosen & Stucker, 2015).

4.3. Katman Kalınlığı (Layer Thickness)

Her katmanın kalınlığı, üretim süresini ve yüzey kalitesini etkiler. İnce katmanlar, detaylı ve hassas üretimi sağlarken, daha uzun üretim sürelerine yol açabilir (Yadroitsev & Smurov, 2011).

4.4. Tarama Stratejisi (Scanning Strategy)

Lazerin tarama deseni, iç gerilmeleri ve çatlak oluşumunu önlemek için optimize edilmelidir. Çapraz tarama, paralel tarama ve rastgele tarama gibi stratejiler kullanılmaktadır (DebRoy et al., 2018).

4.5. Toz Özellikleri (Powder Characteristics)

Metal tozlarının parçacık boyutu, şekli ve akışkanlığı, üretim sürecinde tutarlılığı sağlamak açısından önemli parametrelerdir. Küresel şekilli tozlar, daha iyi bir dolgu ve erime davranışı sergiler (Gibson et al., 2015).

SLM sürecinde, üretim parametrelerinin optimizasyonu, parçaların mekanik özelliklerini, yüzey kalitesini ve genel üretim verimliliğini artırmak için kritik öneme sahiptir. Günümüzde, bu optimizasyonu gerçekleştirmek için çeşitli yöntemler kullanılmaktadır. Taguchi yöntemi, deney tasarımı ve analizinde kullanılan istatistiksel bir yaklaşımdır. Bu yöntem, proses parametrelerinin optimal seviyelerini belirlemek ve varyasyonu minimize etmek için kullanılır. Örneğin, bir çalışmada, SLM ile üretilen Ti6Al4V alaşımının yüzey pürüzlülüğü üzerine lazer gücü, tarama hızı, katman kalınlığı ve tarama mesafesi gibi parametrelerin etkisi Taguchi L16 ortogonal dizisi kullanılarak incelenmiştir (Aydın & Özer, 2022). Son yıllarda, yapay zeka ve makine öğrenmesi teknikleri, SLM proses parametrelerinin optimizasyonunda giderek daha fazla kullanılmaktadır. Özellikle, Gaussian süreç regresyonu gibi yöntemler, proses parametreleri

ile çıktı özellikleri arasındaki karmaşık ilişkileri modelleyerek optimal parametre setlerinin tahmin edilmesine olanak tanır. Bu yaklaşımlar, deneysel maliyetleri azaltırken, prosesin verimliliğini artırır (Asadi et al., 2020). Parçacık Sürü Optimizasyonu (PSO – Particle Swarm Optimization), doğal sürü davranışlarından esinlenen bir optimizasyon tekniğidir. SLM prosesinde, PSO kullanılarak proses parametrelerinin optimal değerleri belirlenebilir. Bu yöntem, özellikle yüksek boyutlu parametre uzaylarında etkili sonuçlar sunar (Asadi et al., 2020).

SLM yönteminde üretim parametrelerinin optimizasyonu, üretilen parçaların kalitesini ve performansını doğrudan etkiler. Günümüzde, deneysel tasarım yöntemleri, yapay zeka ve makine öğrenmesi teknikleri gibi çeşitli optimizasyon yaklaşımları kullanılmaktadır. Bu yöntemlerin entegrasyonu ve geliştirilmesi, SLM teknolojisinin endüstriyel uygulamalarını daha da genişletecektir.

5. SLM YÖNTEMİYLE ÜRETİLEN MALZEMELERİN YAPISAL ÖZELLİKLERİ

5.1. Mikro Yapı ve Kristalizasyon Mekanizması

Seçici Lazer Eritme (SLM – Selective Laser Melting) yöntemi, metal tozlarının lazer enerjisi kullanılarak katman katman eritilip birleştirilmesiyle yüksek yoğunluklu ve karmaşık geometrili parçaların üretildiği bir eklemeli imalat teknolojisidir. Bu yöntemle üretilen malzemeler, yüksek mekanik dayanım, ince mikro yapı ve düşük gözeneklilik gibi özellikler sunmaktadır (DebRoy et al., 2018). Ancak, üretim sürecinde iç gerilmeler, mikro çatlaklar ve anizotropik mekanik davranışlar gibi bazı yapısal dezavantajlar da ortaya çıkabilmektedir (Gibson, Rosen & Stucker, 2015).

SLM yöntemiyle üretilen metallerde mikro yapı, yüksek soğuma hızları nedeniyle ince taneli ve dendritik bir yapı gösterir. SLM sürecinde kullanılan lazer enerjisi ve tarama stratejisi, malzemenin kristalleşme kinetiğini doğrudan etkiler. Örneğin, Ti-6Al-4V alaşımı, ince kolonlu dendritik taneler içeren martensitik α' fazı oluşturur, bu da yüksek mukavemet sağlamasına rağmen kırılganlık riskini artırır (Thijs, Verhaeghe, Craeghs, Humbeeck & Kruth, 2010).

Ayrıca, SLM ile üretilen 316L paslanmaz çeliğin mikro yapısı, geleneksel döküm veya dövme teknikleriyle üretilenlere kıyasla daha homojen ve ince tanelidir. Yüksek enerji girdisi ve hızlı katılaşma, hücresel dendritik yapılar oluşturur ve bu da sertliği artırır (Spierings, Schneider & Eggenberger, 2011).

SLM ile üretilen malzemelerin yoğunluğu, üretim parametreleriyle doğrudan ilişkilidir. Lazer gücü, tarama hızı ve katman kalınlığı gibi faktörler uygun şekilde optimize edilmezse, parça içinde gözenekler oluşabilir ve bu da mekanik özellikleri olumsuz etkileyebilir (Yadroitsev & Smurov, 2011). Yapılan araştırmalar, SLM ile %99,9'a varan yoğunlukta parçalar üretilebileceğini ancak üretim sürecinin hassas kontrol gerektirdiğini göstermektedir (Kruth, Froyen, Van Vaerenbergh, Mercelis, Rombouts & Lauwers, 2004).

5.2. Mekanik Özellikler

SLM ile üretilen metal parçalar, geleneksel üretim yöntemleriyle yapılanlara kıyasla daha yüksek çekme dayanımı ve sertlik gösterebilir. Örneğin, Ti-6Al-4V alaşımı için yapılan çalışmalar, SLM ile üretilen numunelerin çekme dayanımının 1200 MPa seviyelerine ulaşabildiğini göstermektedir (Thijs et al., 2010). Benzer şekilde, SLM ile üretilen paslanmaz çelik 316L parçaları, geleneksel yöntemlere kıyasla daha ince taneli mikro yapı nedeniyle %20'ye kadar daha yüksek sertlik sunmaktadır (Spierings et al., 2011).

SLM yöntemiyle üretilen parçaların yorulma dayanımı, yüzey pürüzlülüğü ve iç kusurlara bağlı olarak değişiklik göstermektedir. Yüzeyde oluşan mikro çatlaklar ve gözenekler, yorulma dayanımını düşürebilmektedir (Leuders, Lieneke, Lammers, Tröster, Niendorf & Weißgärber, 2014). Yüzey sonrası işlemler (örneğin kumlama, polisaj ve ısıl işlemler) uygulanarak bu olumsuzluklar minimize edilebilir ve yorulma ömrü artırılabilir.

SLM süreci, katmanlı bir üretim yöntemi olduğu için parçalar anizotropik mekanik davranışlar gösterebilir. Üretim yönüne bağlı olarak malzemenin çekme dayanımı ve süneklik değerleri değişebilir (Gibson et al., 2015). Bu durum, özellikle havacılık ve biyomedikal uygulamalarında dikkate alınması gereken kritik bir faktördür.

SLM yöntemiyle üretilen metal parçalar, yüksek mekanik dayanım, ince mikro yapı ve optimize edilmiş yoğunluk gibi avantajlar sunmaktadır. Ancak, üretim sürecinde iç gerilmeler, gözeneklilik ve yön bağımlı mekanik davranışlar gibi bazı zorluklarla karşılaşılabilmektedir. Bu nedenle, SLM üretim parametrelerinin optimize edilmesi ve sonradan işleme yöntemlerinin uygulanması, parçaların performansını artırmada kritik bir rol oynamaktadır.

6. SLM YÖNTEMİYLE ÜRETİMDE KARŞILAŞILAN ZORLUKLAR VE ÇÖZÜM YÖNTEMLERİ

Seçici Lazer Eritme (SLM – Selective Laser Melting) yöntemi, metal eklemeli imalat teknolojileri arasında en yaygın kullanılan yöntemlerden biridir. Yüksek hassasiyet ve malzeme verimliliği sağlamasına rağmen, bu süreçte mikro çatlak oluşumu, iç gerilmeler, gözeneklilik, yüzey pürüzlülüğü ve anizotropik mekanik özellikler gibi çeşitli zorluklarla karşılaşılmaktadır

(Gibson, Rosen & Stucker, 2015). Bu problemlerin üstesinden gelmek için optimizasyon çalışmaları, üretim sonrası işlemler ve ileri üretim teknikleri gibi çeşitli çözüm yöntemleri geliştirilmiştir (DebRoy et al., 2018).

SLM yöntemiyle üretimde hızlı ısıtma ve soğutma döngüleri, malzeme içinde büyük iç gerilmelerin birikmesine neden olur. Bu gerilmeler zamanla mikro çatlak oluşumuna yol açarak malzemenin mekanik özelliklerini olumsuz etkileyebilir (Leuders, Lieneke, Lammers, Tröster, Niendorf & Weißgärber, 2014). Çözüm: Isıl İşlemler: Gerilim giderme tavlaması ve yaşlandırma işlemleri uygulanarak iç gerilmeler azaltılabilir. Optimum Tarama Stratejisi: Çapraz tarama veya rastgele tarama gibi stratejiler kullanılarak termal gradyanlar düşürülebilir (DebRoy et al., 2018).

Gözeneklilik, parçanın mekanik dayanımını ve yorulma direncini düşüren önemli bir faktördür. Düşük lazer enerjisi yoğunluğu veya yetersiz toz yatağı homojenliği, gözenek oluşumunu artırabilir (Spierings, Schneider & Eggenberger, 2011). Çözüm: Lazer Parametre Optimizasyonu: Lazer gücü ve tarama hızı optimize edilerek enerji yoğunluğu artırılmalıdır. Gaz Destekli Üretim: Argon veya nitrojen gazı kullanılarak oksidasyon önlenebilir ve yoğunluk artırılabilir (Kruth, Froyen, Van Vaerenbergh, Mercelis, Rombouts & Lauwers, 2004).

SLM ile üretilen parçaların yüzeyi genellikle yüksek pürüzlülük gösterir ve bu da hassas mekanik uygulamalar için ek işlem gerektirir (Yadroitsev & Smurov, 2011). Çözüm: Sonradan İşleme: Mekanik polisaj, kumlama ve elektro-parlatma yöntemleri uygulanabilir. Optimum Toz Boyutu Seçimi: Küresel ve ince taneli tozlar kullanılarak yüzey kalitesi iyileştirilebilir (Thijs, Verhaeghe, Craeghs, Humbeeck & Kruth, 2010).

SLM yöntemi katmanlı bir üretim süreci olduğu için parçaların mekanik özellikleri üretim yönüne bağlı olarak

değişebilir. Z yönünde üretilen numuneler genellikle daha düşük süneklik gösterir (Leuders et al., 2014). Çözüm: Farklı Tarama Stratejileri Kullanımı: Çapraz tarama veya dönüşümlü tarama stratejileri anizotropiyi azaltabilir. Çok Yönlü Isıl İşlemler: Homojen kristal büyümesi sağlanarak mekanik özelliklerde iyileştirme yapılabilir (Gibson et al., 2015).

SLM yöntemiyle üretim, yüksek mekanik dayanım, karmaşık geometri ve malzeme verimliliği gibi avantajlar sunarken, iç gerilmeler, gözeneklilik, yüzey pürüzlülüğü ve anizotropik mekanik özellikler gibi bazı üretim zorluklarıyla karşılaşılmaktadır. Bu problemlerin önüne geçmek için lazer parametre optimizasyonu, farklı tarama stratejileri ve çeşitli üretim sonrası işlemler uygulanmaktadır. Gelişen yapay zeka ve makine öğrenmesi teknikleri ile birlikte, gelecekte SLM üretim sürecinin daha verimli hale getirilmesi ve üretim zorluklarının minimize edilmesi hedeflenmektedir.

7. SLM UYGULAMA ALANLARI VE ENDÜSTRİYEL KULLANIM ÖRNEKLERİ

Seçici Lazer Eritme (SLM – Selective Laser Melting) yöntemi, metal eklemeli imalat teknolojileri arasında en gelişmiş yöntemlerden biri olup, havacılık, otomotiv, biyomedikal, enerji ve kalıpçılık gibi birçok endüstride yaygın olarak kullanılmaktadır. Karmaşık geometrilere sahip, yüksek dayanımlı ve özelleştirilmiş parçalar üretebilmesi, SLM yöntemini geleneksel üretim tekniklerine kıyasla daha avantajlı hale getirmektedir (Gibson, Rosen & Stucker, 2015). Son yıllarda, üretim süreçlerindeki optimizasyon çalışmaları ve gelişmiş malzeme kullanımı sayesinde SLM'nin endüstriyel uygulama alanları hızla genişlemektedir (DebRoy et al., 2018).

Havacılık sektörü, SLM teknolojisinin en yaygın kullanıldığı alanlardan biridir. Titanyum, süper alaşımlar ve hafif

metallerin SLM ile işlenebilmesi, uçak motorları ve uzay araçları için kritik parçaların üretilmesine olanak sağlamaktadır (Gibson et al., 2015). General Electric (GE), SLM ile üretilen yakıt enjektörlerini LEAP motorlarında kullanarak %25 daha hafif ve %30 daha verimli parçalar üretmiştir (Frazier, 2014). NASA, roket motor bileşenlerini üretmek için SLM teknolojisini kullanarak parçaların üretim süresini %50 azaltmış ve maliyetleri düşürmüştür (Thompson, Bian, Shamsaei & Yadollahi, 2015).

SLM yöntemi, hafif ve yüksek mukavemetli parçalar üretme ihtiyacı nedeniyle otomotiv sektöründe de büyük bir ilgi görmektedir. Geleneksel döküm ve talaşlı imalat tekniklerine kıyasla, karmaşık yapılı motor bileşenleri ve şasi parçaları SLM ile daha verimli şekilde üretilebilmektedir (Levy, Schindel & Kruth, 2003). Bugatti, Chiron modelinde kullanılan titanyum fren kaliperlerini SLM yöntemiyle üreterek parçaların ağırlığını düşürmeyi ve mukavemetini artırmayı başarmıştır (DebRoy et al., 2018). BMW, prototip motor parçaları ve şasi bileşenlerini SLM ile üreterek test sürelerini kısaltmış ve üretim maliyetlerini azaltmıştır (Spierings, Schneider & Eggenberger, 2011).

SLM teknolojisi, kişiye özel implant ve protez üretiminde devrim yaratmıştır. Geleneksel üretim yöntemleri ile üretilemeyen karmaşık tasarımlar, hastaya özel uyarlamalar sayesinde daha ergonomik ve dayanıklı hale getirilebilmektedir (Kruth, Froyen, Van Vaerenbergh, Mercelis, Rombouts & Lauwers, 2004). Ortopedik implantlar (kalça, diz protezleri), biyouyumlu alaşımlar (örneğin Ti-6Al-4V) kullanılarak SLM ile üretilmektedir (Thijs, Verhaeghe, Craeghs, Humbeeck & Kruth, 2010). Kafatası ve çene implantları, hastaya özel tasarımlarla SLM yöntemiyle üretilmekte ve cerrahi başarı oranı artırılmaktadır (Leuders, Lieneke, Lammers, Tröster, Niendorf & Weißgärber, 2014).

SLM, enerji sektöründe özellikle türbin kanatları, ısı değiştiriciler ve kompleks boru sistemleri üretiminde yaygın olarak kullanılmaktadır. Ayrıca, savunma sanayiinde hafif ve dayanıklı parçalar üretmek için de tercih edilmektedir (Yadroitsev & Smurov, 2011). Siemens, gaz türbinlerinde kullanılan soğutmalı türbin kanatlarını SLM ile üreterek verimliliği artırmıştır (Frazier, 2014). ABD Savunma Bakanlığı (DoD), hafif ve mukavemetli silah parçalarını ve zırh bileşenlerini SLM ile üretmeyi araştırmaktadır (DebRoy et al., 2018).

SLM, kalıp üretiminde hassas ve dayanıklı parçalar üretme avantajı sunduğundan, plastik enjeksiyon kalıpları ve metal döküm kalıpları üretiminde giderek daha fazla kullanılmaktadır (Kruth et al., 2004). Volkswagen, motor bileşenlerinin döküm kalıplarını SLM ile üreterek üretim sürelerini ve maliyetlerini düşürmüştür (Spierings et al., 2011). Mold & Die Industry, SLM kullanarak soğutma kanalları içeren enjeksiyon kalıpları üretmekte ve böylece döküm süresini kısaltmaktadır (Levy et al., 2003).

SLM yöntemi, havacılıktan otomotive, biyomedikalden enerji sektörüne kadar geniş bir kullanım alanına sahiptir. Geleneksel üretim yöntemleriyle mümkün olmayan hafif, dayanıklı ve karmaşık parçaların üretimi için SLM giderek daha fazla tercih edilmektedir. Özellikle havacılık, savunma sanayii ve medikal sektörlerde özelleştirilmiş ve yüksek performanslı parçaların üretiminde büyük avantajlar sağlamaktadır. Gelecekte, SLM teknolojisinin yeni malzemeler ve optimizasyon teknikleriyle geliştirilmesi, üretim süreçlerinde daha geniş çapta benimsenmesini sağlayacaktır. Ayrıca, makine öğrenimi ve yapay zeka destekli süreç kontrol sistemleri, SLM üretiminin verimliliğini artırmada kritik bir rol oynayacaktır.

8. SONUÇ VE GELECEK PERSPEKTİFLERİ

Seçici Lazer Eritme (SLM – Selective Laser Melting) yöntemi, metal eklemeli imalat teknolojileri içinde en yaygın kullanılan yöntemlerden biri olarak, havacılık, otomotiv, medikal, enerji ve savunma sanayii gibi birçok sektörde önemli bir yer edinmiştir. Karmaşık geometrilere sahip, yüksek mukavemetli ve özelleştirilmiş parçalar üretebilme yeteneği, SLM'yi geleneksel üretim yöntemlerine kıyasla daha avantajlı hale getirmektedir (Gibson, Rosen & Stucker, 2015). Bununla birlikte, iç gerilmeler, yüzey pürüzlülüğü, gözeneklilik ve anizotropik mekanik davranışlar gibi üretim sürecine dair zorluklar, teknolojinin daha da geliştirilmesini gerektirmektedir (DebRoy et al., 2018).

SLM yöntemi, malzeme bilimi, lazer teknolojileri ve eklemeli üretim süreçlerindeki gelişmelerle birlikte sürekli olarak optimize edilmektedir. Günümüzde Ti-6Al-4V, paslanmaz çelik, Inconel ve Al-Si alaşımları gibi yüksek performanslı metallerin SLM ile üretimi yaygın hale gelmiştir (Frazier, 2014). Ayrıca, üretim sonrası işlemler (ısı işlemleri, mekanik yüzey işlemleri, HIP – Hot Isostatic Pressing gibi yöntemler) kullanılarak, SLM ile üretilen parçaların mekanik özellikleri iyileştirilmektedir (Leuders, Lieneke, Lammers, Tröster, Niendorf & Weißgärber, 2014).

Günümüzde havacılık ve uzay sanayii, SLM kullanımının en yaygın olduğu alanlardan biridir. NASA ve General Electric (GE) gibi kuruluşlar, roket motorları, türbin bileşenleri ve yakıt enjektörleri gibi kritik parçaların üretiminde SLM'yi aktif olarak kullanmaktadır (Thompson, Bian, Shamsaei & Yadollahi, 2015). Benzer şekilde, otomotiv ve medikal sektörlerinde de hafif, dayanıklı ve kişiye özel üretim ihtiyaçları nedeniyle SLM teknolojisine olan talep giderek artmaktadır (Spierings, Schneider & Eggenberger, 2011).

Mevcut SLM süreçleri genellikle Ti-6Al-4V, paslanmaz çelik ve Inconel gibi geleneksel alaşımlarla sınırlıdır. Ancak, kompozit malzemeler, bakır alaşımları ve fonksiyonel dereceli malzemeler (FGM) gibi yeni malzemelerin SLM ile işlenebilirliğinin artırılması için çalışmalar devam etmektedir (Yadroitsev & Smurov, 2011). Nano-parçacık takviyeli metal tozları, daha yüksek mekanik performans ve termal direnç sağlamak amacıyla geliştirilmekte ve test edilmektedir (Kruth, Froyen, Van Vaerenbergh, Mercelis, Rombouts & Lauwers, 2004).

SLM süreçlerinde lazer gücü, tarama hızı, katman kalınlığı ve toz morfolojisi gibi parametrelerin optimizasyonu, genellikle deneysel çalışmalarla belirlenmektedir. Ancak, makine öğrenmesi ve yapay zeka tabanlı optimizasyon yöntemleri, üretim sürecinin daha verimli hale getirilmesine olanak tanımaktadır (DebRoy et al., 2018). Özellikle derin öğrenme ve görüntü işleme teknikleri, SLM sürecinde gerçek zamanlı kalite kontrolü sağlamak için kullanılmaktadır (Thompson et al., 2015).

SLM'nin gelecekteki en önemli gelişmelerinden biri, çok malzemeli üretim süreçlerinin geliştirilmesi olacaktır. Fonksiyonel dereceli malzemeler (FGM) ve farklı metal kombinasyonlarının aynı üretim sürecinde birleştirilmesi, çok amaçlı mühendislik çözümleri sunabilir (Leuders et al., 2014). Ayrıca, CNC işleme ve SLM'nin bir arada kullanıldığı hibrit üretim teknikleri, yüzey kalitesini iyileştirme ve üretim hızını artırma açısından büyük potansiyel taşımaktadır (Frazier, 2014).

SLM'nin mikro ve nano ölçekte üretim kabiliyeti, özellikle biyomedikal ve elektronik sektörleri için büyük bir araştırma alanıdır. Hücre mühendisliği, biyosensörler ve mikro robotik sistemler gibi ileri teknoloji uygulamaları için SLM ile ultra hassas metal yapılar üretilmesi hedeflenmektedir (Spierings et al., 2011).

SLM yöntemi, hassas ve yüksek mukavemetli parçalar üretme kabiliyeti sayesinde günümüzde birçok endüstride yaygın olarak kullanılmaktadır. Havacılık, otomotiv, medikal ve enerji sektörlerinde giderek daha fazla benimsenen bu teknoloji, geleneksel üretim yöntemlerine kıyasla daha esnek ve özelleştirilmiş üretim imkânı sunmaktadır. Ancak, gözeneklilik, iç gerilmeler ve yüzey pürüzlülüğü gibi zorlukların aşılması için sürekli gelişim ve optimizasyon gerekmektedir.

Gelecekte, yeni malzeme geliştirme çalışmaları, yapay zeka destekli süreç optimizasyonu, çok malzemeli üretim teknikleri ve mikro/nano üretim uygulamaları, SLM'nin daha geniş bir kullanım alanına yayılmasını sağlayacaktır. Hibrit üretim sistemlerinin geliştirilmesi ve akıllı üretim teknolojilerinin entegrasyonu, SLM'nin sanayi 4.0 ve dijital üretim ekosistemine entegrasyonunu hızlandıracaktır.

Sonuç olarak, SLM yöntemi, geleceğin üretim teknolojileri arasında yerini sağlamlaştırmış olup, sürekli araştırma ve inovasyon ile daha yüksek verimlilik ve kalite seviyelerine ulaşacaktır.

KAYNAKÇA

ASTM International. (2015). *ASTM 52900: Standard terminology for additive manufacturing – General principles – Terminology.* ASTM International.

Asadi, F., Olleak, A. A., Yi, J., & Guo, Y. (2020). Gaussian process (GP)-based learning control of selective laser melting process. *arXiv preprint arXiv:2010.04712.* Retrieved from https://arxiv.org/abs/2010.04712

Aydın, D. S., & Özer, G. (2022). Farklı üretim parametrelerinin SLM yöntemiyle üretilen Ti6Al4V alaşımının yüzey kalitesi üzerindeki etkilerinin Taguchi yöntemi ile incelenmesi. *International Journal of Innovative Engineering Applications, 6*(2), 230-236. Retrieved from https://dergipark.org.tr/tr/download/article-file/2355651

DebRoy, T., Wei, H. L., Zuback, J. S., Mukherjee, T., Elmer, J. W., Milewski, J. O., ... & Zhang, W. (2018). Additive manufacturing of metallic components – Process, structure and properties. *Progress in Materials Science, 92,* 112-224.

Frazier, W. E. (2014). Metal additive manufacturing: A review. *Journal of Materials Engineering and Performance, 23*(6), 1917-1928.

Gibson, I., Rosen, D. W., & Stucker, B. (2015). *Additive manufacturing technologies: 3D printing, rapid prototyping, and direct digital manufacturing.* Springer.

Gupta, M. (2021). *3D printing and additive manufacturing technologies.* CRC Press.

Kruth, J. P., Froyen, L., Van Vaerenbergh, J., Mercelis, P., Rombouts, M., & Lauwers, B. (2004). Selective laser melting of iron-based powder. *Journal of Materials Processing Technology, 149*(1-3), 616-622.

Kruth, J. P., Mercelis, P., Van Vaerenbergh, J., Froyen, L., & Rombouts, M. (2005). Binding mechanisms in selective laser sintering and selective laser melting. *Rapid Prototyping Journal, 11*(1), 26-36.

Levy, G. N., Schindel, R., & Kruth, J. P. (2003). Rapid manufacturing and rapid tooling with layer manufacturing (LM) technologies. *CIRP Annals, 52*(2), 589-609.

Leuders, S., Lieneke, T., Lammers, S., Tröster, T., Niendorf, T., & Weißgärber, T. (2014). On the fatigue properties of selective laser melted Ti-6Al-4V: Role of ductility and internal defects. *Materials Research Letters, 2*(6), 255-260.

Padmakumar, M. (2020). Additive manufacturing of tungsten carbide hardmetal parts by selective laser melting (SLM), selective laser sintering (SLS) and binder jet 3D printing (BJ3DP) techniques. *Lasers in Manufacturing and Materials Processing, 7*(3), 338-371.

Spierings, A. B., Schneider, M., & Eggenberger, R. (2011). Comparison of density measurement techniques for additive manufactured metallic parts. *Rapid Prototyping Journal, 17*(5), 380-386.

Thijs, L., Verhaeghe, F., Craeghs, T., Humbeeck, J. V., & Kruth, J. P. (2010). A study of the microstructural evolution during selective laser melting of Ti–6Al–4V. *Acta Materialia, 58*(9), 3303-3312.

Thompson, S. M., Bian, L., Shamsaei, N., & Yadollahi, A. (2015). An overview of Direct Laser Deposition for additive manufacturing. *Additive Manufacturing, 8*, 36-62.

Yadroitsev, I., & Smurov, I. (2011). Selective laser melting technology: From the single laser melted track stability to

3D parts of complex shape. *Physics Procedia, 12*, 264-270.

MECHANICAL ENGINEERING FROM AN ACADEMIC PERSPECTIVE

yaz
yayınları

YAZ Yayınları
M.İhtisas OSB Mah. 4A Cad. No:3/3
İscehisar / AFYONKARAHİSAR
Tel : (0 531) 880 92 99
yazyayinlari@gmail.com • www.yazyayinlari.com